The development of in vitro techniques capable of characterising gas powered floating dosage forms

Chapman, James Anthony

Award date:
2002

Awarding institution:
University of Bath

THE DEVELOPMENT OF *IN VITRO* TECHNIQUES CAPABLE OF CHARACTERISING GAS POWERED FLOATING DOSAGE FORMS

submitted by

James Anthony Chapman B.Pharm. (Hons), M.R.Pharm.S.

for the degree of Doctor of Philosophy

of the University of Bath, February 2002

ProQuest LLC
789 East Eisenhower Parkway
P.O. Box 1346
Ann Arbor, MI 48106-1346

Acknowledgements

I would like to thank both of my supervisors, Mike Tobyn and John Staniforth for their guidance and support throughout my project. This work would not have been possible without the sponsorship of Ranbaxy Ltd, who I thank for their generous support.

I would also like to thank the following: Naresh Talwar for his invaluable help and advice on tablet formulations and his constant willingness to lend his thoughts, Graham Graham Kay for providing much needed moral support throughout the years, Fraser Manov-Steele for always being available to answer my questions and his general help around the laboratory, David Simpson for his help with the mercury porosimetry work, everyone at the department of material sciences for their help with the ASAP work, Steven Edge, Mop Aydin and Martyn Clarke for keeping me sane by providing some much needed football banter and to all my friends at the University of Bath who have helped me to complete this project. Special thanks goes to Martyn Fawley for keeping me amused with his cinnamon tricks.

Finally, I would like to thank my parents and my beautiful fiancée Stephanie for all their help and for sticking by me during some tough times.

Abstract

Retention of a drug delivery system in the stomach is one way of improving and controlling the absorption of drugs that have an absorption window in the upper small intestine. By releasing the drug at a controlled rate across this main absorption site for a prolonged period, improved blood levels, and therefore better tolerated dosage regimes, can be achieved.

Gas-powered floating delivery systems have emerged as one of the most promising of the gastric retention methods currently in development. However, at present, gas-powered floating dosage forms do not have a standardised battery of *in vitro* tests that are predicative of *in vivo* results. There is therefore a need for a rationalised approach to floating dosage form design, which will enable us to evolve a proper mechanistic understanding of the behaviour of such dosage forms, thus improving the accurate prediction of *in vivo* behaviour.

The most important factor to consider when designing floating dosage forms is the ability of the formulation to float upon the gastric fluids. It is also vital to quantitate the floating profile of the dosage form over a functional time period. An apparatus has therefore been developed that accurately measures the resultant weight of a dosage form at predetermined intervals over an elongated time period.

The controlled production of gas from a floating dosage form offers considerable benefits to the formulator. A novel *in vitro* pressure vessel, capable of assessing the real time production of gas from a formulation over a designated time period, has therefore been designed and tested.

The extent to which a polymer system swells upon hydration *in vivo* has a direct effect on the density of floating dosage forms. An *in vitro* method capable of accurately measuring the dynamic swelling of a dosage form has therefore been developed.

The apparatus have been extensively tested using a selection of manufactured gas powered floating dosage forms. The relationship between the parameters has been investigated in detail and possible *in vivo – in vitro* correlation discussed.

Acknowledgements ii
Abstract iii
Figures: viii
Tables: xi
CHAPTER 1 ..... **1**
GENERAL INTRODUCTION **1**
1.1 Gastrointestinal transit and drug absorption 2
1.2 Gastric emptying 2
1.2.1 Postprandial emptying 3
1.2.2 Interdigestive emptying 3
1.2.3 Factors affecting gastric emptying rate 3
1.3 Gastric emptying of dosage forms 4
1.4 Controlling the gastrointestinal transit of dosage forms 5
1.4.1 Physical methods of delaying gastric emptying 6
1.4.1.1 Floating systems 6
1.4.1.2 Bioadhesive systems 8
1.4.1.3 Other systems 9
1.4.2 Physiological methods of delaying gastric emptying 9
1.4.3 Pharmacological methods of delaying gastric emptying 9
1.5 Aims and objectives 10
CHAPTER 2 ..... **11**
MATERIALS AND METHODS **11**
2.1 Introduction 12
2.2 Materials 13
2.3 Methods 14
2.3.1 Mercury porosimetry 14
2.3.2 Surface area analysis by nitrogen adsorption 14
2.3.3 Measurement of Bulk density 15
2.3.4 Measurement of Tablet Strength 15
2.3.5 Measurement of Tablet Weight 15
CHAPTER 3 ..... **16**
BUOYANCY APPARATUS DESIGN AND DEVELOPMENT **16**
3.1 Introduction 17

3.2 Background 17
3.3 Original Apparatus Design 19
3.4 Initial Method 24
3.5 Initial Modifications to Original Design 24
3.6 Secondary Method and Results 26
3.7 Further Modifications to Method 29
3.8 Final Method 33
CHAPTER 4 36
PRESSURE VESSEL DESIGN AND DEVELOPMENT 36
4.1 Introduction 37
4.2 Background 37
4.3 Original apparatus design 38
4.3.1 Theory behind apparatus measurements / specifications 38
4.3.2 Experimental design 40
4.4 Initial calibration methodology 42
4.5 Modifications to the original design 45
4.6 Initial calibration results 45
4.7 Secondary modifications to vessel design 48
4.8 Further modifications to methodology 50
4.9 Validation of final apparatus and method 58
4.9.1 Blank runs using final pressure apparatus 58
4.9.2 Calibration of final pressure apparatus 62
CHAPTER 5 70
IN VITRO ANALYSIS OF A GAS-POWERED, FLOATING DOSAGE FORM 70
5.1 Introduction 71
5.2 Choice of dosage form 71
5.3 Manufacture of dosage forms 72
5.3.1 Initial manufacturing method 72
5.4 Results from initial batch 73
5.4.1 Weight variation 73
5.4.2 Hardness testing 74
5.4.3 Buoyancy testing 75
5.4.4 Helium pycnometry and mercury porosimetry 78
5.4.4.1 Helium pycnometry and calculations 78

5.4.4.2 Mercury porosimetry 79
5.5 Changes to blending methodology 81
5.6 Formulation, manufacture and testing of blends 81
5.6.1 Weight variation 82
5.6.2 Hardness testing 83
5.6.3 Buoyancy testing 84
5.6.4 Pressure vessel testing 87
5.6.5 Mercury porosimetry 90
5.6.6 Nitrogen adsorption 91
5.6.7 Development of an apparatus capable of quantifying tablet swelling 94
5.6.7.1 Introduction 94
5.6.7.2 Original apparatus design 95
5.6.7.3 Results from original apparatus 96
5.6.7.4 Modifications to the apparatus 97
5.6.7.5 Final methodology 98
5.6.7.6 Results from blend 2 98
5.6.8 Discussion of blend 2 characteristics 102
5.7 Formulation and testing of secondary blends 107
5.7.1 Results from blend 3 108
5.7.1.1 Weight variation 108
5.7.1.2 Hardness testing 109
5.7.1.3 Buoyancy testing 110
5.7.1.4 Pressure vessel testing 113
5.7.1.5 Mercury porosimetry 117
5.7.1.6 Nitrogen adsorption 118
5.7.1.7 Swelling studies 119
5.7.2 Discussion of blend 3 characteristics 123
5.7.3 Results from blend 4 127
5.7.3.1 Weight variation 127
5.7.3.2 Hardness testing 128
5.7.3.3 Buoyancy testing 128
5.7.3.4 Pressure vessel testing 131
5.7.3.5 Mercury porosimetry 135
5.7.3.6 Nitrogen adsorption 135

5.7.3.7 Swelling studies 136
5.7.4 Discussion of blend 4 characteristics 140
5.8 Blend comparisons 143
5.8.1 Comparison of buoyancy results 143
5.8.2 Comparison of pressure vessel results 147
5.8.3 Comparison of swelling results 149
5.9 Summary 151
CHAPTER 6 152
CASE STUDY OF A FLOATING SYSTEM (1) 152
6.1 Manufacture of the aerogel system 153
6.2 Buoyancy testing 154
6.3 Pressure vessel testing 157
6.4 Swelling studies 161
6.5 Discussion of the aerogel capsule characteristics 165
CHAPTER 7 170
CASE STUDY OF A FLOATING SYSTEM (2) 170
7.1 Discussion of in vivo results 171
7.2 In vitro buoyancy results 172
7.3 Conclusions 174
CHAPTER 8 175
DISCUSSION AND CONCLUSIONS 175
8.1 General discussion 176
8.2 Further work 178
CHAPTER 9 179
REFERENCES 179

Figures:

Figure 1 Schematic of a previous buoyancy apparatus 19
Figure 2 A schematic of the initial buoyancy device 20
Figure 3 A picture of the buoyancy apparatus 21
Figure 4 Dimensions and structure of Force Transmitter Device (FTD) 22
Figure 5 A photograph of the FTD and water bath assembly 23
Figure 6 A graph to show the effect of water loss on resultant weight whilst using the original apparatus 25
Figure 7 A graph to show the effect of water loss on resultant weight whilst using the modified test method 28
Figure 8 A graph to show the effect of water loss on resultant weight when silicon oil and Tween 20 had been added to the surface of the medium 30
Figure 9 A graph to show the effect of water loss on resultant weight when water loss is limited by insulating spheres 32
Figure 10 A graph to show the effect of fluid loss on resultant weight when using simulated gastric fluid as a medium 35
Figure 11 Photograph of pressure vessel 41
Figure 12 Schematic of pressure vessel design 42
Figure 13 A graph to show the relationship between CO_2 addition and pressure in a closed vessel containing CO_2 free water 44
Figure 14 A graph to show the relationship between CO_2 and pressure in a closed vessel containing different mediums 47
Figure 15 A graph to show the "warming up" effect of the pressure transducer 50
Figure 16 A graph to show the relationship between pressure and time when the medium in the vessel had been preheated prior to the vessel being sealed 51
Figure 17 A graph to show the relationship between pressure and time when the medium in the vessel has been heated after the sealing of the vessel 52
Figure 18 A graph to show to relationship between pressure and time during and after heating SGF to 37°C in the pressure apparatus with insert 57
Figure 19 A graph to show results of the pressure vessel methodology using blank run conditions 60
Figure 20 A graph to show the average of the five pressure vessel runs using blank conditions 61

Figure 21 A graph to show the calibration curves for the pressure vessel containing SGF 63
Figure 22 A graph to show the average calibration curve for the pressure vessel containing SGF 64
Figure 23 A graph to show the calibration curves for the pressure vessel containing no medium 66
Figure 24 A graph to show the average calibration curve for the pressure vessel containing no medium 67
Figure 25 A graph to show the effect that medium presence has on the calibration curve for the pressure vessel 68
Figure 26 A graph to show the resultant weight profiles of three tablets from blend 1 ... 76
Figure 27 A graph to show the resultant weight profiles of five tablets from blend 2 85
Figure 28 A graph to show the carbon dioxide release rate for five blend 2 tablets 88
Figure 29 A graph to show the rate of gas release during consecutive 1.5-minute periods for blend 2 89
Figure 30 A digital photograph of the housing structure and mesh 96
Figure 31 Two digital photographs showing the swelling of a blend 2 tablet 97
Figure 32 Sample digital photographs of tablet swelling process 99
Figure 33 A graph to show the image analysis data for blend 2 101
Figure 34 A graph to show the normalised dynamic testing data sets for blend 2 106
Figure 35 A graph to show the resultant weight profiles of five tablets from blend 3 ... 111
Figure 36 A graph to show the carbon dioxide release rate for five blend 3 tablets 115
Figure 37 A graph to show the rate of gas release during consecutive 1.5-minute periods for blend 3 116
Figure 38 Sample digital photographs of tablet swelling process 120
Figure 39 A graph to show the image analysis data for blend 3 122
Figure 40 A graph to show the normalised dynamic testing data sets for blend 3 126
Figure 41 A graph to show the resultant weight profiles of five tablets from blend 4 ... 129
Figure 42 A graph to show the carbon dioxide release rate for five blend 4 tablets 133
Figure 43 A graph to show the rate of gas release during consecutive 1.5-minute periods for blend 4 134
Figure 44 Sample digital photographs of tablet swelling process 137
Figure 45 A graph to show the image analysis data for blend 4 139
Figure 46 A graph to show the normalised dynamic testing data sets for blend 4 142

Figure 47 A graph to show the comparison of resultant weight profiles for the three test blends 146
Figure 48 A graph to show the comparison of gas release profiles for the test blends .. 148
Figure 49 A graph to show the comparison of swelling profiles for the test blends 150
Figure 50 A graph to show the resultant weight profile of five aerogel capsules 155
Figure 51 A graph to show the average resultant weight profile for the aerogel capsules 156
Figure 52 A graph to show the carbon dioxide release rate for five aerogel capsules ... 159
Figure 53 A graph to show the average rate of gas release for the aerogel capsules 160
Figure 54 Sample digital photographs of the capsule swelling process 162
Figure 55 A graph to show the image analysis data for the aerogel capsules 164
Figure 56 A graph to show the normalised data for gas release from aerogel capsules 166
Figure 57 A graph to show the normalised dynamic testing data sets for the aerogel capsules 169
Figure 58 A graph to show the resultant weight profiles for the generic capsules 173

Tables:

Table 1. Materials that have been used during the course of the study 13
Table 2 Total weight gain on the FTD over an 8-hour period using Millipore water as a medium 31
Table 3 Total weight gain on the FTD over an 8-hour period using SGF as a medium ... 34
Table 4 Blend Constituents of initial test formulation 72
Table 5 A table to show the weight variation in batch 1 74
Table 6 A table to show the hardness variation in batch 1 75
Table 7 A table to show the mercury porosimetry results for tablets made from blend 1 80
Table 8 A table to show the weight variation in batch 2 83
Table 9 A table to show the hardness variation in batch 2 84
Table 10 A table to show the buoyancy force data for blend 2 86
Table 11 CO_2 release data for the five blend 2 tablets 90
Table 12 A table to show the mercury porosimetry results for tablets made from blend 2 91
Table 13 Results from BET surface area analysis on blend 2 93
Table 14 Cross-sectional area data for blend 2 100
Table 15 Blend constituents of formulations 3 and 4 107
Table 16 A table to show the weight variation in batch 3 109
Table 17 A table to show the hardness variation in batch 3 110
Table 18 A table to show the buoyancy force data for blend 3 113
Table 19 CO_2 release data for the five blend 3 tablets 117
Table 20 A table to show the mercury porosimetry results for tablets made from blend 3 118
Table 21 Results from BET surface area analysis on blend 3 119
Table 22 Cross-sectional area data for blend 3 121
Table 23 A table to show the weight variation in batch 4 127
Table 24 A table to show the hardness variation in batch 4 128
Table 25 A table to show the buoyancy force data for blend 4 131
Table 26 CO_2 release data for five blend 4 tablets 132
Table 27 A table to show the mercury porosimetry results for tablets made from blend 4 135
Table 28 Results from BET surface area analysis on blend 4 136
Table 29 Cross-sectional area data for blend 4 138

Table 30 Comparison of blend constituents 143
Table 31 Average pressure generated per hour for test blends 149
Table 32 Peak swelling size comparison for test blends 151
Table 33 Qualitative composition of aerogel capsules 153
Table 34 A table to show the buoyancy force data for aerogel capsules 157
Table 35 CO_2 release data for five aerogel capsules 161
Table 36 Cross-sectional area data for the aerogel capsules 163
Table 37 Comparative dissolution results for Omeprazole formulations 171
Table 38 Comparative *in vivo* Cmax values of omeprazole formulations 172

CHAPTER 1

GENERAL INTRODUCTION

1.1 Gastrointestinal transit and drug absorption

It is generally recognised that the main absorption site of drugs in humans is the small intestine, due to its high relative surface area and associated uptake sites (Davis et al, 1986a). It has also been shown that the colon acts as an absorption site for some drugs such as theophylline (Yuen et al, 1993). Other drugs, such as ciprofloxacin, diazepam, frusemide and various ACE inhibitors, have been shown to have a small preferential site of absorption located in the upper small intestine, known as an "absorption window" (Harder et al, 1990; Chan et al 1994; Grass and Morehead, 1989). However, the extent of drug absorption in a segment of the GI tract depends on the rate of absorption, as well as the time available for the absorption to occur (Rouge et al, 1996).

When drugs with absorption windows are formulated in normal controlled release dosage forms, some of the drug will be released after the main absorption site has been passed, resulting in incomplete delivery. The delivery site has to therefore be controlled, in order to improve the absorption of certain drugs. It follows that the gastric residence time of a dosage form will markedly influence both the rate of absorption and the total absorption of many drugs.

As previously mentioned, for some drugs it may be preferential to target the colon for delivery. This would be the case if local action was required or for compounds such as peptides that would otherwise be metabolised in the small intestine. Indeed, delivery systems have been investigated that would allow colon specific targeting (Gliko-Kabir et al 2000a and b).

1.2 Gastric emptying

The stomach is anatomically divided into three parts: fundus, body and antrum (or pylorus). The proximal stomach, made up of the fundus and body regions, serves as a reservoir for ingested materials while the distal region (antrum) is the major site of mixing motions, acting as a pump to accomplish gastric emptying.

1.2.1 Postprandial emptying

The stomach has the ability to empty different meal constituents at different rates, even when they are ingested simultaneously (Christensen et al, 1985). Resistance to the flow of liquids across the pylorus is relatively small therefore they empty from the stomach rapidly. Resistance to digestible solids, however, is much greater, resulting in the need for solids to be broken down before they can be emptied from the stomach (Weiner et al, 1981). Any particles that are too large to pass through the pylorus are returned back into the distal stomach for further digestion as many times as is necessary. Indigestible solids larger than approximately 2mm are thought to be retained to some degree during the postprandial period (Kelly, 1981).

1.2.2 Interdigestive emptying

After the stomach has finished emptying the contents of a meal, all that remains is mucus, cellular debris and any indigestible solids over approximately 2mm in diameter. A special mechanism called the interdigestive myoelectric complex (IMMC or housekeeper wave) exists to flush out the contents of the fasted stomach (Code and Marlett, 1975). The complex occurs in four phases of differing activity. It is the 2^{nd} and 3^{rd} phases that are the most powerful, with contractions in phase 3 being powerful enough to sweep the fasting stomach contents out into the duodenum. In the fasted state the complex is thought to occur at roughly 2 hourly intervals, but the actual duration and onset of each cycle varies both inter and intra subject.

1.2.3 Factors affecting gastric emptying rate

Fatty acids are known to reduce the rate of gastric emptying. This is regulated by duodenojejunal receptors that are sensitive to fatty acids. The important factor in determining the degree of slowing is the chain length of the fatty acid. The 14-carbon chain myristic acid is known to have to the greatest effect (Hunt and Knox, 1968).

The number of calories delivered to the duodenum tends be at a constant rate of approximately 2 kcal/min (Brener et al, 1983). Therefore the greater the concentration of energy (kcal/ml) in the stomach contents, the less volume is transferred per minute to the

duodenum. There are possibly duodenal receptors that are sensitive to the fatty acid anions produced during triglyceride digestion (Hunt, 1980).

Any increase in the acidity of the stomach contents also causes a decrease in stomach emptying rate. This is again due to duodenal receptors, which appear to maintain the pH of the duodenum at 6.5 (Hunt and Knox, 1972).

Some drugs are capable of having an effect on the rate of gastric emptying. Anticholinergics, antihistamines, tricyclic antidepressants, phenothiazines and propantheline have all been known to delay gastric emptying, which can be attributed to their antimuscarinic effects. Metoclopramide, cholinergics and nicotine have all been shown to increase emptying rate.

1.3 Gastric emptying of dosage forms

The gastric emptying of dosage forms were measured in early studies by employing X-ray examinations to follow the GI transit of radiopaque formulations (Wagner et al, 1958). This method suffers from the modification of the dosage form's characteristics which inevitably result from the incorporation of barium sulphate.

More recently the advent of gamma scintigraphy has enabled workers to compile useful information concerning the gastric emptying of various drug delivery systems (Bechgaard et al, 1985; Wilson and Hardy, 1985; Davis et al, 1986b; Sangekar et al, 1987).

The emptying of controlled release dosage forms from the stomach will depend upon the presence or absence of food and the size of the ingested system. Food influences the gastric retention time of dosage forms in that it delays the onset of the IMMC, thus any indigestible matter bigger than the cut-off size of the pylorus, e.g. a large dosage form, will be retained throughout the postprandial period. If a large dosage form is given to a patient who is in the fasting state then the gastric retention time is dependent upon the onset of the next IMMC, which could theoretically be anything from 1 minute to 2 hours later as discussed earlier. Kaus et al proved the importance of food, when they administered perspex capsules to fasted patients (1984a). The time the capsules took to empty from the stomach was erratic, due to the variation in onset of the IMMC, therefore the size and the shape of a dosage form makes no difference to the gastric residence time if the stomach is in the fasted state. It has also been shown that the presence of food in the stomach slows the emptying rate of multiparticulate systems (O'Reilly et al, 1987).

It has been shown that the composition of the meal is also important in relation to the absorption of theophylline from a controlled release single unit dosage form (Karim et al, 1985), which is probably indicative of an altered gastric residence time. Davis et al found that an osmotic device, of 7 mm diameter, was retained in the stomach for over 10 hours after ingestion of a high calorie breakfast, whilst the same dosage form was retained for a much shorter duration after a low calorie breakfast (1984).

The size of a dosage form will have an effect on gastric residence time when food has been consumed. There is always the possibility that the formulation will empty due to chance, along with any digested food, if it has a diameter smaller than the pyloric cut-off size. This cut-off size was thought to be 2mm, which had been extrapolated from dog studies (Khosla and Davis, 1990). However, more recent studies have shown that the critical size could be as high as 12mm, although it is more likely a graduated scale (Timmermans and Moes, 1993). Attention must be paid if designing such a dosage form because there is a risk of causing gastric obstruction if a nondisintegrating formulation, bigger than the resting pyloric diameter, is swallowed (Khosla and Davis, 1990). However, studies so far have only taken the initial size of the formulation into consideration when discussing the effect of size on gastric retention. It may be more relevant to measure the robustness of a formulation, as it is possible that a large 'fluffy' tablet may be able to pass through the pylorus if it has a relatively small robust centre. This may be the case in formulations that consist mainly of hydrogels such as hydroxypropylmethylcellulose (HPMC).

1.4 Controlling the gastrointestinal transit of dosage forms

Numerous approaches have been developed recently in an attempt to control the transport of dosage forms through the GI tract, with special attention being given to prolonging the residence time in the stomach. Retention of a drug delivery system in the stomach is one way of improving and controlling the absorption of drugs with an absorption window in the upper small intestine, by releasing the drug at a controlled rate over the main absorption site for a prolonged period. Topical drug delivery to the gastric mucosa, for example, antibiotic administration for *Helicobacter pylori* eradication in the treatment of peptic ulcer disease, would also be facilitated (Yang et al, 1999).

The methods used thus far to delay gastric emptying can be divided into three sub-sections; physical, physiological and pharmacological.

1.4.1 Physical methods of delaying gastric emptying

Physical methods that formulators have tried to utilise include floating systems, bioadhesive systems, rapidly swelling systems, high-density pellets and a shape system.

1.4.1.1 Floating systems

Floating systems have attracted attention from scientists interested in increasing the gastric retention time of controlled release devices, and indeed there has been some success achieved in this field since the earliest description in 1975 (Sheth and Tossounian). Various formulations have been considered including, capsules (Timmermans et al, 1989; Cook et al, 1990; Oth et al, 1992; Timmermans and Moes, 1994; Menon et al, 1994; Mazer et al, 1998), tablets (Ingani et al, 1987; Hilton and Deasy, 1992; Desai and Bolton, 1993; Yang and Fassihi, 1996), and multiparticulate or granular systems (Ichikawa et al, 1991; Thanoo et al, 1993; Yuasa et al, 1996; Iannuccelli et al, 1998a and b; Whitehead et al, 1999). The systems can be classified, in terms of behaviour, into either monolithic (tablets and capsules) or multiparticulate dosage forms, both of which aim to remain buoyant on the gastric contents, which have a density of approximately 1.004g/cm^3 (Lentner, 1981), without affecting the intrinsic rate of gastric emptying. It follows that in order for the floating dosage form to be effective, it must be taken when there is a medium to float upon in the stomach. Many studies have indeed demonstrated the failure of floating dosage forms to remain in the stomach under fasting conditions. For instance, Sugito et al (1990) showed that tablets with a density of 0.86 remained in the stomach for longer than tablets with a density of 1.33, when taken after a light breakfast. However, when the same dosage forms were taken under fasted conditions no difference between gastric residence times was detected. A small problem with this study was the different size of the dosage forms used, as the diameter of the tablets could have had an effect on the gastric emptying. The reason for the failures is the so-called housekeeper wave of the IMMC that was mentioned previously. Such a limitation must therefore be taken into account when considering the use of floating dosage forms. However, providing that the formulation is capable of remaining buoyant and a gastric medium is available, then the digestive state of the subject

becomes the rate-limiting step. The floating dosage form is in effect, due to its distance from the pylorus, protected from a random, early and erratic emptying during the digestive phase, even if the size of the dosage form is smaller than diameter of the pyloric opening (Timmermans et al, 1989).

A number of investigations, however, have come to the conclusion that the density of a dosage form does not significantly influence its gastric residence time (Davis et al, 1986d; Kaus, 1987). Davis and co-workers (1986d) did not detect any gastric residence time differences relating to density when comparing either floating capsules or tablets with non-floating tablets, in a study using gamma scintigraphy. They found that food was the major factor controlling the gastric emptying of both dosage forms. However it has been confirmed since, in an *in vitro* experiment (Timmermans and Moes, 1990c), that the floating forms used in the experiment produced quite unsteady and inappropriate floating characteristics and often sank after a few hours. It could be possible that the units float *in vivo*, but even still the study is significantly flawed due to the size difference (6.9mm for the floating capsule to 10.0mm for the non-floating tablet) in the dosage forms chosen for the study. We can therefore draw no conclusions about buoyancy / density, from the study.

Kaus agreed with the conclusion made by Davis in a published letter (1987), the focus of the letter was based on a previous article that showed no difference in the gastric residence times of two indigestible Perspex units (Kaus et al, 1984a), with gravities of 1.03 and 1.61mg/mm^3. As the capsules are made of Perspex, it therefore follows that their densities cannot change with time, and as neither of the capsules have a density significantly less than that of the gastric fluids, we cannot expect either of them to float with any degree of certainty. However, the study was actually carried out in the fasting state, which as discussed earlier, is not an appropriate time to administer floating dosage forms due to the IMMC.

The size of the dosage forms can be a critical factor when comparing the gastric residence times of formulations. It has been proven that as the dosage form becomes bigger (4.8-7.5-9.9mm), the gastric residence time for both floating and non-floating formulations becomes longer (Timmermans et al, 1989). It has also been shown, in the same publication, that the difference in gastric retention time, between floating and non-floating devices, is more pronounced at the smaller and medium sizes. The data from this experiment was taken after the patients had consumed a small breakfast prior to administering the dosage form, with no more food being taken until the end of the trial. It proves the theory that the floating of the dosage form avoids the random emptying seen

with the non-floating formulations out of the pylorus along with portions of digested matter. It is consequently emptied at the end of the digestive cycle by the housekeeper wave. The reason that size retards emptying is that a bigger object is less likely to be emptied randomly through the pyloric sphincter. The gastric residence time for large floating capsules (9.9mm) was not statistically different from identically sized non-floating capsules. This is because once a certain size is reached, the dosage form will not be emptied until the IMMC, thus nullifying any advantage induced by floating.

Multiparticulate systems were initially developed in order to overcome the 'all or nothing' gastric emptying seen with some monolithic dosage forms (i.e. if the tablet/capsule gets ejected from the stomach randomly, no more drug is absorbed, therefore the patient is under-dosed). They also provide less chance of damage to the gastric mucosa which can be associated with some drugs. Floating multiparticulate systems do show an increased gastric residence time when compared to non-floating equivalents (Whitehead et al, 1999). This correlates with the thoughts of Timmermans et al (1989).

1.4.1.2 Bioadhesive systems

As an alternative approach to increasing the gastric residence time of dosage forms, mucoadhesive substances that adhere to the gastric mucosa have been proposed. The potential of bioadhesive polymers has been widely discussed in the literature (Park and Robinson, 1984; Ch'ng et al, 1985; Longer et al, 1985; Duchene et al, 1988; Harris et al, 1989; Li et al, 1993), however a lot of the work has focused on the development of suitable *in vitro* techniques and theoretical assessments of the structural requirements needed for bioadhesion. Many successful materials have indeed been found during *in vitro* tests, resulting in some detailed structural hypothesis of chemical groups that aid mucoadhesion (Tobyn et al, 1996). Some materials that show promise include sodium carboxymethylcellulose, sodium alginate and polyacrylic acid. One of the problems associated with the use of bioadhesive systems for stomach retention devices is that they rely on attachment to mucin on the gastric mucosa. The turnover of mucin in the human stomach is, however, quite rapid, which would make it very difficult to adhere a controlled release gastric mucoadhesive formulation to the stomach wall for any significant period of time (Gupta et al, 1990). We should also consider that, due to the intimate contact required, some drugs have the potential to exhibit an adverse effect on the mucosa itself. The future for gastric mucoadhesive formulations may lie in the co-formulation of

bioadhesive and floating properties into a system (Matharu and Sanghavi, 1992, Rosa Jimenez-Castellanos et al, 1994, Chueh et al, 1995) but much work still remains to be done.

1.4.1.3 Other systems

Other physical methods used to increase the gastric residence time include the use of high density pellet systems which may reside in the lower part of the antrum (Bechgaard and Ladefoged, 1978) and the use of rapidly swelling systems that are retained due to their size, before degrading (Agyilirah et al, 1991; Deshpande et al, 1997). The use of different shaped units has also been investigated in dog studies (Cargill et al, 1988). However, the use of large irregular shaped units in human volunteers may prove to be dangerous, due to the risk of permanent pyloric obstruction. Ion exchange resins have also been attempted (Thairs et al 1998) but the turnover of the gastric mucosa may limit the maximum gastric residence time.

1.4.2 Physiological methods of delaying gastric emptying

The delaying of gastric emptying using a physiological mechanism requires the incorporation of a material into the dosage form that is known to stimulate the duodenal receptors responsible for the regulation of gastric emptying. This has been attempted in an *in vivo* study (Groning and Heun, 1984), which incorporated myristic acid, as the triethanolamine salt for increased solubility, into the dosage form. The study highlighted a major problem with this technique, as the responses seen in the experiment varied greatly from individual to individual, depending on the effect of the myristic acid on each individual's receptors. This would therefore lead to variable results on potential patients, which would not be acceptable to clinicians.

1.4.3 Pharmacological methods of delaying gastric emptying

This method involves adding a stomach motility reducing agent, such as propantheline, into the dosage form (Watanabe et al, 1976). This may prolong the gastric residence time as a result of reducing gastric motility. However, this is not really a viable option for use in many patients, due to the intrinsic interference with the natural workings

of the stomach, which would affect absorption and digestion of foodstuffs, as well as introducing the possibility of systemic side effects.

1.5 Aims and objectives

Floating systems appear to be the most promising of all the methods utilised so far to increase the gastric retention time of dosage forms. The dosage form of choice appears to be a gas powered device which has the ability to remain buoyant on the stomach contents for the duration of drug release. A powered device would offer extra insurance against sinking *in vivo*, which would minimise the incidence of random emptying that has been seen with some of the previous inactive floating formulations (Davis et al, 1986d; Kaus et al, 1984a). There is therefore a need for a rationalised approach to gas powered, floating dosage form design, which can be achieved using novel, *in vitro* experimental design. This would enable us to evolve a proper mechanistic understanding of the behaviour of gas powered, floating dosage forms, which have been designed to remain in the stomach for long, reproducible, periods of time.

Such dosage forms do not have current pharmacopoeial testing methods associated with them, hence it is important that methods are designed which accurately assess the pertinent properties of gas powered floating dosage forms.

Floating dosage forms, in particular, have been shown to have a low degree of *in vitro – in vivo* correlation. The aim of this study was therefore to design and utilise several *in vitro* techniques capable of assessing, and optimising, the important characteristics of gas-powered floating dosage forms, which in turn would lead to *in vivo* success.

It was considered particularly important to develop apparatus capable of quantifying dosage form buoyancy, gas release rate and the degree of polymer swelling within a formulation. These parameters will be discussed in parallel to assess the effect that each has on the floating properties of a formulation.

CHAPTER 2

MATERIALS AND METHODS

2.1 Introduction

This chapter will discuss the routine methods used to evaluate the physical characteristics of the pharmaceutical solids used in this study. Further chapters will then be used to describe, in detail, the novel *in vitro* methods that apply specifically to floating dosage form characterisation. All materials used during the course of the study are listed in Table 1, Section 2.2., Page 13.

Physical characterisation of pharmaceutical solids can be conducted at three primary levels; the molecular level (properties associated with individual molecules), the particulate level (properties pertaining to individual solid particles) and the bulk level (properties associated with an assembly of particles) (Brittain et al, 1991). This chapter is concerned essentially with the bulk physical properties of dosage forms.

Bulk physical properties can be defined in terms of material structure, porosity, pore size distribution and surface area. Tablet properties, such as hardness and weight variation, are well-recognised parameters used within the pharmaceutical industry. Specific surface areas can be measured using gas adsorption techniques, which depend on the ability to predict the number of adsorbate molecules required to exactly cover the surface of a material with a single layer of inert gas (Brittain et al, 1991). Accuracy of the technique is highly dependent on material properties and experimental parameters.

Quantitative estimates of pore volume, pore diameter and pore area can be obtained using the technique of mercury porosimetry. This is based on capillary rise phenomena whereby a pressure is required to make a non-wetting liquid move up narrow capillaries (Ganderton and Selkirk, 1969). Quantitative data is obtained by relating pressure applied, and volume of mercury intruded, to pore size distribution, pore volume and pore surface area. Mercury porosimetry has gained popularity as a research tool due to the simplicity of the technique and the wide range of data that can be generated (Dees and Polderman, 1981). Due to its ease of use, mercury porosimetry is often used as a black box, which produces pore size distributions (Van Brakel et al, 1981). However, basic limitations of the technique exist and problems may arise if it is applied to materials for which it has not been properly tested. To ensure the data obtained is truly representative of the porous material; potential sources of error need to be thoroughly evaluated and care must be taken with interpretation of results.

In this study, floating dosage forms were analysed using mercury porosimetry and gas adsorption techniques. The objective was to determine the suitability of these methods, alone and in combination, for characterising specific surface area, bulk density, porosity, pore area and pore size distribution of floating dosage forms.

To achieve this it was necessary to; (1) ensure that the techniques gave information which was truly representative of the porous body; (2) assess whether the measurements obtained would be potentially useful for physical properties / *in vitro* behaviour correlation studies.

2.2 Materials

Table 1. Materials that have been used during the course of the study

Material	Manufacturer	Batch Number
Ciprofloxacin	Ranbaxy	-
Sodium Bicarbonate	BDH	K25190714839
Xanthan Gum	Monsanto	64165V
Sodium Alginate	Monsanto	59346A
X-linked PVP	BASF	379138
Magnesium Stearate	BDH	30120362
Talc	Degussa	0891
Carvedilol	Cadila Healthcare	9CD003
Dried Glucose syrup	Roquette	655310
Xantural 75	Monsanto	830370K
Calcium Carbonate (precipitated) Heavy	BDH	K26038699905
Ammonium Bicarbonate	BDH	K25366774844
Lubritab	Mendell	666812603X
Emcocel 90M	Mendell	E9B8A01X
Mercury	Belgrave Mercury Ltd	-
Tween 20	Aldrich	-
Silicone oil	Aldrich	-
Sodium Chloride	Aldrich	4041440408011
Hydrochloric Acid	Fischer	K24810951805

2.3 Methods

2.3.1 Mercury porosimetry

Pore size determinations were made using a Micromeritics Autopore II porosimeter (Type 9220, Micromeritics Instruments Co., Georgia, USA) capable of operating in the range of 3.4 to 414,000kNm^{-2}. The porosimeter was equipped with a low-pressure chamber operating from atmospheric pressure (172kNm^{-2}) down to 3.4kNm^{-2} and a high-pressure chamber operating from 172 up to 414,000kNm^{-2}. The pressure at which mercury could be introduced into the penetrometer (fill pressure) could be controlled between 3.4 and 69kNm^{-2}. Assuming the contact angle of the mercury to be 130° and the surface tension of mercury to be 485.0gcm/s^2 respectively, pores having median diameters in the range 360 to 0.003μm could be analysed. A hydraulic pump generated pressure and the movement of mercury in the penetrometer stem was followed using a conductance detector.

Tablets were tested one at a time in a solid penetrometer that had a stem volume of 1.131ml. One tablet was used in each test and the test was run in duplicate to assess reproducibility. Samples were evacuated down to a pressure of 50μmHg to remove adsorbed gases and moisture. The penetrometer, fill pressure and sample size were carefully selected to ensure that between 10 and 90% of the stem volume was used in each run. Measurements were carried out at a consistent room temperature of 21°C using an equilibration time of 5s. The surface tension, contact angle and density of mercury at 21°C were taken to be 485.0gcm/s^2, 130° and 13.5g/ml respectively. Between 30 to 50 points in the required range were taken.

2.3.2 Surface area analysis by nitrogen adsorption

Nitrogen adsorption onto the surface of tablets was measured using a surface area analyser (ASAP 2010, Micromeretics Instruments Co., Georgia, USA). Ideally the surface area being measured should be in the region of 20m^2. However, since the surface area of the tablets was expected to be low (in common with many pharmaceutical products), it was decided that three tablets should be used for each analysis in order to increase the available

surface area for measurement. To accommodate three tablets, a glass sample tube with a volume of approximately $30cm^3$ was used. Outgassing the samples was necessary before testing to remove physio-adsorbed gases and vapours, which can alter surface potential and block or fill pores. Vacuum pumping down to a pressure of 8mmHg outgased the samples. The samples were outgased directly on the analysis port; thus negating the need for port transfer after outgassing so that no atmospheric gas was able to enter the tube. After outgassing, the sample was cooled to the boiling point of nitrogen (77K) by immersing the sample holder into a dewar filled with liquid nitrogen. The sample was exposed to increasing partial pressures of nitrogen and the volume of gas adsorbed was measured at each partial pressure.

2.3.3 Measurement of Bulk density

Bulk density was calculated from mercury porosimetry results.

2.3.4 Measurement of Tablet Strength

The crushing strength of tablets were determined using a Schleuniger 2E tensile tester (Dr. K. Schleuniger & Co., Switzerland). Ten tablets were tested in order to assess reproducibility. Tablets were crushed along the longest face. Measuring tablet strength is an established technique to ensure that a batch of tablets has been manufactured within recommended limits.

2.3.5 Measurement of Tablet Weight

The weight of tablets was measured using an A and D HM120 balance (Oxford, UK). Ten tablets from each batch were assessed in order to determine the reproducibility of the tableting process.

CHAPTER 3

BUOYANCY APPARATUS DESIGN AND DEVELOPMENT

3.1 Introduction

The rational design of *in vitro* experiments is essential for the thorough understanding of any dosage form. Indeed, a large number of physical and / or chemical properties exhibited by pharmaceutical products can be measured. It is perhaps even more important when we are considering the various intrinsic factors that influence the ability of a formulation to float. Floating dosage forms do not have current pharmacopoeial testing methods associated with them, hence it is important that methods are designed which can assess the integral properties of such dosage forms.

The most important factor to consider when designing floating dosage forms is obviously the ability of a formulation to float upon the gastric fluids.

3.2 Background

Until recently, the main parameters that had been used to describe the adequacy of dosage form buoyancy were bulk density and, in some experiments, the duration of floating. It is, however, not enough to say whether a dosage form floats or not, as it is much more preferable to quantitate the force with which the formulation is floating. It is also vital to assess the buoyancy profile of the dosage form over a functional time period, rather than taking a singular pre-testing density measurement. A common misjudgement is that delivery systems travel in an uncontrollable way through the length of the gastrointestinal tract. This has in turn led to a lack of correlation between *in vitro / in vivo* results. For instance, Davis has shown the absence of correlation between the cumulative data of *in vitro* release and *in vivo* absorption for a drug given to fasted patients in the form of a monolithic osmotic tablet (1986c). Many other investigations in humans have also led to conflicting conclusions when using floating dosage systems. Studies have shown systems thought to float *in vitro* that did not provide a significantly prolonged gastric retention time when compared with non-floating systems *in vivo* (Bechgaard and Ladefoged, 1978; Davis et al, 1986d; Kaus, 1987; Sangekar et al, 1987).

According to the known properties of fluids (Cromer, 1981), it is possible to note that although density may express whether an object will float, it does not represent the

magnitude of the floating forces produced by the object. In addition to this, a single density determination that is made prior to immersion does not enable one to foresee the floating force evolution of a dosage form, as the dry material of which it is made progressively reacts or interacts with the medium surrounding it.

These problems have recently been overcome with the invention of a piece of equipment that is capable of measuring the buoyancy force of a dosage form over a period of time (Timmermans and Moes, 1990a and b). A schematic of the apparatus is shown below in Figure 1 (page 19). The equipment consists of an electronic toploader balance <1> and a force transmitter device <6,7,8> (FTD) that extends vertically down from the measuring module of the balance into the opening of a test container <12>. Rigid connection between the upper end of the FTD and the junction point of the electromagnetic measuring module is ensured in such a way that all vertical upward or downward displacements of the FTD are perceived by the measuring module and displayed by the balance. The lower end of the FTD holds a test sample totally submerged in the test solvent at a constant immersion depth. The test solvent is maintained at a constant temperature, in an environment free from vibrations, by a water bath <13>. A draft protection assembly covers the pan of the balance <2>. The data is collected and plotted by a paper chart recorder <29>. A liquid compensating system is in place as an attempt to counteract the effects of evaporation from the test container <17-24>.

This apparatus makes it possible to determine the force with which a dosage form floats over a period of time. It then becomes possible to optimise the floating capabilities of a formulation before commencing *in vivo* testing. The apparatus has been used to assess some of the previous work carried out on floating dosage forms (Timmermans and Moes, 1990c).

Using apparatus of this kind would make it possible to determine the robustness of a particular floating dosage form, and also to gain an indication of what to expect when looking for correlation between *in vivo* and *in vitro* results. The kinetics of dissolution, floating, swelling or disintegration can be determined from use of such an apparatus. The measuring process also operates in a non-destructive manner, allowing the real behaviour of the dosage form to be examined. The profiles produced may in turn be analysed to establish the important characteristics and properties of tested materials.

Figure 1 Schematic of a previous buoyancy apparatus (Timmermans and Moes, 1990c)

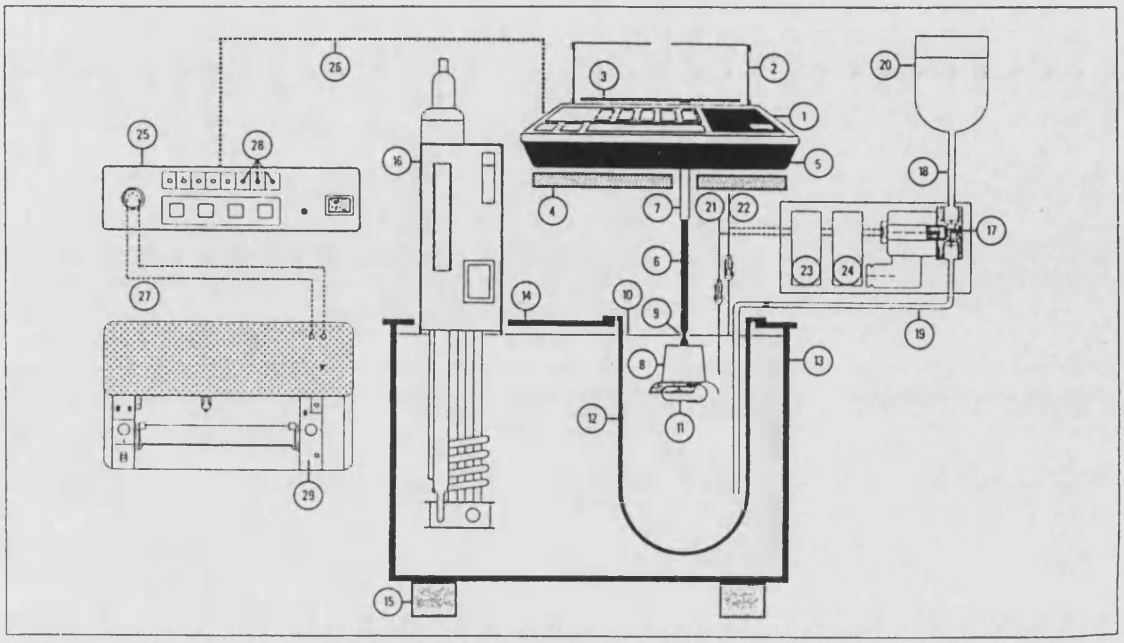

Fig. 1 Schematic view of the resultant-weight measuring apparatus in full assembly.
① to ⑪: measuring system
⑫ to ⑯: test bath arrangement
⑰ to ㉔: liquid level compensating system
㉕ to ㉙: recording means

3.3 Original Apparatus Design

The equipment described above was used as a starting point for the design of an apparatus that could be used, in the laboratory, for the detailed assessment of dosage form buoyancy over a predetermined period of time. See Figure 2, page 20, for a schematic of the new apparatus and Figure 3, page 21, for a digital photograph.

The new apparatus consisted of four main sections, which can be categorised as follows:

1. *Balance assembly.* An A&D HM120 balance (Oxford, UK) was mounted on a raised pedestal to enable it to sit directly above the test medium. The A&D HM120 balance was chosen because it has a connection point to the underneath of the balance enabling direct access for the FTD connection.

2. *Force transmitter device.* The force transmitter device is shown enlarged in Figure 4, page 22, it is also photographed in Figure 5, page 23. It consists of a PTFE / stainless steel shaft, which ends in a basket device for tablet capture. PTFE was chosen as the

material for the upper part of the device so as to prevent magnetisation of the electromagnetic measuring module on the balance. Stainless steel was used for the remainder of the shaft so as to limit interaction with the test medium being used, and also to provide rigidity to the device. A waist was built into the main shaft at the point where the device would be in contact with the surface of the test medium, in order to limit the effect of evaporation during the test period. The basket itself was made from a stainless steel mesh and was moulded into a half cylinder that would contain the floating dosage forms. A meshwork structure was chosen so as to limit the interaction that occurs between the sample and the holder. A meshwork holder also allows the medium access to the majority of the dosage form, thus helping to limit spurious readings.

3. *Test Medium.* The medium is contained in a modified dissolution vessel capable of holding quantities of up to 1 Litre. The medium was covered during heating in order to prevent evaporation.

4. *Circulating water bath.* A Grant Y6 (Royston, UK) water bath was used. The water is circulated and heated, so as to enable temperature maintenance and control.

Figure 2 A schematic of the initial buoyancy device

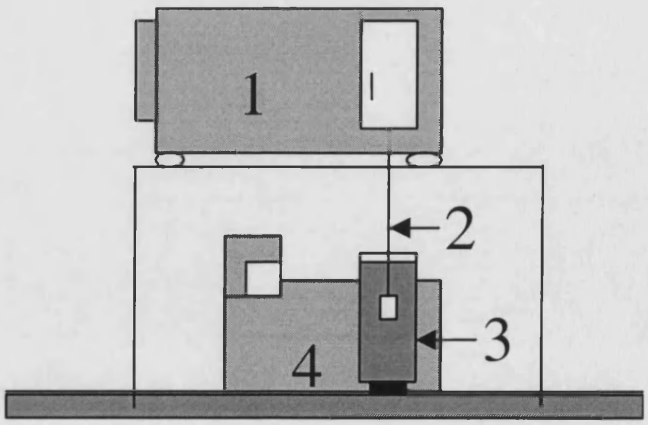

Figure 3 **A picture of the buoyancy apparatus**

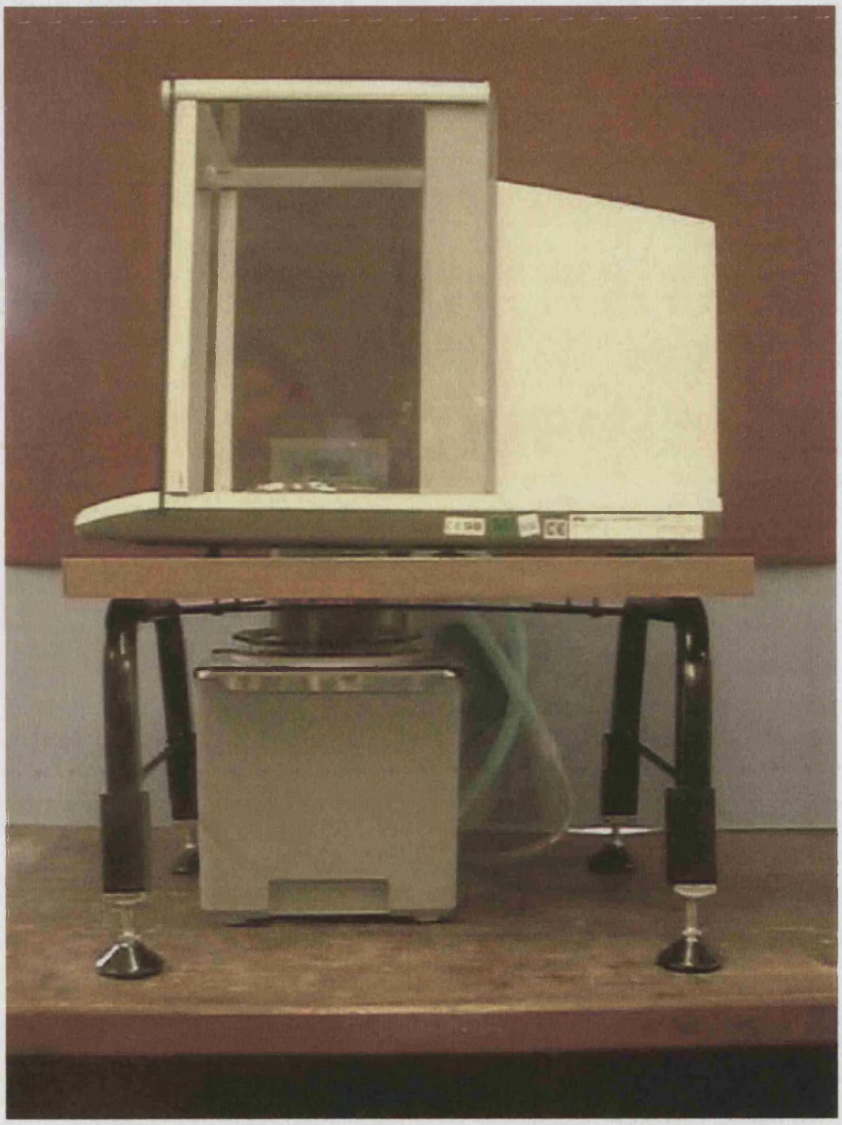

Figure 4 **Dimensions and structure of Force Transmitter Device (FTD)**

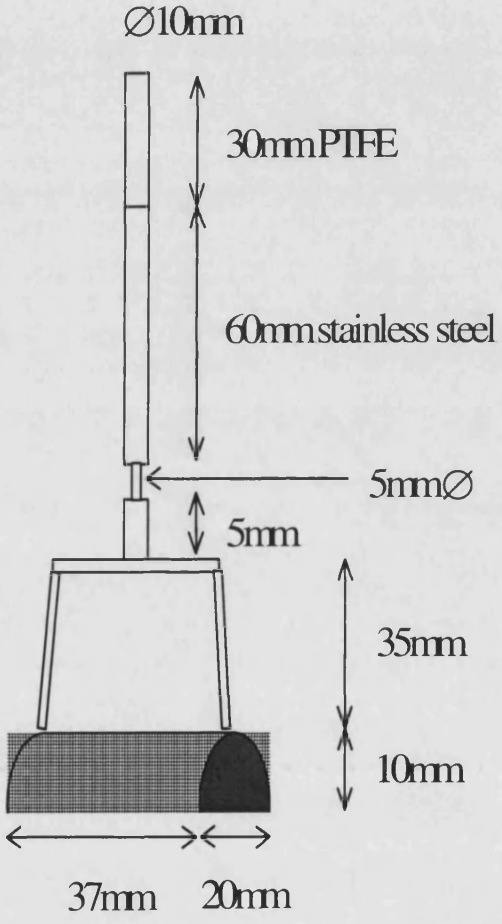

Figure 5 **A photograph of the FTD and water bath assembly**

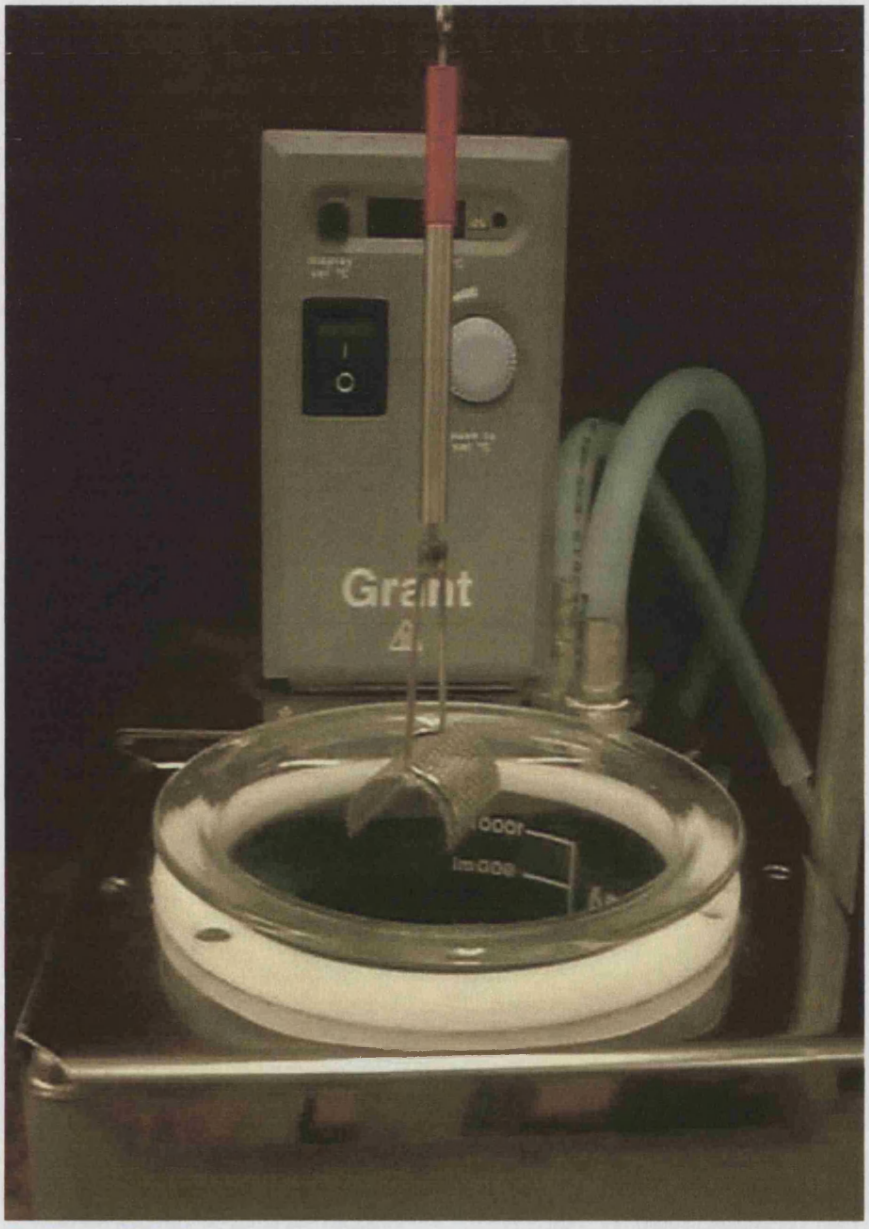

3.4 Initial Method

1000mls of Millipore water, measured in a volumetric flask, were placed into the modified dissolution vessel and heated to 37.0°C. The heating process took approximately 1.5 hours, and was conducted whilst the vessel was covered with a modified dissolution vessel top. The FTD was connected to the balance and the unit was lowered into the dissolution vessel so that the meniscus of the water was level with the mid-point on the waist of the FTD. The balance was then zeroed and readings from the balance were taken at intervals of 1 hour over a 4-hour period. The run was repeated 4 times to assess reproducibility.

3.5 Initial Modifications to Original Design

The results (see Figure 6, page 25) that were seen from the 4 runs were too erratic for the method to be considered reproducible enough to be used to compare floating tablets in future work. The graphs all showed an increase in resultant weight, which was due to the loss of water from the system. The variations in the results were thought to be mainly due to 2 factors:

1. The temperature in the laboratory varied noticeably from day to day. This would certainly have had an effect on the evaporation of the water from the dissolution vessel during the course of the experiment. In order to minimise the variation that was seen, it was decided to move the vessel to a laboratory where the temperature of the air could be controlled.
2. The waist that had been designed into the FTD, to minimise the effect of evaporation on the change in balance weight, was having a detrimental effect on reproducibility. This was due to the level of the water dropping more than had been expected over the course of the experiment. As the water level approached the bottom of the waist, it was thought that the surface tension of the water 'attracted' the FTD to the surface, and therefore a change in the gradient of the buoyancy graph was seen, adding to the unpredictability of the system.

Figure 6 **A graph to show the effect of water loss on resultant weight whilst using the original apparatus**

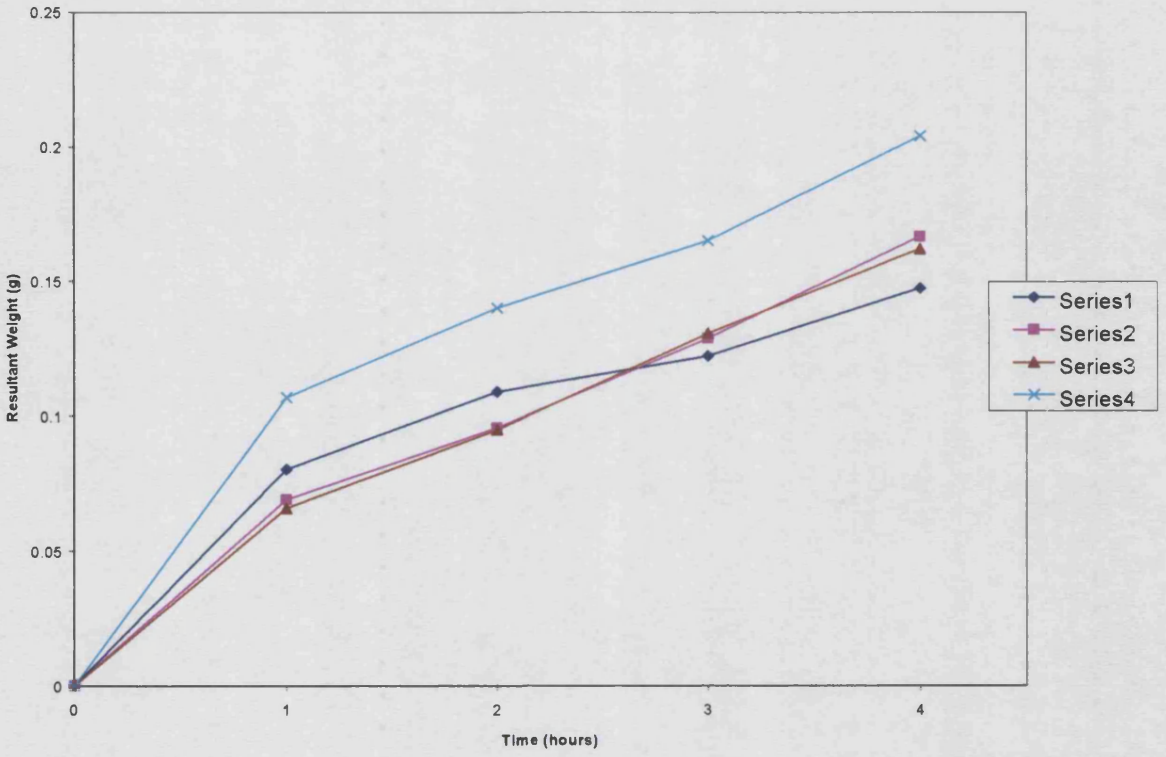

Another problem the experiments highlighted was that taking 4 or 5 data points over a 4-hour period was insufficient to accurately assess the buoyancy profile. For example, the exact time point at which the waist was affected by the surface tension of the water was impossible to deduce. This problem can be overcome by linking the vessel to a computer capable of constantly logging data points at a predetermined rate. The overall graph would then show exactly what was happening at any particular time point, enabling a better understanding of the mechanisms that are involved, rather than the ambiguous picture currently being portrayed.

Software called Collect (A&D, Oxford, UK) was installed onto a personal computer, which was in turn connected to the balance by an RS232 interface cable. The RS232 interface is used to convert the digital readings of the balance to an analogue output that the computer can recognise. The settings on the Collect program can then be adjusted to the users specification for any particular run, and the data readout can be collected from the balance at predetermined time points directly into a compatible spreadsheet package.

A further alteration to the design of the apparatus was the addition of a piece of mesh to the bottom of the FTD in order to render it capable of holding a tablet before immersion. This alteration was made before any further work was continued.

In order to minimise the effect that any dissolved gases may have had on buoyancy, it was decided that any fluid used in future experiments should be degassed with Helium for approximately 1 hour.

3.6 Secondary Method and Results

The improvements from the previous experiment were all put into place before the work continued. A second run using the revised apparatus was conducted according to the following revised methodology:

1000mls of Millipore water were measured out into a volumetric flask. Helium was then bubbled through the water for 1 hour, to remove dissolved gases. The degassed water was transferred to the modified dissolution vessel and heated to 37.0°C, which took approximately 1.5 hours. During heating the vessel was covered with a plastic top to keep evaporation to a minimum. The temperature of the water was checked using a mercury

thermometer before the experiment was started, to ensure the medium had been stabilised at 37°C.

The FTD was then connected to the balance and the unit was lowered into the dissolution vessel. The balance was zeroed and the reading from the balance was taken at intervals of 60 seconds, using the Collect software, over a period of 8 hours.

The experiments were conducted in a room where the temperature of the air was controlled at 20°C. The run was repeated five times in order to assess the reproducibility of the technique. The results can be found in Figure 7, on page 28.

The graphs that were produced showed two distinct phases. The first phase occurred during the first hour of the test, and was characterised by an apparent increase in the weight of the FTD. It is thought that this increase was due to the heating up of the probe, combined with water loss through evaporation. As the probe heats up it will undergo an amount of expansion, thereby changing the density of the probe. As part of the probe is situated in the medium during the test, any change in density will affect the force that is being measured by the balance. The second phase continued from the first hour, until the end of the 8-hour test period, during which the gradient remained almost constant. It is therefore thought that the second phase is purely the result of water loss through evaporation, resulting in less of the probe being submerged in the water.

The 5 runs were grouped more closely together than in the previous experiment, but were still not deemed suitable as a baseline for future experiments as the resultant weight gain on the probe was still too high. It was decided therefore to try and reduce the amount of evaporation of water from the vessel so that the overall change in weight could be reduced.

It was thought that there was a degree of unpredictability about the graphs being produced. It is possible that this was due to condensation of the evaporated water onto the FTD that would then slowly aggregate before dripping back into the test medium. Limiting the degree of evaporation from the medium would also help to solve this problem.

Again, there were seen to be sudden forces of attraction caused by the waist in the FTD being drawn towards the surface of the liquid in the vessel by the surface tension. In order to solve this problem the waist was filled in using a piece of PTFE with the same diameter as the rest of the shaft, thereby producing a shaft of even diameter throughout.

Figure 7 **A graph to show the effect of water loss on resultant weight whilst using the modified test method**

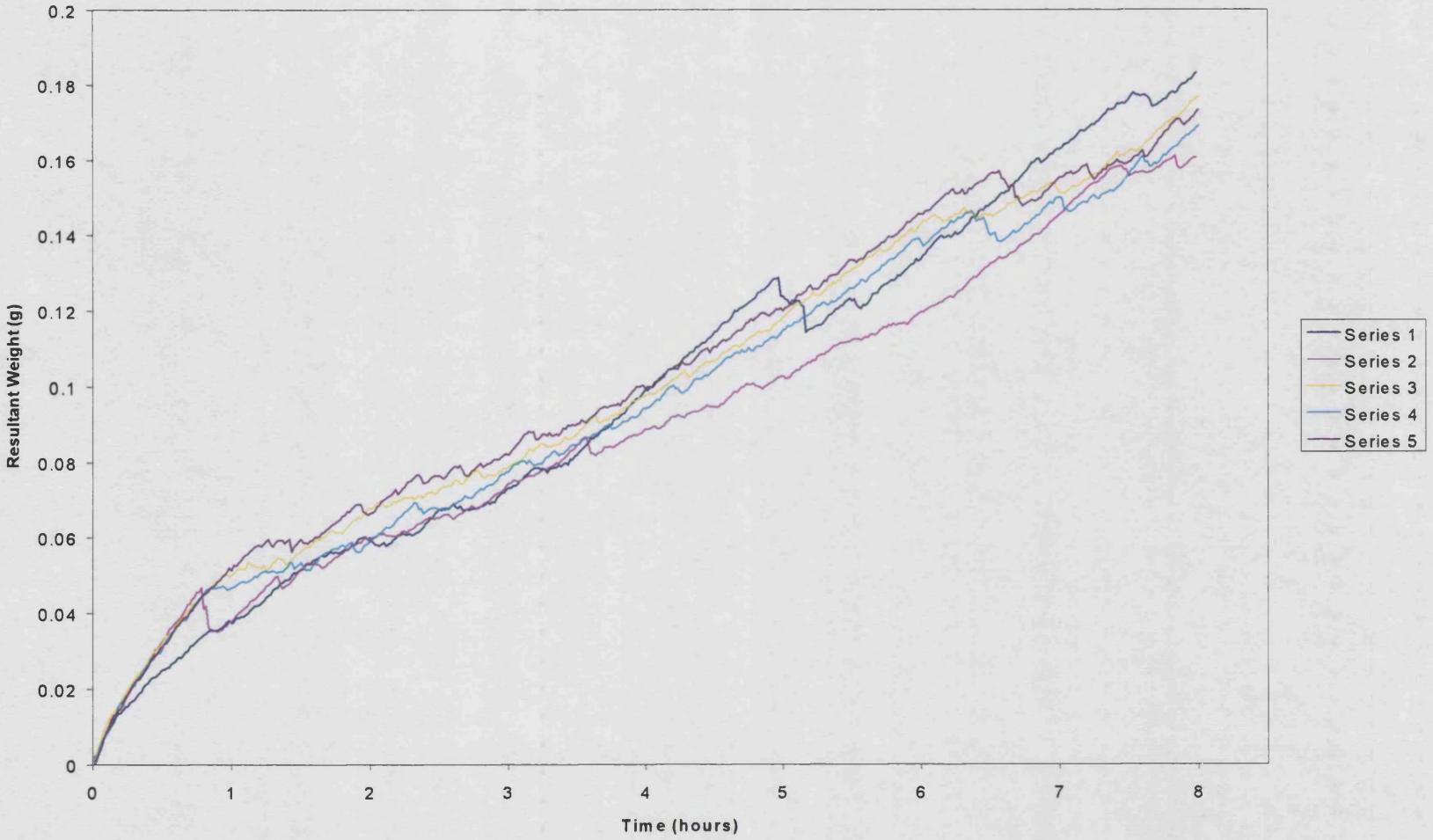

3.7 Further Modifications to Method

In order to reduce the evaporation of water from the vessel during testing it was decided to try to place a layer of oil on top of the water. The theory behind this was that the oil would then form a barrier on top of the vessel through which the water would not evaporate. Silicone oil was used as the test agent for this experiment as this was readily available in the laboratory.

A drop of the oil was placed onto the surface of the water. However, the oil simply formed a discreet blob on the surface of the water, which clearly would not be capable of limiting the water evaporation as desired. It was decided therefore to mix some of the silicon oil with a few drops of Tween 20 before addition to the water. This mixture was shaken thoroughly before placing one drop onto the surface of the water.

As expected, the Tween 20 helped the partitioning of the oil and the mixture quickly spread itself over the surface of the water. A test run was then performed, as before, in order to see if the addition of the oil would hinder evaporation of the water.

The results of this run can be seen in Figure 8, page 30. The weight gain on the FTD over the course of the experiment was approximately 2/3 of the previous weight gain seen before oil addition. A heating up phase of the FTD was also still being seen, so it was decided to modify the method by placing the FTD probe into the medium during the equilibration of the fluid to 37°C. This would ensure that the FTD would be at the same temperature as the medium at the start of the testing period.

Even though using the oil had reduced the evaporation of the water during testing, it was decided that there was potential for the oil to interfere with dosage forms during future testing. An alternative way of minimising evaporation was to use insulating spheres, such as those used to maintain the temperature of water baths, on top of the water. Such spheres would not interfere chemically with any future test formulations.

Figure 8 **A graph to show the effect of water loss on resultant weight when silicon oil and Tween 20 had been added to the surface of the medium**

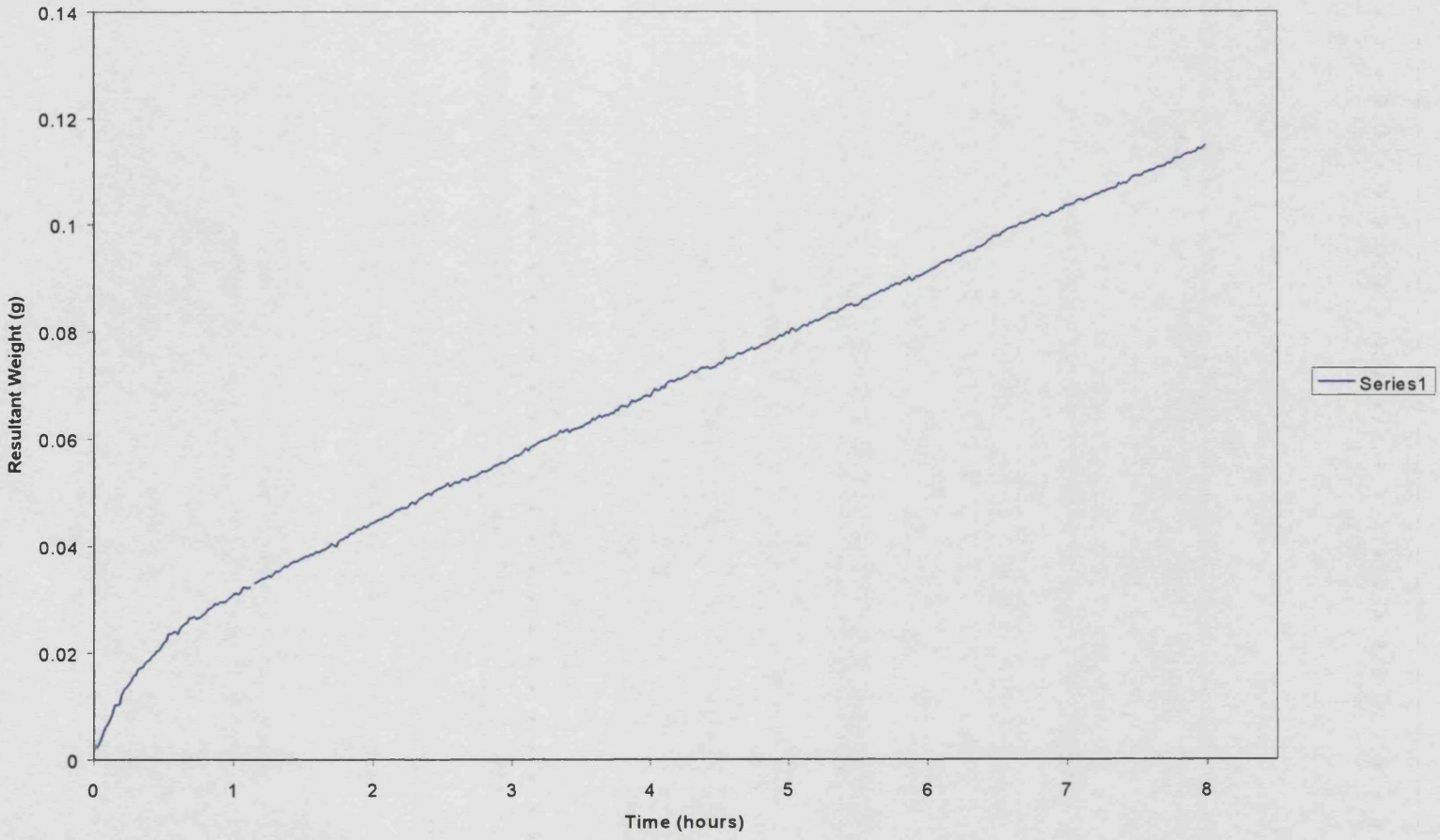

In order to accommodate the spheres into the system, it was first necessary to ensure that the spheres did not affect the FTD on its path into the vessel. A piece of hard plastic tubing was therefore cut to size to surround the FTD and prevent the spheres from knocking the FTD during testing. The tubing was attached to the top of the balance holder by a rubber seal so that it could easily be removed / reattached. The test was then performed as before, being repeated five times in order to assess reproducibility. The results are shown in Figure 9, page 32.

The overall water loss was reduced so that the effective weight gain on the FTD was approximately 0.05g over the 8-hour period. This was deemed to be satisfactory for the purposes of the buoyancy apparatus, as it was thought the degree of error would be minimal compared to the buoyancy / sinking effect which would be seen when a tablet was added. The weight gain for each tablet run is shown below in Table 2, page 31. The standard deviation of the weight gains for the individual runs was seen to be 0.00371, which was deemed to be satisfactory for this type of test.

Table 2 **Total weight gain on the FTD over an 8-hour period using Millipore water as a medium**

Run number	Weight gain (g)
1	0.0527
2	0.0522
3	0.0552
4	0.0453
5	0.0502
Mean	0.0511
Standard deviation	0.00371

Figure 9 **A graph to show the effect of water loss on resultant weight when water loss is limited by insulating spheres**

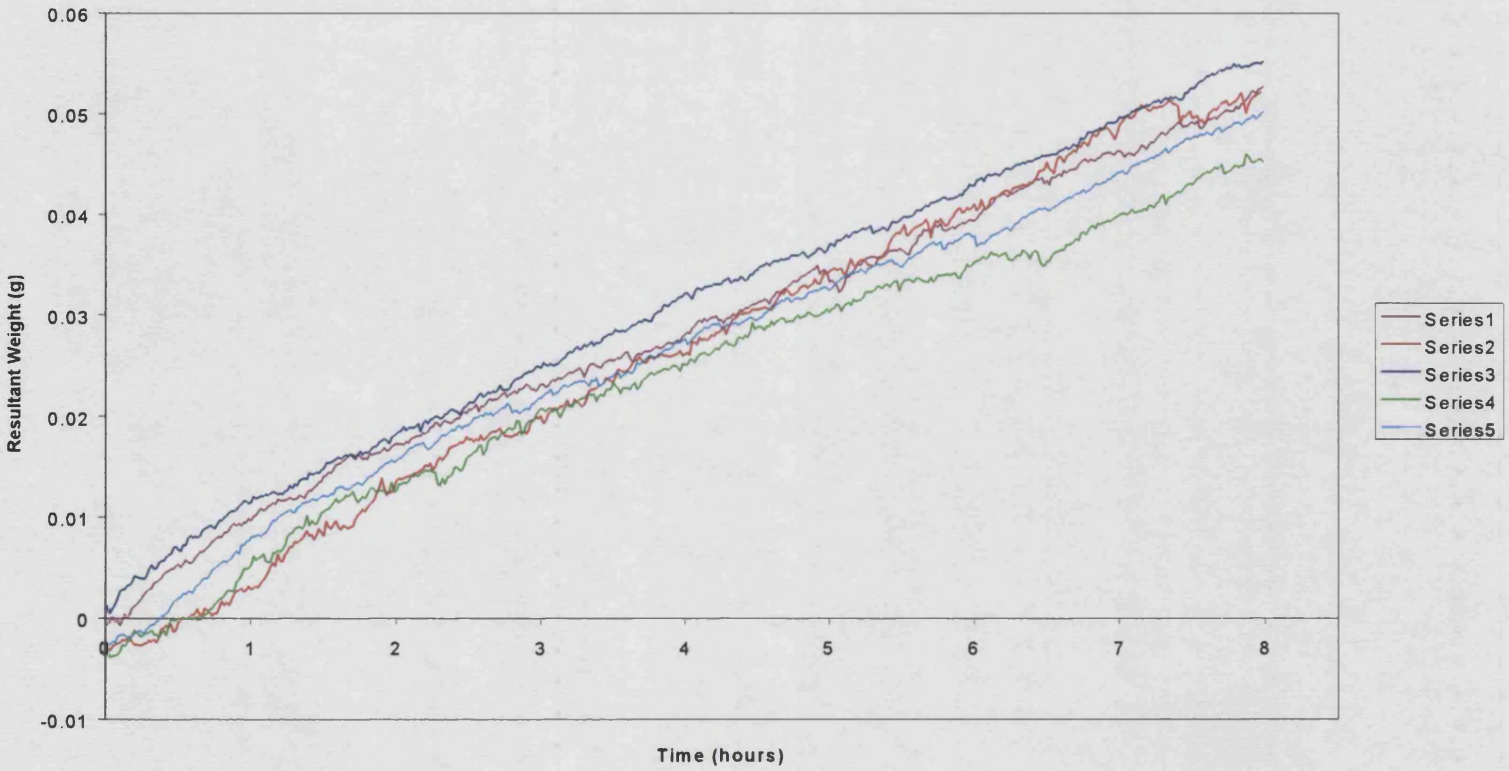

All of the runs to this point had been performed using Millipore water as a medium, however when using floating dosage forms the test will need to be performed with simulated gastric fluid in order to mimic stomach conditions. The effect of evaporation will, however, vary depending on the medium being used at the time. A baseline blank run was therefore performed using simulated gastric fluid. The simulated gastric fluid (SGF) medium was produced according to Formula 1.

Formula 1 :

Sodium Chloride	2.0g
Hydrochloric Acid	7.0mls
Millipore Water to	1000mls

3.8 Final Method

The following method was used for the pre-testing of the system, as well for all future tests using the apparatus:

- The SGF was produced according to Formula 1 and was then degassed by bubbling Helium through the mixture for 1 hour.
- 1000mls of SGF were transferred to the modified dissolution vessel. The loose FTD was placed in the fluid and the top of the vessel was covered with the modified dissolution top. The water bath was then heated to 37°C. The heating up process took 1.5 hours, and the temperature was checked using a mercury thermometer before testing began.
- Once 37°C had been reached, the top was removed from the vessel and the FTD was taken out, quickly dried, using paper tissue, and then connected to the balance, with the protective shield surrounding the top portion of the FTD.
- The balance assembly / FTD was then placed back into the fluid and the insulating spheres added over the surface of the medium in a monolayer.
- The balance was tared.
- The balance was then lifted out of the water bath and held for approximately 3 seconds, in order to simulate the process of tablet addition (in future runs the dosage form will

be added at this point), before being re-submerged. The data collection was then started.

- The run was performed over an 8-hour period, with data being taken every 5 seconds.

The average overall weight gain was 0.04g (see results in Figure 10, page 35), which was similar to the results achieved when Millipore water was used. An approximate difference of 0.015g was found between the overall weight gains of the 5 runs, with a standard deviation of 0.00652, which was deemed appropriate for this study (see Table 3, page 34).

Table 3 Total weight gain on the FTD over an 8-hour period using SGF as a medium

Run number	Weight gain (g)
1	0.0494
2	0.0391
3	0.0518
4	0.0419
5	0.0368
Mean	0.0438
Standard deviation	0.00652

The apparatus was therefore ready to be used as a comparative test for floating dosage forms. The testing of floating dosage forms will be discussed in future chapters.

Figure 10 **A graph to show the effect of fluid loss on resultant weight when using simulated gastric fluid as a medium**

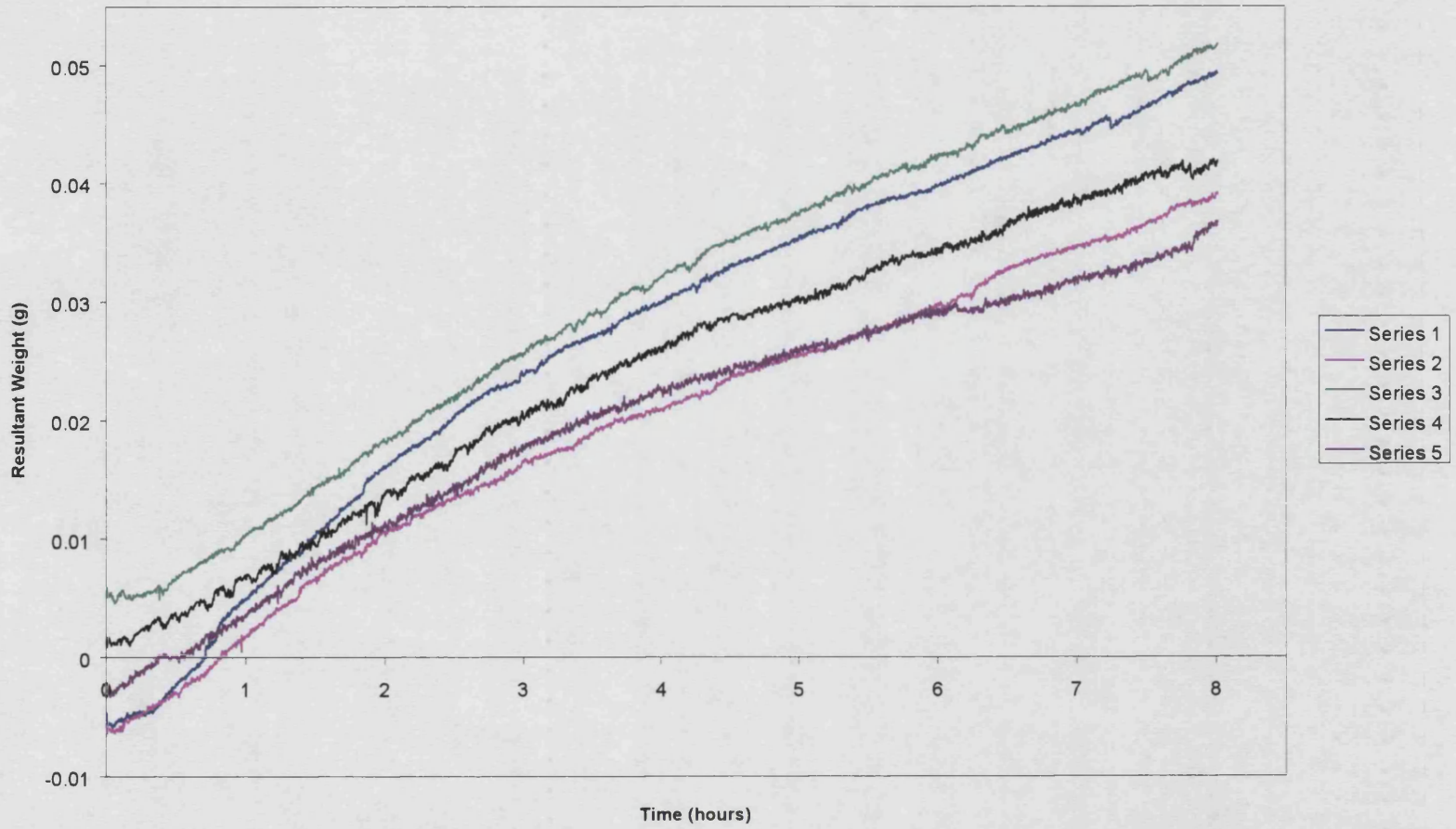

CHAPTER 4

PRESSURE VESSEL DESIGN AND DEVELOPMENT

4.1 Introduction

The release of gas from a component within a floating dosage form, if controlled properly, offers considerable benefits for the formulator. It can enable dosage forms to have their own floating power generator and can considerably increase swelling if a coating were applied to the outside of a tablet. Obviously, this production of gas has to be at a predetermined rate and has to take into account the swelling / gel strength of the polymer matrix into which it is embedded. It is therefore of benefit to have an *in vitro* technique capable of measuring the rate and extent of gas release from a tablet system.

4.2 Background

The release of gas from a component within a dosage form is of considerable interest in various pharmaceutical systems. The controlled production of gas is capable of aiding tablet disintegration, as in effervescent dosage forms, and of conveying buoyancy to floating dosage forms (Ingani et al, 1987; Yang et al, 1999). Both these systems would benefit from an *in vitro* technique capable of fully characterising and accurately quantifying the rate and extent of gas production by the dosage form, thereby allowing the optimisation of a formulation.

According to the ideal gas law (see Equation 3, page 39) an inversely proportional relationship exists between volume and pressure in a closed system, assuming the temperature in the system remains constant. It is therefore possible to calculate any change in the gaseous volume of a closed system, by measuring the pressure change that occurs within that system.

Some work has been conducted previously which looked at the production of gas after a reaction involving sodium bicarbonate powder (Fordtran et al, 1984). However the system used relied on the measurement of a displaced volume of gas after the bicarbonate had reacted. This technique is not accurate enough for studies on floating dosage forms as the amount of gas produced is envisaged to be relatively small. Also, the experiment only yields the total quantity of gas produced by the system, when it is the rate of production that is integral to this study.

A pressure device for measuring gas release from effervescent systems has also been attempted previously (Anderson et al, 1982). The experiment consisted of a closed plastic vessel containing a test medium, into which the test tablet was dropped at time zero. A pressure monitor was attached which measured the rate of pressure change as the gas was released from the effervescent system. Unfortunately in this experiment, a vessel made from an unspecified plastic had been used. Some plastics may become slightly deformed under increased pressures, which would mean that the internal volume of the vessel would not remain constant throughout the duration of the experiment, leading to potentially erroneous results. The pressure monitor used was also only accurate to 2psi, which would not be sufficiently accurate to measure the much smaller change in pressure envisaged with a gas powered floating system. However, the main flaw in the experiment was that the close relationship between pressure and temperature had been largely ignored. The vessel itself was not temperature regulated, which would cause fluctuations in the pressure within the vessel as the gas expanded / constricted due to temperature fluctuations.

4.3 Original apparatus design

4.3.1 Theory behind apparatus measurements / specifications

A gas powered floating dosage form must have the capability to produce gas at a predictable, reproducible rate. It is therefore essential that we have a piece of apparatus capable of measuring the rate of gas evolution from a dosage form *in vitro*.

Currently, the most widely used gaseous system in pharmaceutical effervescent formulations is carbon dioxide. Carbon dioxide is normally produced using the reaction that occurs between citric acid and sodium bicarbonate, when catalysed by water (see Equation 1, page 38).

Equation 1

E.g., Citric acid + $3NaHCO_3$ $3H_2O$ + $3CO_2$ + Citric residue

Rmm = 192 Rmm = 84

Therefore, the reaction of 1 mole (192g) of citric acid with 3 moles (252g) of sodium bicarbonate yields 3 moles of carbon dioxide. The volume of 1 mole of gas at 273K is 22.4dm^3 (24dm^3 at 298K). Therefore the 3 moles of CO_2 generated in the reaction have a volume of 72dm^3 at 298K, assuming the reaction goes to completion.

In a gas powered floating dosage form, it is envisaged that the maximum amount of sodium bicarbonate present in the formulation would be somewhere in the region of 60mg. Any more sodium bicarbonate than this would begin to cause problems with the size of the dosage form that would need to be produced.

The ratio of the components needed to fulfil the reaction shown above are 1.3125g sodium bicarbonate : 1g citric acid. Therefore if we use the theoretical maximum of 60mg of sodium bicarbonate the above equation becomes:

Equation 2

60mg $NaHCO_3$ + 46mg Citric acid 0.017 dm^3 of CO_2 at 298K (17cm^3)

We can therefore assume the maximum amount of CO_2 that would be produced in a gas powered floating dosage form would be in the region of 17cm^3.

The ideal gas law is stated in Equation 3:

Equation 3

PV=nRT where: P = Pressure (Pa)
V = Volume (L)
n = moles of gas X
R = Gas constant
T = Temperature (K)

Rearranging the equation enables us to establish a relationship between Pressure and Volume: $P \propto 1/V$, assuming that the temperature remains constant. Therefore in a theoretical 100cm^3 closed system resting at 1 Bar pressure, a 0.1 cm^3 addition of gas will result in a pressure rise of 1mbar, if the gas behaves ideally. It follows that an addition of 17cm^3 of CO_2, into the same system, would yield an increase in pressure of 170mbar.

Based on the work reviewed previously, a rationally designed pressure vessel would present a viable system for *in vitro* measurement of gas release from a floating dosage form. The data that has been considered above dictates that the design of any pressure vessel should be loosely based on a $100cm^3$ gas system, and be attached to a pressure transducer capable of measuring between 0 and 170mbar.

4.3.2 Experimental design

As shown in Figure 11, page 41, the pressure vessel consists of a main glass assembly that is detachable into two sections, separated by a ground glass joint designed to convey an airtight seal. Glass was the medium of choice for the body of the vessel for two reasons. Firstly, the glass structure would enable us to see into the vessel during experimentation. Secondly, glass is unlikely to swell upon prolonged heating, thus ensuring that the internal volume of the vessel remains constant throughout the duration of the experiment. Figure 12, page 42 shows a schematic of the vessel. When in use, the ground glass joints are covered with a silicone sealant to avoid the possibility of escaping gas. The internal volume of the vessel was approximately $200cm^3$, so it is envisaged that approximately $100cm^3$ of airspace will remain once a medium has been added. This volume is in keeping with the theory discussed above.

The lower section of the vessel has been designed to contain the sample being tested, along with any medium being used. The vessel, containing a stirring flea, sits on a Heidolph MR 300 C (Schwabach, Germany) magnetic heated stirrer, set at 100 rpm in order to agitate the medium, hence replicating stomach conditions and providing a more even dissolution. A water bath surrounds the lower portion of the vessel such that the internal medium temperature can be set to 37°C.

The upper section of the vessel has been designed to include both a means of monitoring internal pressure, and an inlet / outlet valve for gaseous addition / release. The valve itself consists of a modified subaseal piece, which is screwed into place directly onto the glass vessel. A Druck PDCR 820 (Leicester, UK) pressure transducer conducts the monitoring of the internal pressure. The transducer has a range of 200mbar and an accuracy of 1mbar pressure, which is in correlation with the theory above. The transducer is linked to a digital output device that facilitates the reading of pressure levels at various time points.

Figure 11 Photograph of pressure vessel

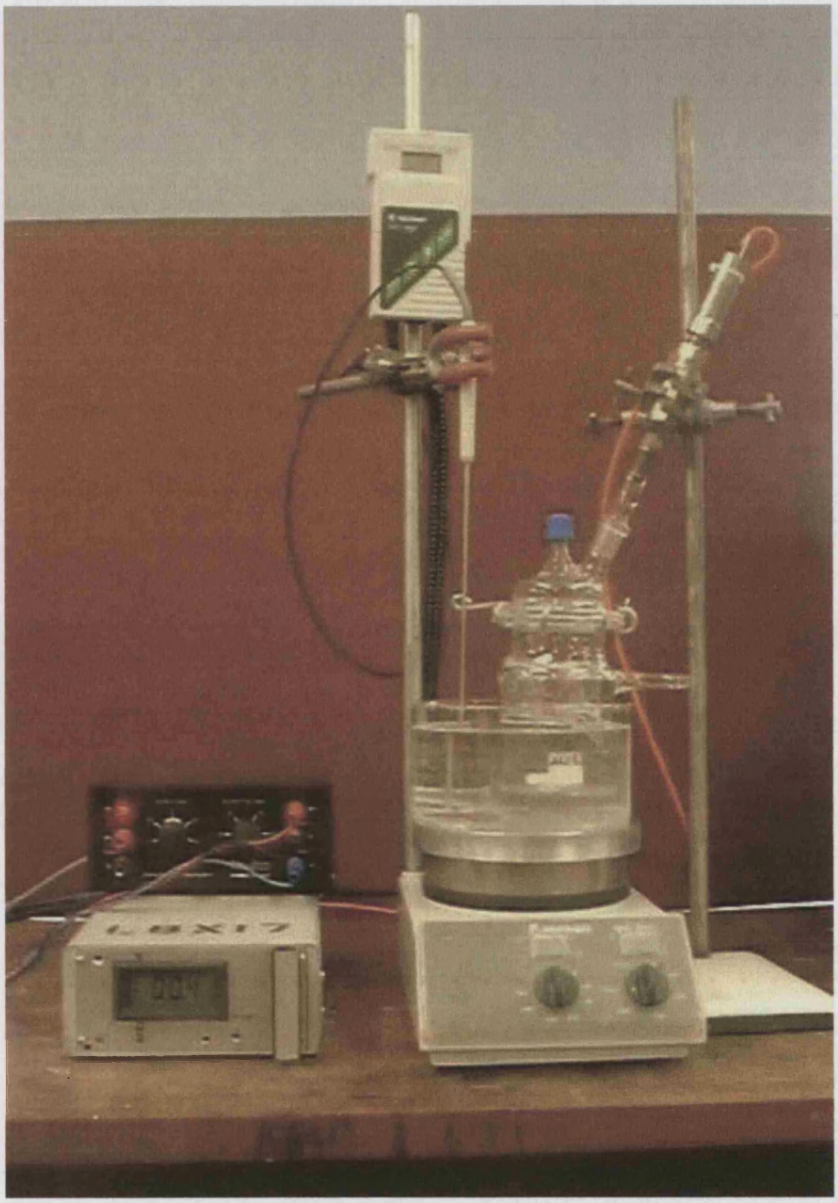

Figure 12 Schematic of pressure vessel design

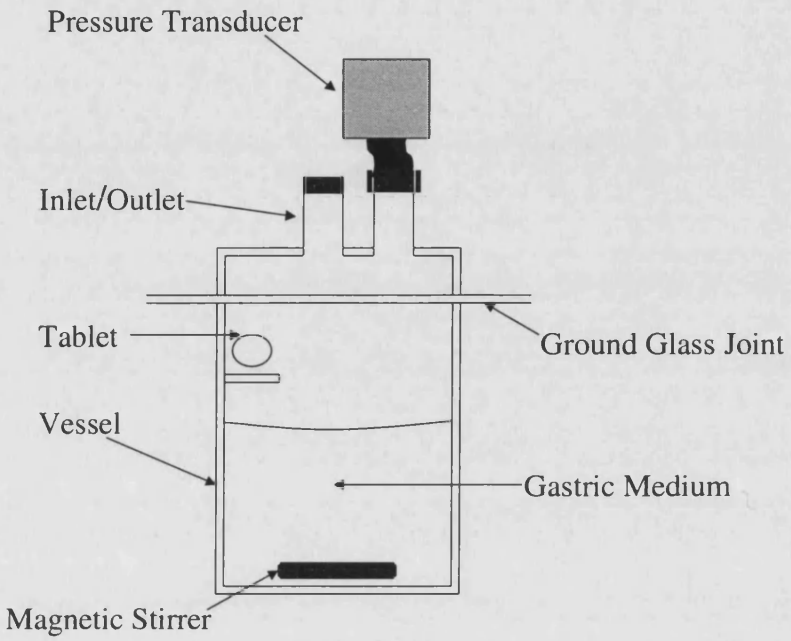

4.4 Initial calibration methodology

The calibration method used consisted of the addition of known aliquots of CO_2 into the closed pressure vessel, in order to assess the change in internal pressure. Decarbonated water was used as the medium in the vessel, so as to ensure that all CO_2 produced came from the gaseous additions. Decarbonated water also had the advantage of being an easily reproducible medium to make.

The decarbonated water was produced by vigorously boiling reverse osmosis water for 10 minutes, and then cooling whilst protecting from the atmosphere (British Pharmacopoeia, 1993). 90mls of this medium were then measured using a 100ml-measuring cylinder, before transferring them to the pressure vessel. The pressure vessel was then heated to 37°C on the heated magnetic stirrer, with the stirrer speed set to 100rpm. This process took approximately 90minutes to stabilise, after which time the vessel was sealed and the pressure reading zeroed.

The carbon dioxide itself was produced using cardice. A conical flask was first purged with CO_2 gas from a compressed cylinder. The cardice was then added to the purged flask and the top covered with a subaseal bung, using a needle to vent. A Weber scientific BS 1263 5ml-glass syringe, attached to a needle, was then used to collect known amounts of pure CO_2 gas from the flask. The syringe was allowed to equilibrate to atmospheric pressure, before injecting the required amount of CO_2 through the inlet valve and into the decarbonated water in the pressure vessel. The CO_2 was injected directly into the medium in order to mimic the effects of gas release from a tablet. The pressure readings were taken 5 minutes after the addition of the CO_2, in order to give the system time to equilibrate. 1ml of CO_2 was added initially followed by 5ml additions until near maximum pressure (200mbar) was reached. See Figure 13, page 44 for the results.

Figure 13 **A graph to show the relationship between CO_2 addition and pressure in a closed vessel containing CO_2 free water**

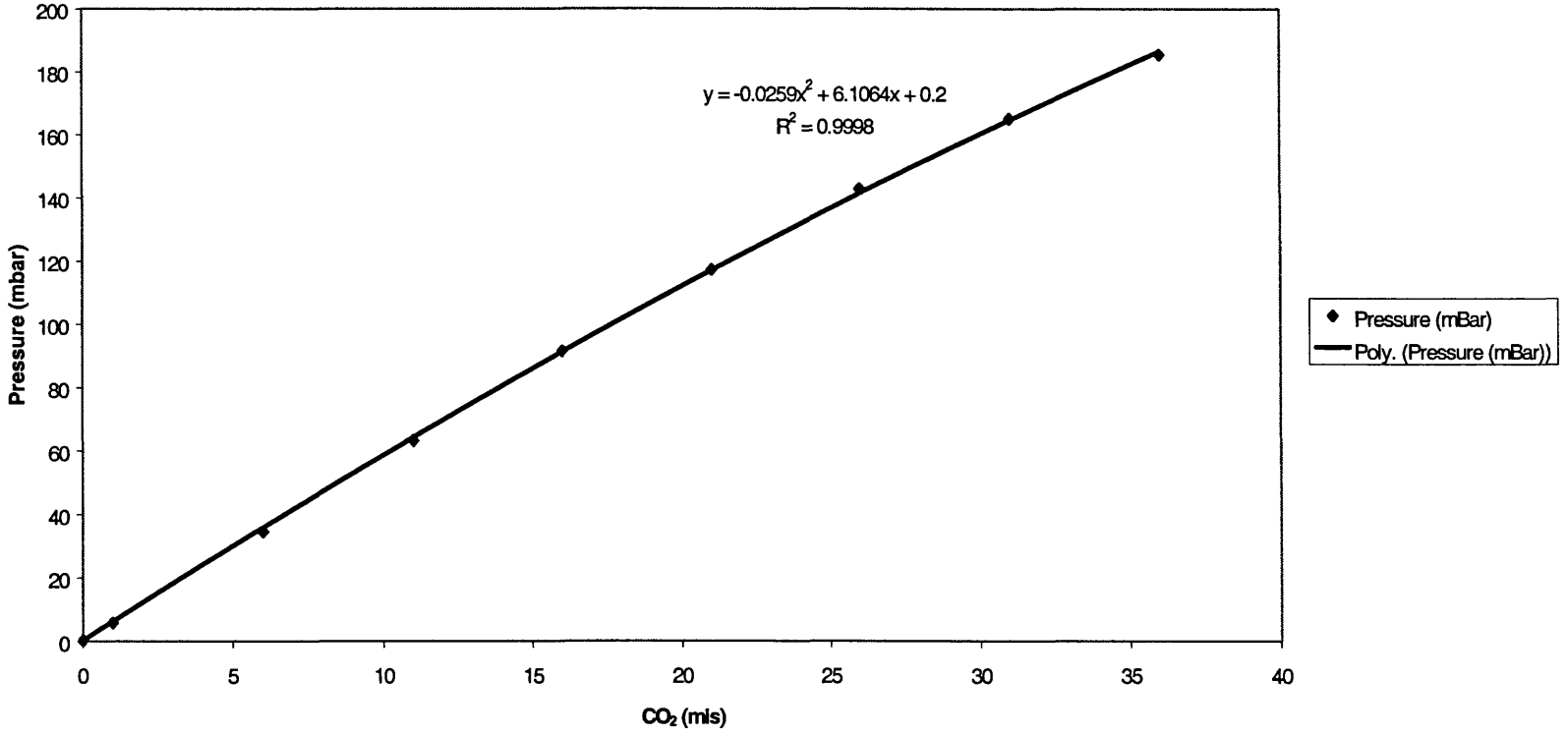

4.5 Modifications to the original design

Initial results from the experiment (Figure 13, page 44) indicated that pressure was being lost from the vessel to some degree. The first modification was to add a firm support around the ground glass joint of the pressure vessel to ensure that no gas was leaking from this area.

When the experiment was rerun however, it was noticed that the pressure in the vessel was dropping rapidly as the needle was inserted past the septum. The experiment was therefore terminated. Upon further investigation a leak was eventually located through a small aperture in between the needle and the glass syringe. The gap was sealed with PTFE tape and the experiment repeated.

During the next rerun of the experiment, gas was found to be leaking from the subaseal septum on the inlet / outlet valve. The experiment was therefore terminated again. This loss of gas was deemed to be the result of repeated piercing of the septum with the syringe needle and highlighted the need for the septum to be replaced before each run.

The corrected experimental calibration was then conducted in triplicate in order to assess reproducibility. The experiment was repeated using simulated gastric fluid as the medium and also when the pressure vessel was empty, to see the effect that the medium has on the pressure levels seen. The simulated gastric fluid was produced according to Formula 1, page 33.

4.6 Initial calibration results

The calibration proved to be similar for each of the individual conditions, see Figure 14, page 47. The slight error seen could have been due to a multitude of factors. The accuracy of the syringe being used to inject gas introduces a certain error, as does the operator. The air temperature while the gas was being measured was not kept constant and so will have an effect on the number of moles of gas being injected into the vessel, which in turn will directly affect the pressure reading within the vessel. The water bath keeping the pressure vessel at 37°C also had a limitation as the temperature fluctuated slightly as

the heated bath came on. It is perhaps this factor that made the most difference to the results.

The overall graphs followed distinctly different patterns, depending on the presence, or lack, of fluid in the vessel. When the fluid was present in the vessel, the calibration curve could be fitted to a quadratic equation. However, when no fluid was present in the vessel a linear calibration was produced.

The predictable curve seen when fluid is used in the vessel is probably due to the experimental conditions. The pressure readings were taken 5 minutes after the addition of CO_2, and not when the pressure in the vessel had reached equilibrium. When the CO_2 is first injected into the vessel the pressure reading reaches a peak level before dropping off slowly, until finally equilibrium is reached. This is thought to represent the slow incorporation of injected CO_2 gas into the liquid phase, presumably as carbonic acid. This transition causes the pressure in the gas phase of the system to slowly decrease until equilibrium is reached. However, as the overall pressure in the vessel increases with each further addition of gas, so the rate of CO_2 transition increases. This therefore leads to the predictable curve seen in the calibration graph.

There is a small difference between the decarbonated water graph and the simulated gastric fluid graph, although this difference may not be statistically valid (Figure 14, page 47). The acidic nature of the gastric fluid could help to explain this perceived difference. The acidic gastric fluid would not form carbonic acid as readily as the decarbonated water. This would therefore lead to more moles of CO_2 remaining in the gaseous phase at equilibrium, and hence a higher pressure detected in that phase by the transducer.

The calibration performed without liquid further proves the equilibration theory, and validates the fact that no leaks are occurring in the vessel. A linear response was seen, as expected, due to the inverse relationship that exists between volume and pressure. We can therefore deduce that the curve seen previously was due to the presence of fluid in the vessel. The overall pressure levels seen were much lower when compared with the fluid filled vessels, due to the increase in the gaseous phase volume that occurs when the fluid is removed.

Figure 14 **A graph to show the relationship between CO_2 and pressure in a closed vessel containing different mediums**

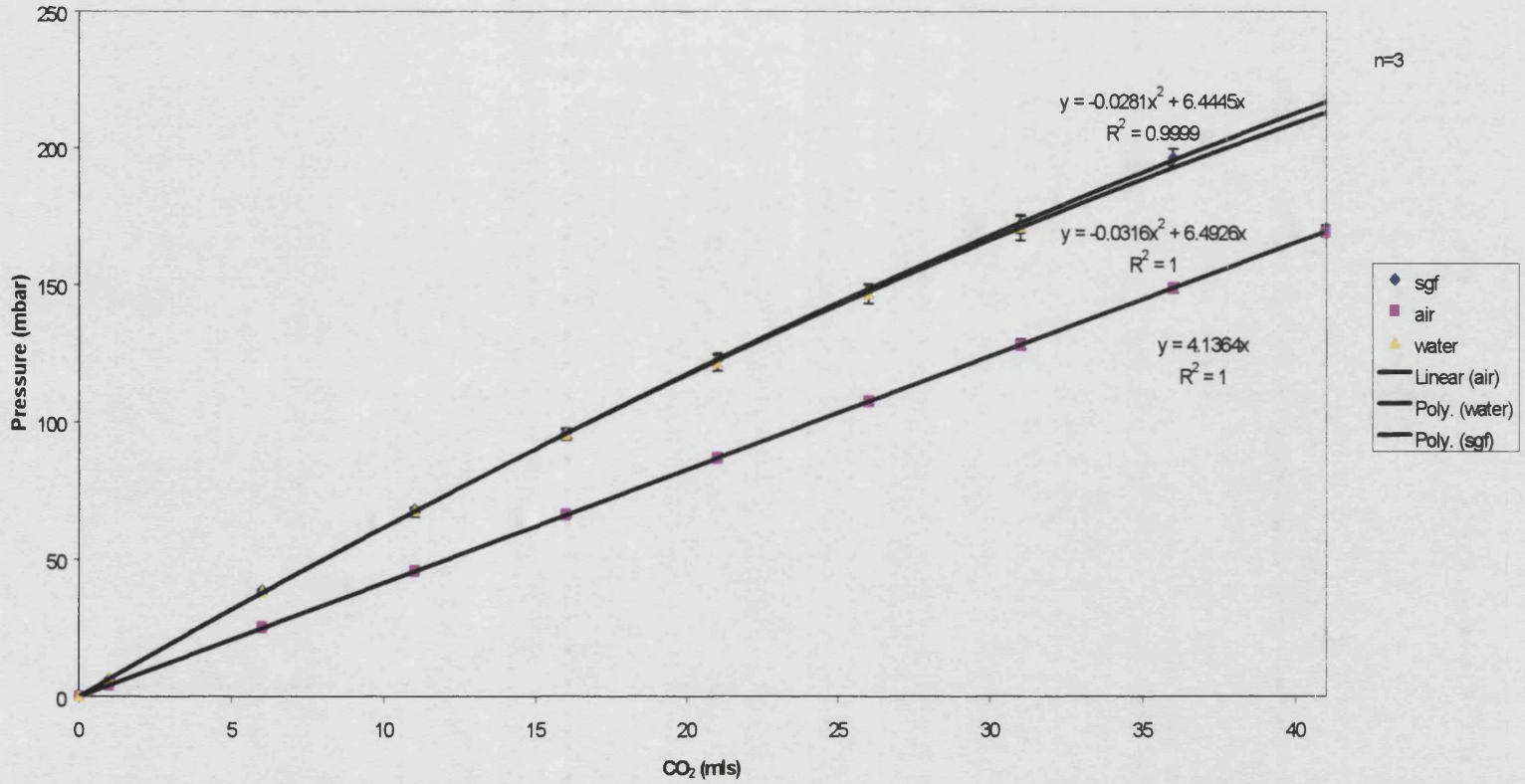

4.7 Secondary modifications to vessel design

The experiments performed on the initial vessel provided useful information regarding the relationship between pressure and medium. However, it was decided that there were some factors that could be altered to improve the reproducibility of the experiments.

Firstly, the temperature of the air / medium inside the vessel cannot have been constant throughout the course of the experiment, due the inadequate temperature regulation device and the inherent fluctuation in air temperature. Any fluctuation in the temperature inside the vessel would have a direct effect on the pressure inside the vessel therefore it is essential to try to keep the temperature constant throughout the duration of the experiment. It was decided to do this in two ways. Firstly, it was decided to move the experiment into a laboratory with regulated air temperature control, so that all experiments could be run at the same external air temperature. The second change was to discard the previous water bath arrangement that had shown temperature fluctuations during the course of the experiment. Such fluctuations were deemed to be a direct cause of the majority of the error seen during calibration. It was decided to replace the water bath arrangement with a water jacket connected to a circulating water bath (Grant Y6, Royston, UK), as this was considered the best way to maintain a constant temperature. Therefore, both the internal and external temperatures would now be kept constant for the duration and repetition of future experiments, leading to a reduction of overall error.

In order for a glass water jacket to be added it was necessary for the vessel to become slightly larger. This was due the difficulty encountered when fitting a glass jacket around the existing structure. This obviously led to the requirement for re-calibration of the new apparatus, as the internal volume had altered which would inevitably change the pressure readings seen when equivalent levels of gas were added.

A second factor thought to have a degree of error associated with it was the speed of stirring due to the stirring flea. It was noticed that when the stirring speed was increased, the time for equilibration of pressure in the vessel decreased. During the calibration experiment there was a delay between gaseous addition and the recording of the pressure reading. It was thought that any change in the speed of the stirring flea from day to day might well affect the outcome of the experiment. Such a change would have been

possible, but not easily detected, as the magnetic stirrer used had a non-digital setting system. Had the setting been altered in any way, it may not have been possible to return to the exact same setting as before, thus invalidating any calibrations. Changing the stirring slightly would also effect the dissolution from a dosage form being tested, which would also cause problems during later experiments. It was therefore decided that removing the flea from the system would the best way of achieving reproducible results over the course of an experiment, and to avoid day to day variations.

The third alteration to the system was made to the digital output device. The previous device had been calibrated and set up by in the engineering department at the University of Bath. However, the main flaw with this set up was that the readings had to be taken manually over the experimental period. It would be possible to miss significant events when testing a dosage form in the apparatus if an event happened in between data points. In order to minimise these errors and problems it was decided to link the pressure transducer up to a P.C. via an RS232 interface. The data could then be automatically recorded into a compatible spreadsheet package, at various predetermined time points. This was achieved by using Collect software (A&D instruments, Oxford, UK). In order to utilise the RS232 interface it was first necessary for the device to be returned to the manufacturer for re-calibration and connection to their own digital readout device. The digital device was then connected to the RS232 cable and linked to a compatible P.C..

As the transducer had been re-calibrated and connected to the P.C., it was first decided to conduct a blank run with the transducer completely disconnected from the pressure vessel. The purpose of this experiment was to see if any fluctuation occurred after the pressure transducer was turned on for testing, as it was thought there may be a "warming up" effect. The transducer was switched on and the software was set up to collect data every 5 seconds over a 4-hour period. The results of this run can be seen in Figure 15, page 50.

The graph produced showed that there was indeed a period of "warming up" after turning on the transducer. It was decided therefore to leave the transducer on permanently between experiments, rather than switching on and off as before.

Figure 15 A graph to show the "warming up" effect of the pressure transducer

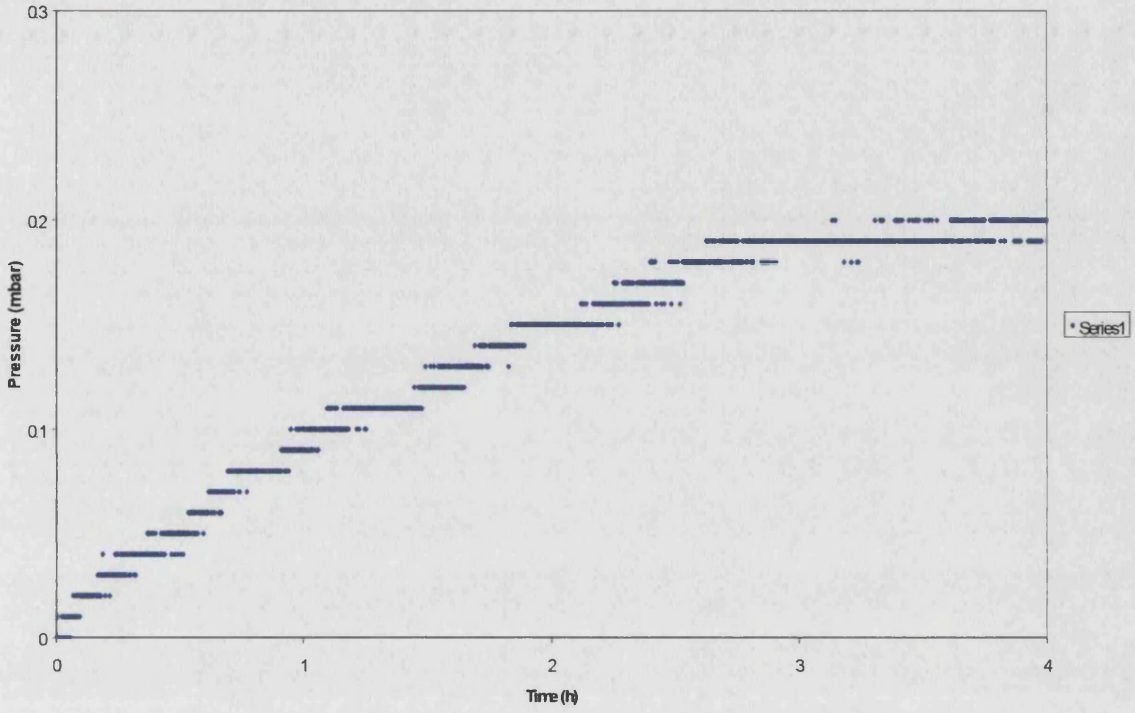

4.8 *Further modifications to methodology*

It was important to establish a reproducible method before any blank runs were conducted with the new apparatus, so that all future experiments could follow the same protocol. In order to achieve this the method must take into account the addition of a dosage form into the apparatus, as this will be an essential part of future work using the vessel.

The addition of a dosage form into the vessel can be achieved in two ways. The medium in the vessel can be heated before the formulation is added, with the vessel then being sealed and the test started. Alternatively, the dosage form can be added prior to heating the medium, with the vessel being sealed from the start. Both of these methods were investigated without dosage forms, in order to investigate the potential problems or advantages that each would bring.

The first to be examined was the heating up of the medium before the theoretical dosage form was added into the vessel. In this experiment, SGF was used as the medium

because SGF will be used in later tests. The SGF was prepared according to Formula 1, page 33. 90mls of medium were placed in the vessel and the vessel jacket was connected to the circulating water bath, which was set to 37°C. The top was left off the pressure vessel during heating. The heating lasted for two hours to ensure that the medium had reached 37°C. The temperature of the medium was checked using a mercury thermometer prior to the start of the test. The top of the vessel was then sealed and data collection was started. Data was collected, using the Collect software, at 5-second intervals for the duration of approximately seven hours. The test was repeated in order to assess the reproducibility of the technique.

The results are shown in Figure 16, page 51. The graphs both showed an increase in pressure at the beginning of the test. This increase was thought to be due to the heating of the air above the warm medium once the vessel had been sealed. This heating up phase precludes this method from further analysis, as it will distort the graph produced when tablets are used in later tests. The pressure in both runs then decreased over the remainder of the test. However, the graphs showed a fluctuation of up to 2 mbar between adjacent points, rather than the straight line that was predicted. This fluctuation was too high for this technique to be used in future runs involving dosage forms.

Figure 16 **A graph to show the relationship between pressure and time when the medium in the vessel had been preheated prior to the vessel being sealed**

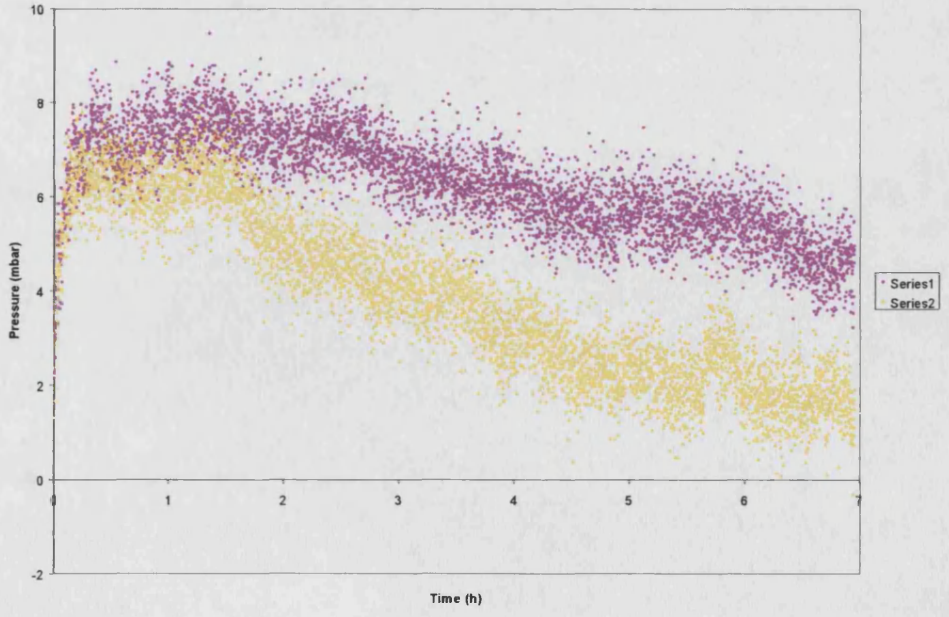

The second technique to be examined was the sealing of the vessel before the medium was heated. 90mls of SGF were again used as the medium. The vessel was heated in the same way as the previous test, only this time the vessel top was on and sealed during heating. After 2 hours the vessel was vented using a fine needle to release the pressure that heating had caused, and then data collection was initiated in the same way as before. The run was again repeated in order to assess reproducibility.

The results are shown in Figure 17, page 52. Both runs showed a general decline over time in a similar fashion to the experiment conducted with the top off during the heating phase. However, this time there was no corresponding increase at the beginning of the test, making this method more viable for future work. This was because the air in the vessel had already reached the same temperature as the medium prior to data collection being initiated. Both runs however, again showed the approximate 2 mbar fluctuation between corresponding points, rather than the expected straight line. This method seemed to work well apart from the rapid pressure fluctuation that was being seen in the vessel.

Figure 17 **A graph to show the relationship between pressure and time when the medium in the vessel has been heated after the sealing of the vessel**

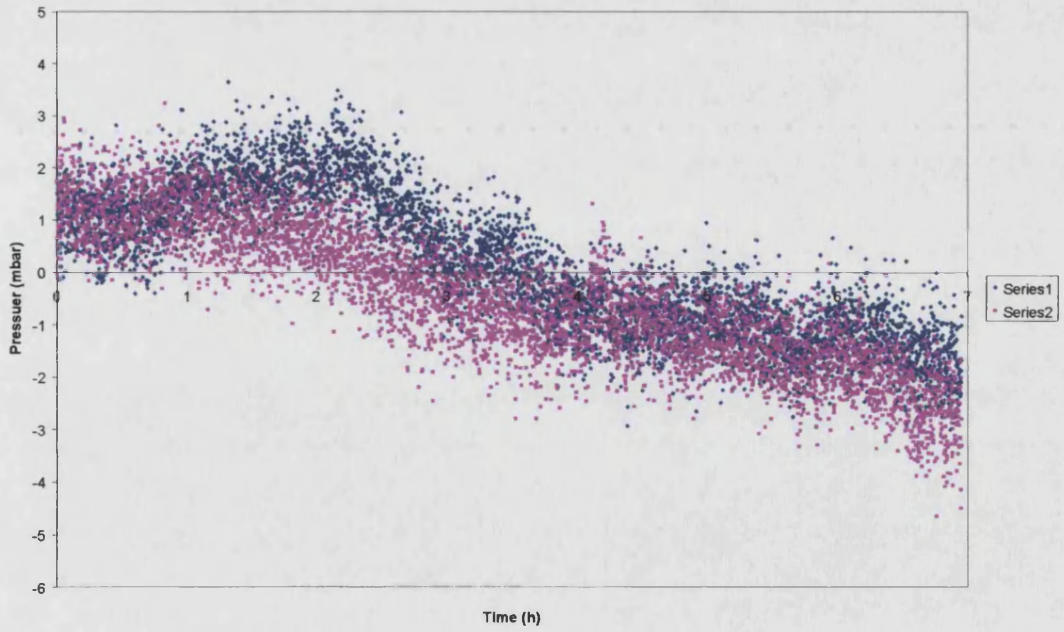

It was likely that the rapid pressure fluctuations were due to a change in the temperature of one of the two phases, within the vessel. The fluctuation can not have been due to the temperature of the medium phase changing for two reasons. Firstly, the changes in pressure were occurring very rapidly, something highlighted by the taking of data points every 5 seconds. It is highly unlikely that the SGF medium could change temperature as rapidly as this. Secondly, the temperature of the circulating water bath was seen to remain constant during the course of the experiment, meaning the medium was also being kept at a constant temperature.

Therefore, it was thought that the pressure fluctuation was due to the temperature of the gaseous phase changing rapidly. It is unlikely that the entire gaseous phase can be changing temperature, and therefore pressure, over the short time periods indicated. It is likely instead, that some sort of temperature cycling was occurring within the gaseous phase of the vessel.

The temperature cycling effect was thought to be due to the increased headspace of approximately 50mls now present in vessel 2. The heated medium was situated at the bottom of this headspace, whilst the pressure transducer measured the pressure at the top. It was likely that the whole of the headspace was not being equally heated by the medium at any one time, and that therefore temperature discrepancies exist between the top and the bottom of the headspace. The mechanism for this action can be explained in 4 steps:

1. The liquid medium is heated to 37°C by the water jacket.
2. The gas immediately above the liquid medium is heated to approximately 37°C and begins to rise with colder air replacing it.
3. As the warm gas rises it displaces colder gas from the top of the vessel where the transducer is monitoring the pressure.
4. The warm gas cools at the top of the vessel and begins to drop, being replaced by gas that has been more recently heated.

Steps 2-4 then continue cycling throughout the duration of the experiment. This theory would explain the rapid changes in pressure seen in the new vessel. It is the slight changes in temperature occurring near to the pressure transducer that accounts for the

variations in pressure that are measured. This is likely, as there is a close relationship between the pressure and temperature of a gas (see Equation 3, page 39).

It is also noticeable that both sets of data show a trend of pressure decreasing slightly over time. It is thought that this is due to the slow evaporation of water over the course of the experiment. As more water evaporates from the SGF medium, so the volume of the gaseous phase increases. If this were taken alone it would explain why the pressure in the vessel is seen to slowly decrease over time, due to the inverse relationship that exists between the volume and pressure of a gas at constant temperatures (see Equation 3, page 39). However, the fact that pressure is proportional to the amount of moles of gas present in the system also has to be taken into account. Therefore as the water evaporates, so the moles of gas in the system increase correspondingly. This leads to an increase in gaseous phase volume as discussed, but also to an increase in the moles of gas present in the gaseous phase. Neither of these two factors would therefore appear to exclusively explain the decrease in pressure over the duration of the experiment, however the system is obviously complex.

The pressure drop could be due to the partial pressure of the water contributing to an overall decrease in the pressure of the gaseous system. According to Dalton's law of partial pressures, the total pressure of a gas mixture is equal to the sum of the partial pressures of the individual gases, providing no chemical reactions take place. Therefore the partial pressure of the evaporated water will have a direct effect on the overall pressure of the gaseous system. It is perhaps this constant change in the constituents and volume of the gaseous system that best explains the pressure drop that is seen in the sealed vessel over time.

The main problem that needed addressing was the pressure fluctuation being seen in the vessel (Figure 16, page 51 and Figure 17, page 52). As discussed above, it was thought that this was due to fluctuations in the temperature of the gas due to a "cycling" effect caused by an increased headspace. In order to remedy this, it was decided to decrease the available headspace. There are two ways of decreasing the headspace. Firstly, it would have been possible to build a new vessel. However, it is possible that the new model may have also shown the fluctuation effect. Instead it was decided to build an insert for the current model, which would occupy part of the headspace in the vessel, thereby decreasing the space available for the gas to occupy. As the primary function of the insert was to prevent the temperature "cycling" of the gas phase, it was decided the best location for the insert would be halfway between the medium and the pressure transducer.

The insert could then regulate the flow of the warmer / cooler gases as they rise and fall within the vessel, thereby stabilising the pressures read by the transducer and creating a more even environment.

The insert was made from perspex to avoid the possibility of interaction with either the medium or gaseous phases. The perspex was cut so that it fitted snugly into the vessel, and a hole was drilled through the middle of the insert to allow gas to pass through. The hole was drilled to an approximate diameter of 1cm.

To ensure that the insert was working as predicted, 3 blank runs were performed according to the following method:

- 1 Litre of SGF was made up according to Formula 1, page 33.
- The SGF was then degassed by bubbling helium through the mixture for 1 hour.
- 90mls of the degassed SGF were then transferred into the pressure vessel using suitably sized pipettes.
- The vessel was sealed shut, using silicon sealant to ensure the vessel was airtight, and a clamp placed around the join to ensure stability. The vessel was then zeroed via the needle vent.
- The circulating water bath was switched on to heat to 37°C and data collection was started.
- Data points were taken every 5 seconds over the course of 7 hours, in order to assess stability.

The results from the 3 runs can be seen in Figure 18, page 57. The graphs show that the insert worked effectively to prevent the rapid fluctuations in pressure seen in previous experiments without the insert. The insert will therefore be used in all future experiments.

The graphs also all show a rapid rise in pressure that stabilises after 1.5 hours until the end of the run. This indicates that the fluid in the vessel is taking approximately 1.5 hours to fully heat up, as after this time the temperature, and therefore the pressure, in the vessel remain constant. It will therefore be necessary to leave a heating time of 2 hours in future experiments to ensure the vessel is stabilised before a formulation is added.
The noticeable difference between the three runs is the pressure at which they stabilise. It was thought this was due to the varying heat of the medium when it was transferred into the vessel. Obviously if the medium was slightly warmer when it was transferred then the

pressure in the vessel would be slightly higher before the vessel was zeroed. It then follows that the change in pressure from the beginning of heating to equilibrium would be less than expected. It is highly probable that the medium was at different temperatures for each of the runs as the medium was degassed in a separate laboratory without temperature control, and therefore likely to suffer from day to day variation. However, although the variation between runs was quite high, it is not of consequence to the methodology, as the vessel will be vented again immediately prior to tablet addition in future runs. This will be done after 2 hours of heating to ensure the equilibrium phase has been reached in the vessel. This second venting prior to tablet addition will mean that all future runs will start at 37°C and at atmospheric pressure.

The final vessel will have to be able to assess the gas release from various dosage forms; therefore the next alteration to the vessel was the design of a mechanism capable of adding a test formulation into the vessel. It was important that the mechanism was finalised at this stage and added to the vessel, so that the calibration of the vessel could be carried out under final test conditions with all components in place. Having previously established that the best method of heating the medium was with the vessel sealed, it was necessary to have the dosage form *in situ* before heating was initiated. This caused a few problems, as it is necessary to protect the dosage form from the SGF medium during the pre-heating phase. The formulation must also be protected from any vapour that may be released during heating of the SGF. The other problem that must be overcome is the mechanism of release of the protected dosage form into the medium, once pre-heating has been completed.

Figure 18 **A graph to show to relationship between pressure and time during and after heating SGF to 37°C in the pressure apparatus with insert**

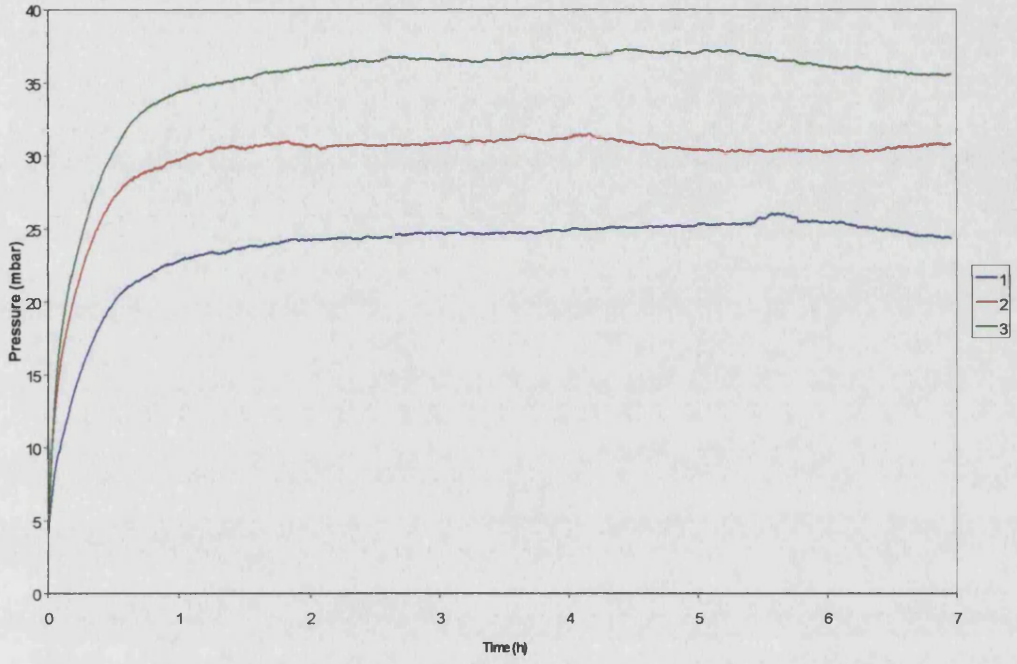

A glass shelf had already been incorporated into the internal structure of the vessel during the early design work. It was therefore necessary to design a structure that could sit on this shelf and protect, then release, the formulation being tested. It was decided to use a piece of hollow perspex tubing as the base for the structure. 30mm of this were cut and one end sealed with a flat, circular piece of perspex. A perspex plug was then made to loosely fit into the free end of the hollow tubing. The plug was manufactured so that it would fall out of the tubing when the tubing was tilted. The plug was then attached to the main structure by a small length of cotton. The length of the cotton was such that it would allow the plug to fall from the tubing when tilted, but so that it would also suspend the plug before it fell into the medium within the vessel. A small amount of silicone sealant was placed around the edges of the plug, so that no vapour from the medium could penetrate, and therefore react, with the test formulation housed inside. The structure was tethered onto the top of the glass tablet shelf inside the vessel, using a plastic pull-tie.

A blank run was performed to test the new mechanism. During the blank run the mechanism was proven to protect a blank tablet from SGF vapour. The vessel was then

tipped to ensure that the plug fell out of the tubing and the tablet dropped into the vessel. As this stage also worked without any problems the vessel was now ready for validation.

4.9 Validation of final apparatus and method

4.9.1 Blank runs using final pressure apparatus

In order to validate the pressure apparatus, it was necessary to perform several blank runs so that the reproducibility of the system could be assessed under test conditions. It was necessary to perform the runs using the conditions that will be used for future tablet runs. The following method was used and repeated a total of five times:

- 1 Litre of SGF was made up according to Formula 1, page 33.
- The SGF was degassed by bubbling Helium through the mixture for 1 hour.
- 90mls of the degassed SGF were then transferred into the pressure vessel using appropriately sized glass pipettes.
- The tablet release mechanism was closed with a small amount of silicon sealant added around the plug section to prevent moisture entering. The previously described insert was added to the top of the vessel to prevent temperature cycling.
- The vessel was sealed shut using silicon sealant to ensure the vessel was airtight and a clamp placed around the join to ensure stability. The vessel was then zeroed via the needle vent.
- The circulating water bath was switched on to heat to 37°C and data collection was started.
- After approximately 2 hours the vessel was re-zeroed via the needle vent.
- Immediately after re-zeroing the vessel was tilted to release the plug from the tablet release mechanism and simulate tablet release.
- Data points were taken every 5 seconds over the course of almost 10 hours, in order to assess stability.

The results from these five runs are shown graphically in Figure 19, page 60. The graphs show that all five runs followed a very similar pattern, as expected. The pressure can be seen to rise in the vessel during the SGF heating phase. Once the SGF has reached

37°C the pressure levels off as equilibrium is attained between the liquid and gaseous phases. The pressure then decreases rapidly to zero due to the venting of the vessel after approximately 2 hours. After venting the runs all exhibit a gradual decline in pressure until the end of the experiment. It was thought this gradual decline was due to the effect that the partial pressure of water vapour has upon the overall pressure of the gaseous system. This phenomenon has been discussed earlier on page 54.

It is noticeable that the pressure in the vessel is dropping below atmospheric pressure during this period, therefore the pressure drop is not simply the vessel leaking. The 5 runs were similar and therefore future experiments will be conducted using the average of these runs as a baseline. Figure 20, page 61 shows an average line of the 5 runs which fits the equation $y = -0.6927x$ with a linear regression r^2 value of 0.9907.

Figure 19 **A graph to show results of the pressure vessel methodology using blank run conditions**

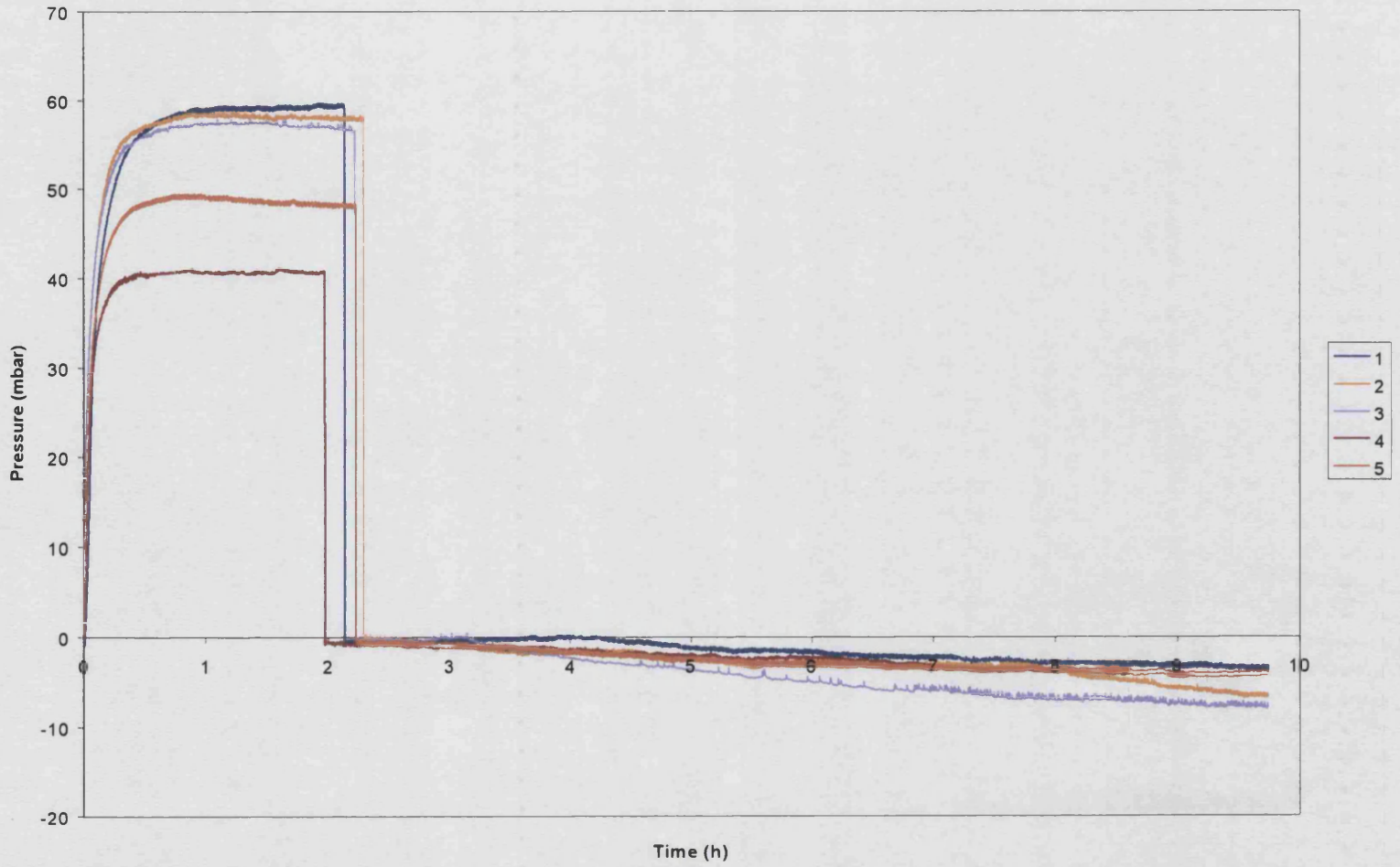

Figure 20 A graph to show the average of the five pressure vessel runs using blank conditions

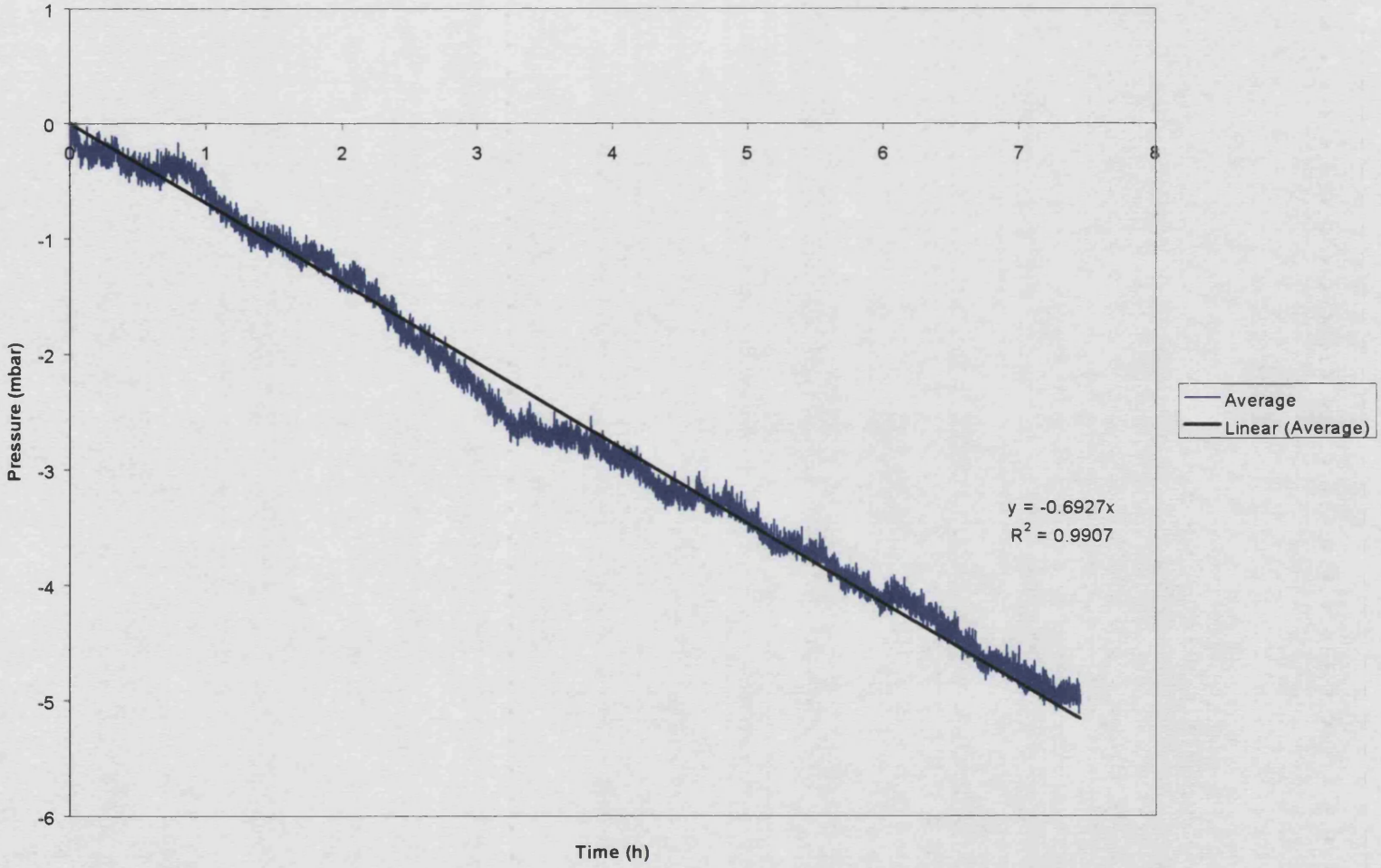

4.9.2 Calibration of final pressure apparatus

The calibration method used consisted of the addition of known aliquots of CO_2 into the closed pressure vessel in order to assess the change in internal pressure produced. The calibration was carried out according to the method outlined below:

- 1L of SGF medium were made up according to Formula 1, page 33. The medium was degassed by bubbling Helium through the fluid for 1 hour.
- 90mls of the mixture were measured out into the pressure vessel using appropriately sized glass pipettes. The pressure vessel was sealed and heated to 37°C, for two hours, after which time the pressure reading was zeroed using a venting needle.
- The aliquots of carbon dioxide were produced using cardice. A conical flask was first purged with CO_2 gas from a compressed cylinder. The cardice was then added to the purged flask and the flask covered with a subaseal, using a needle to vent.
- A Weber scientific BS 1263 5ml-glass syringe, attached to a needle, was used to collect known amounts of pure CO_2 gas from the flask. The syringe was allowed to equilibrate to atmospheric pressure before injecting the required amount of CO_2 through the inlet valve and into the SGF within the pressure vessel. The CO_2 was injected directly into the SGF medium in order to mimic the effects of a tablet.
- The pressure readings were taken 5 minutes after the addition of the CO_2, in order to give the system time to equilibrate. 1ml of CO_2 was added initially followed by further 5ml additions until near maximum pressure (200mbar) was reached.
- The calibration runs were repeated a total of five times to assess reproducibility.

See Figure 21, page 63 for the results of all five runs. The average of the five runs is shown graphically in Figure 22, page 64.

Figure 21 A graph to show the calibration curves for the pressure vessel containing SGF

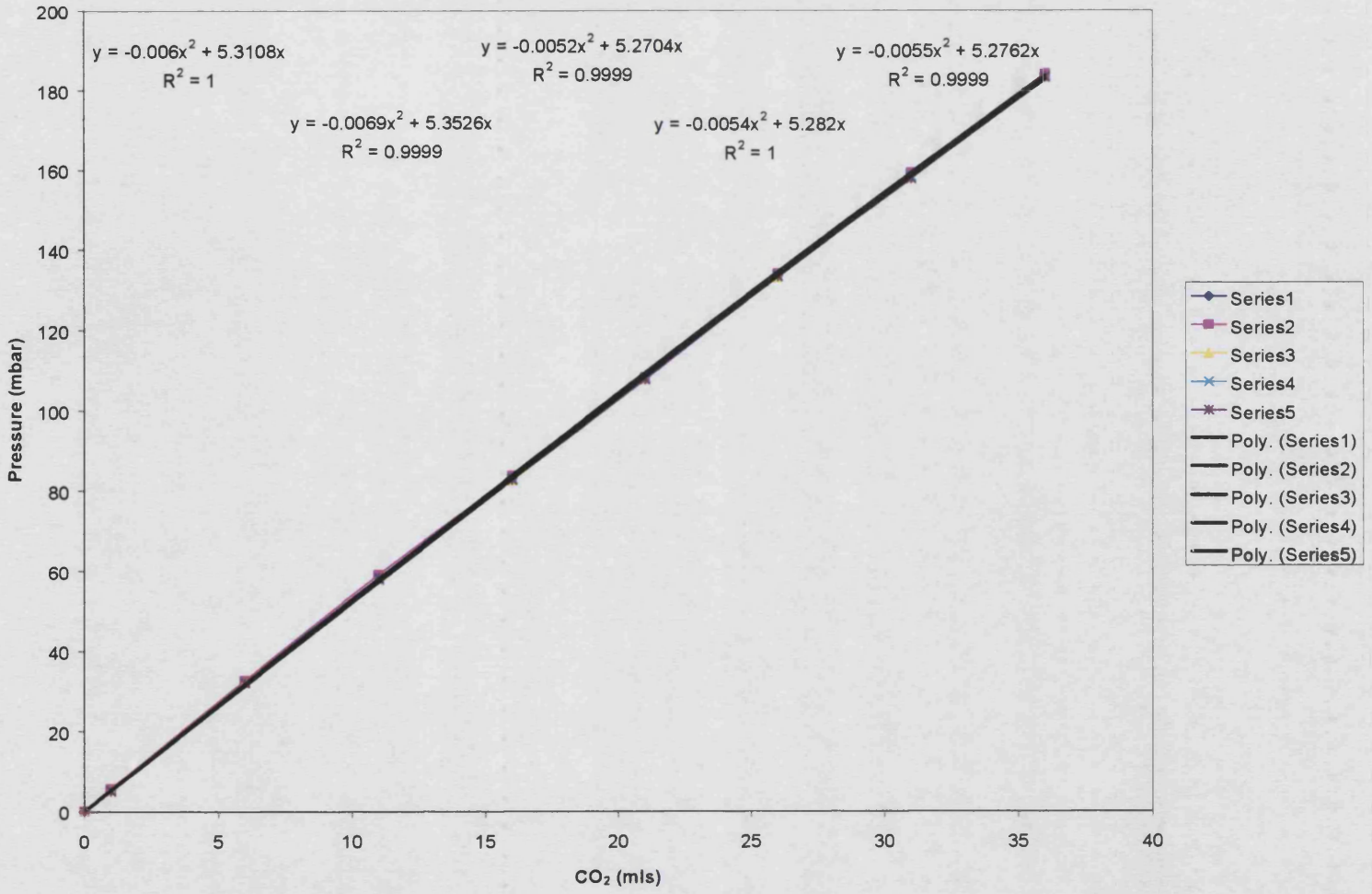

Figure 22 **A graph to show the average calibration curve for the pressure vessel containing SGF**

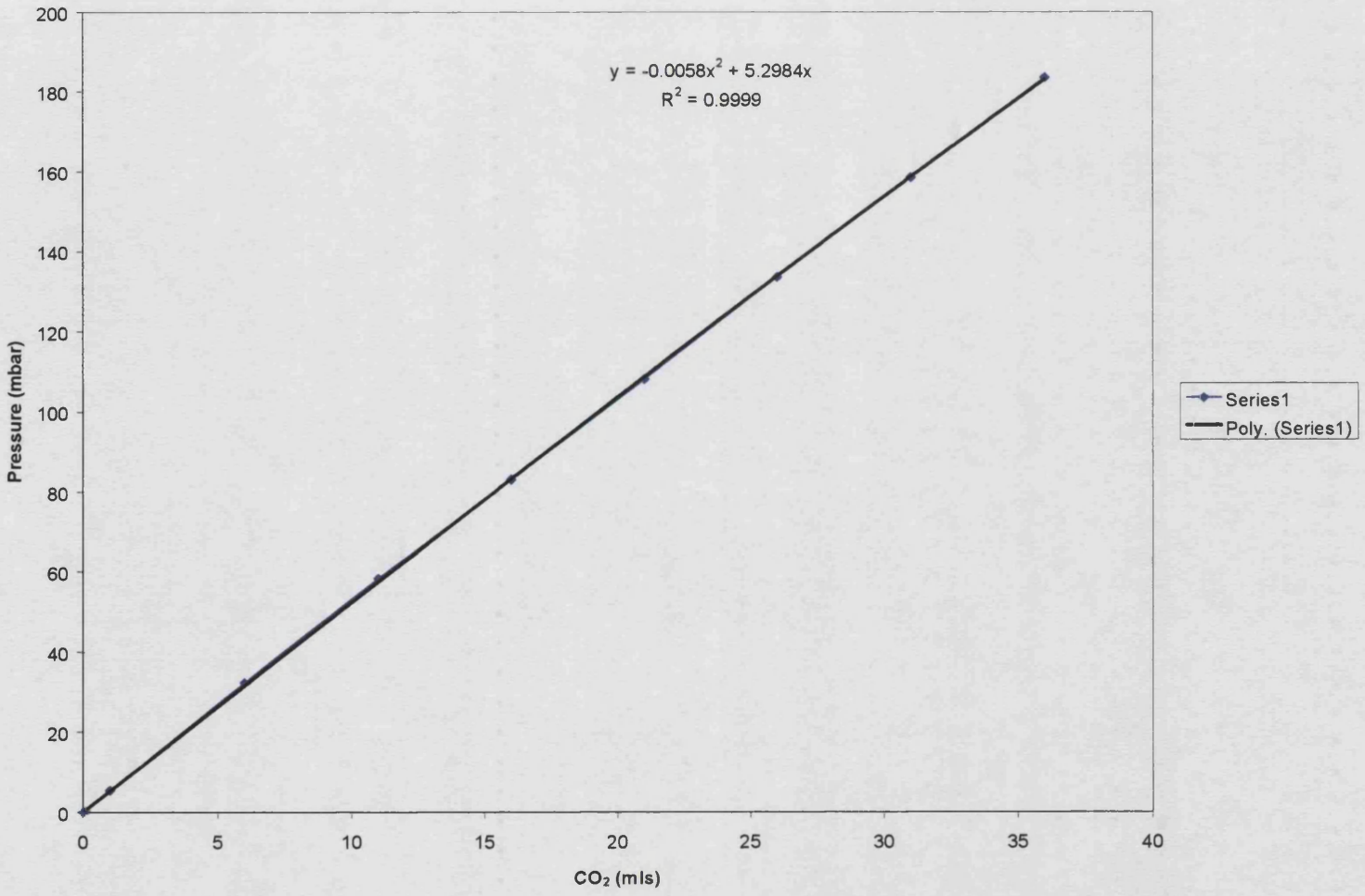

The experiment was repeated when the pressure vessel was empty to assess the effect that medium had on the pressure levels seen. The results for these runs can be found in Figure 23, page 66 and Figure 24, page 67.

The calibrations proved to be reproducible under both sets of conditions. The small error determined between runs has been reduced from previous calibration attempts. This was due to the new experimental parameters introduced into the protocol. The first of these was the moving of the apparatus to a room where temperature can be maintained at 20°C. This helps to maintain the injected gas at a constant temperature and therefore the number of moles of gas being injected into the vessel will be more accurate than before. The addition of a water jacket to the vessel has also helped to maintain accuracy by keeping the internal temperature of the vessel constant, which adds to the reproducibility of the experiment. The small error that is still seen is probably due to the inherent inaccuracy of the syringe being used to inject the gas, as well as a degree of operator error.

Overall, the graphs followed distinctly different patterns, depending on the presence, or lack, of fluid in the vessel. When the fluid was present in the vessel, the calibration curve could be fitted to a quadratic equation. However, when no fluid was present in the vessel a linear calibration was produced. This pattern is in keeping with previous experiments. See Figure 25, page 68 for a comparison of the two calibration runs.

Figure 23 **A graph to show the calibration curves for the pressure vessel containing no medium**

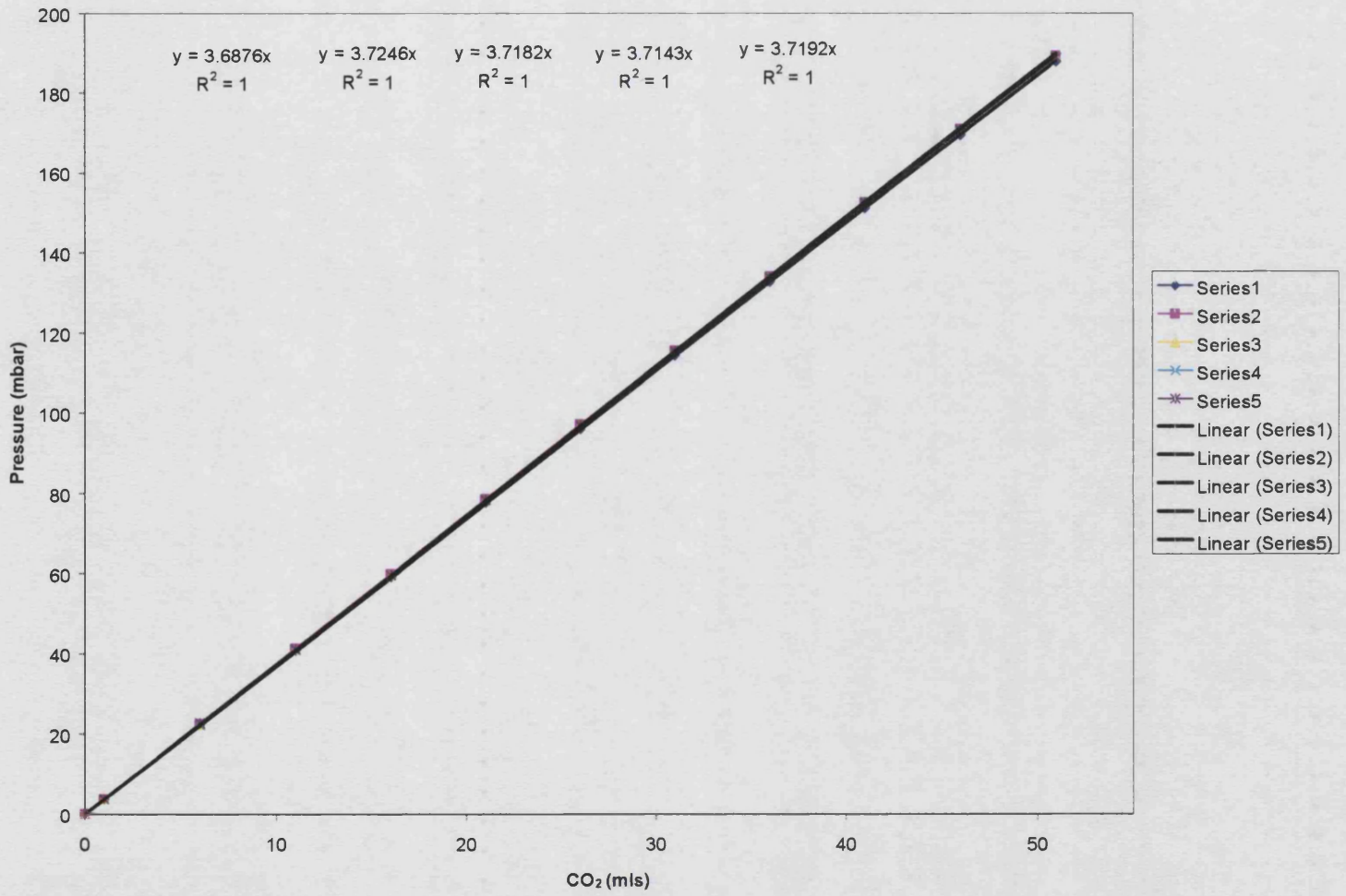

Figure 24 **A graph to show the average calibration curve for the pressure vessel containing no medium**

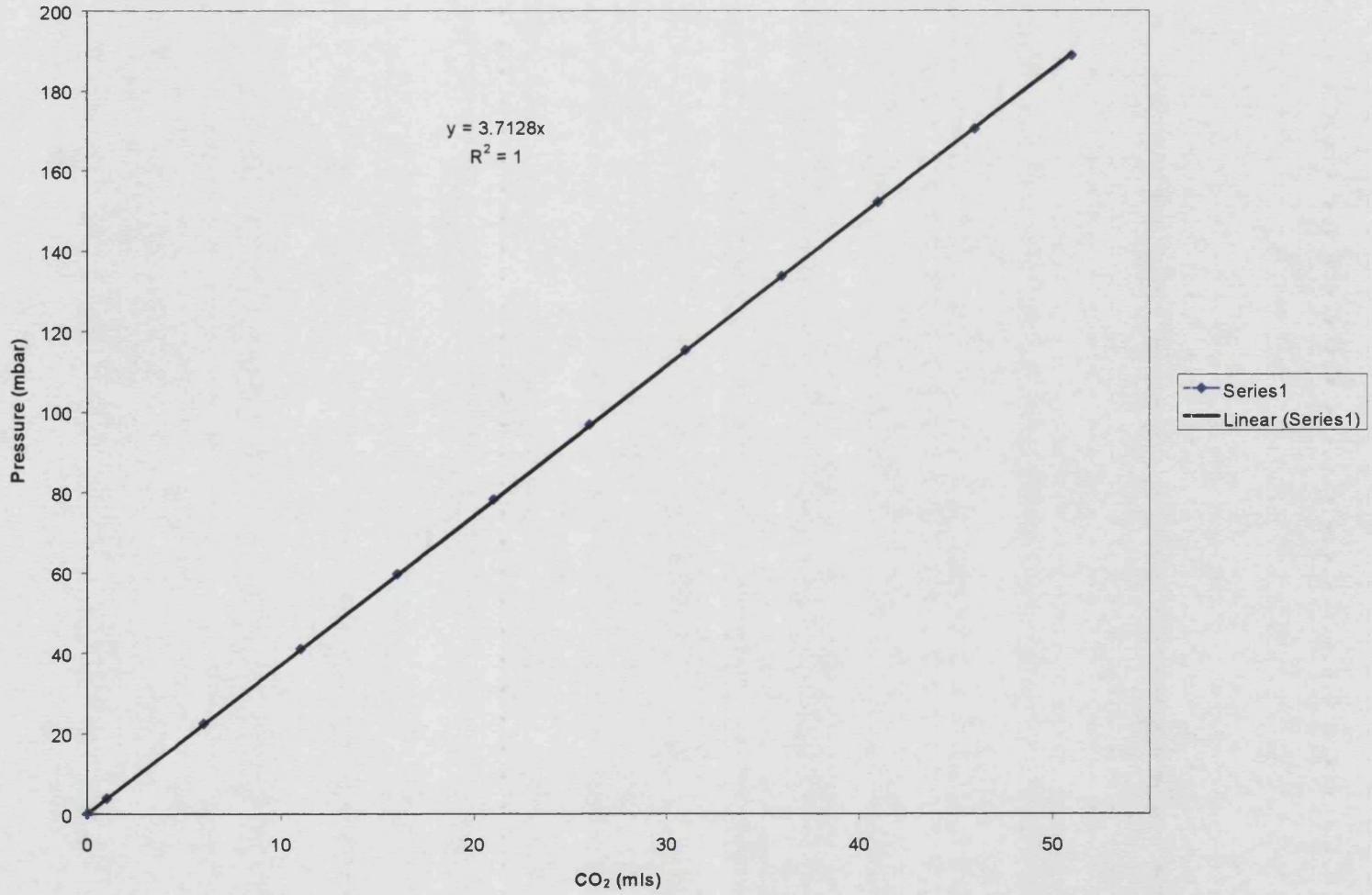

Figure 25 **A graph to show the effect that medium presence has on the calibration curve for the pressure vessel**

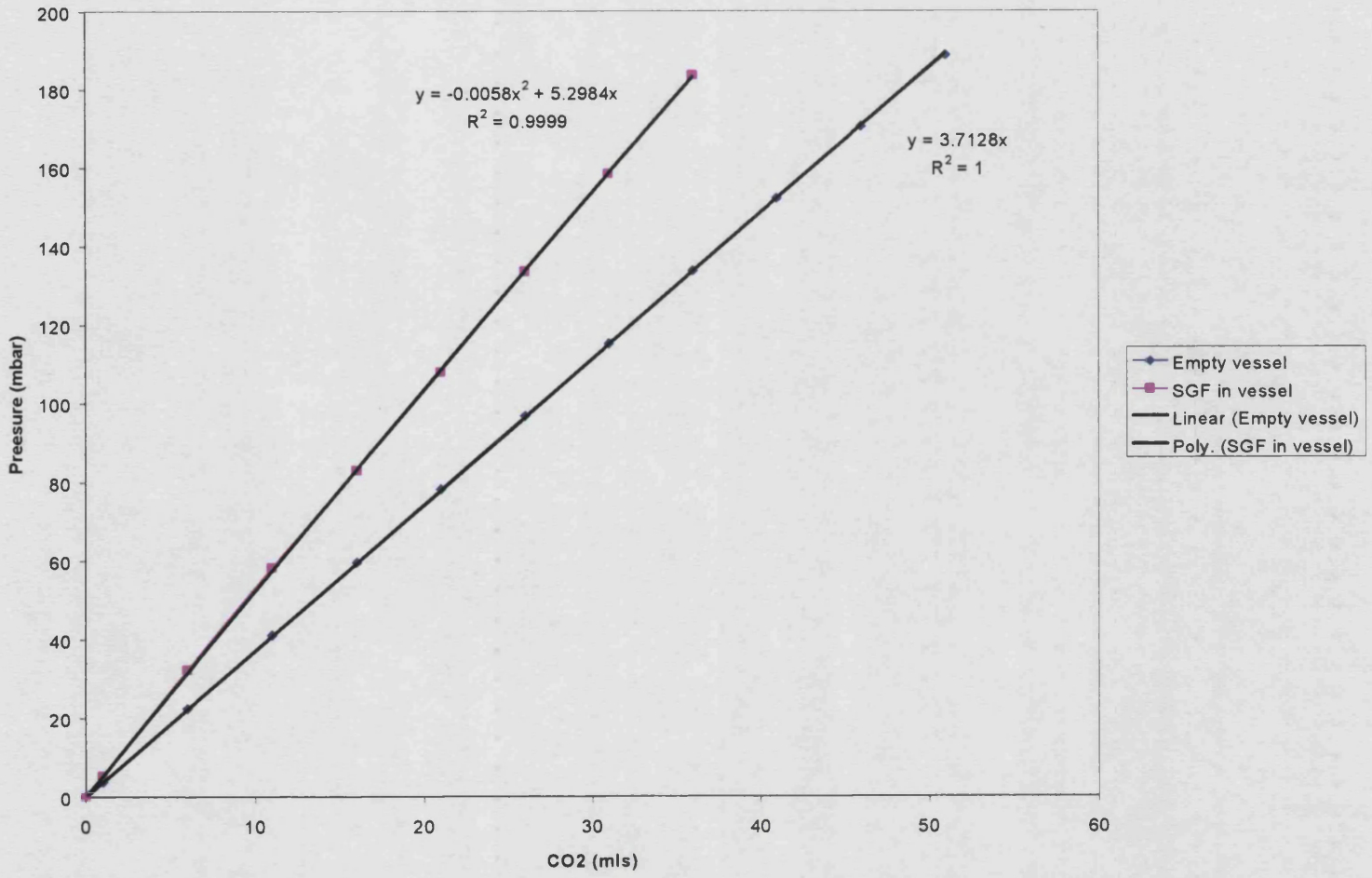

The predictable curve that is seen when SGF fluid is used in the vessel is due to the experimental conditions. The pressure readings were taken 5 minutes after the addition of CO_2, not when the pressure in the vessel had reached equilibrium. When the CO_2 was first injected into the vessel the pressure reading reached a peak level before dropping off slowly, until equilibrium is reached. This is thought to represent the slow incorporation of injected CO_2 gas into the liquid phase, presumably as carbonic acid. This transition causes the pressure in the gas phase of the system to slowly decrease until equilibrium is reached. However, as the overall pressure in the vessel increases with each further addition of gas, so the rate of CO_2 transition increases. This therefore leads to the predictable curve that is seen in the calibration graph.

The calibration performed without liquid further proves the equilibration theory, and validates the fact that no leaks are occurring in the vessel. A linear response was seen as expected, due to the inverse relationship that exists between volume and pressure. We can therefore deduce that the curve seen previously was due to the presence of fluid in the vessel.

The overall pressure levels seen were much lower when compared with the fluid filled vessels. This is due to the increase in the gaseous phase volume that occurs when the fluid is removed from the vessel.

As the vessel has now been calibrated successfully, it is possible to move onto testing dosage forms. The testing of dosage forms will be discussed in future chapters.

CHAPTER 5

IN VITRO ANALYSIS OF A GAS-POWERED, FLOATING DOSAGE FORM

5.1 Introduction

The previous two chapters have discussed the development of apparatus capable of accurately measuring parameters intrinsically associated with gas-powered floating dosage forms. Thus far, methods have been developed that are capable of measuring the buoyancy and/or gas release of a dosage form over a pre-determined time period.

This chapter will discuss the *in vitro* testing of a particular gas-powered floating dosage form using the developed test methods. It will also introduce a test to measure the swelling evolution of dosage forms, before attempting to rationalise the resulting profiles that are seen. The initial surface area of the tablets will also be studied to assess the effect that this has on the buoyancy profile.

It is envisaged that this *in vitro* array of testing methods will be used to explain the buoyancy profiles produced by different dosage forms, thereby allowing the formulator to systematically produce a dosage form with optimal floating capability.

5.2 Choice of dosage form

Before testing could begin, it was first necessary to select a suitable gas-powered floating dosage form. A formulation that had been previously developed by Ranbaxy Ltd (India) was chosen as the initial candidate. This formulation was selected as the constituents/parameters of the tablet were already known and could therefore be easily re-produced in the laboratory (see Table 4, page 72). The tablets selected were known to float *in vivo* for approximately 8 hours, making them an ideal candidate for further investigation. The formulation is described in detail in US patent 6261601.

Table 4 Blend Constituents of initial test formulation

Excipient	mg per tablet
Ciprofloxacin	1000
Sodium Alginate	5
Xanthan Gum	15
Sodium Bicarbonate	200
XL PVP	177
Magnesium Stearate	
Intra-granular	26
Inter-granular	7
Talc	10
Total Weight	1440

5.3 Manufacture of dosage forms

5.3.1 Initial manufacturing method

It was decided to make a 150g batch of the initial blend so that enough tablets would be available for all future tests.

The tablets were prepared according to the following method, which was adapted from the original preparation method (US patent 6261601) for use in the laboratory:

- All excipients, excluding the inter-granular magnesium stearate, were weighed out onto a balance (A&D HF1200G, A&D instruments, Oxford, UK) and placed together into a glass jar. The jar was shaken by hand to roughly mix the excipients.
- The mix was then screened through a 44-mesh sieve (Endecotts, London, UK) in order to break up any aggregates.
- The sieved mix was placed into a clean glass jar and blended on a low shear, turbula mixer (Glen Creston, Stanmore, UK) for 20 minutes at a rate of 20 rpm. The jar size was chosen so that the mixture occupied approximately half of the jar volume, leaving plenty of room for mixing.

- The blend was then slugged using an F-press (Manesty, Liverpool, UK) equipped with 20mm tooling. The dye was hand filled and the F-press was manually operated.
- The slugs were dry-granulated through a 1mm-mesh screen (Frewitt, Fribourg, Switzerland)
- The inter-granular magnesium stearate was weighed out and added to the granular blend, which was then mixed in a glass jar for a further 10 minutes at 20rpm using the same turbula mixer.
- The blend was tabletted using an F-press equipped with specially made caplet tooling, measuring 21.5mm by 10mm. Using an A&D HM120 balance (Oxford, UK), approximately 1.446g of blend was weighed out onto a plastic weighing boat and transferred to the die. The punches were turned over by hand to compact the tablet.
- Each tablet was made to a hardness of approximately 18KPa.

The tablets were weighed out individually and the F-press turned over by hand, so as to decrease the variability that would be seen between tablets. It was imperative that the tablets produced in the batch were as similar as possible at this stage as later tests would be looking at trends between batches.

Approximately 50 tablets were made from the original blend, but many tablets also capped during manufacture. It was thought that the capping was due to the "sticky" nature of the ciprofloxacin.

Problems were also encountered during the initial de-aggregation stage (44-mesh). It was not possible to force some of the ciprofloxacin through the fine mesh and therefore some of the material was lost from the blend.

The tablets that were produced were tested using an array of in vitro tests to assess both their dry and wet parameters.

5.4 Results from initial batch

5.4.1 Weight variation

The tablets were assessed according to the method outlined in section 2.3.5, page 15. Results are shown below in Table 5, page 74.

Table 5 A table to show the weight variation in batch 1

Tablet no.	Weight (g)
1	1.4407
2	1.4391
3	1.4393
4	1.4361
5	1.4412
6	1.4400
7	1.4405
8	1.4406
9	1.4385
10	1.4425
Average	1.4399
Standard deviation	0.001742

The tablets had an average weight of 1.4399g and a standard deviation of 0.001742.

Most of the tablet weights were grouped closely together, however one or two tablets were some distance from the mean. It was thought that this was due to the sticking of the ciprofloxacin onto the punch faces during compaction. It is thought that the batch tightness could be improved in future manufacturing runs.

5.4.2 Hardness testing

The tablets were assessed according to the method outlined in section 2.3.4, page 15.

The results are shown below in Table 6, page 75.

Table 6 A table to show the hardness variation in batch 1

Tablet no.	Hardness (KPa)
1	17.0
2	19.6
3	16.2
4	19.4
5	13.8
Average	17.2
Standard deviation	2.41

The tablets had an average hardness of 17.2KPa, with a standard deviation of 2.41.

The high standard deviation of this batch of tablets caused concern. A variation in tablet hardness will affect the initial density of the dosage form and therefore the floating properties of that dosage form. It is possible that swelling and gas release characteristics may also be affected.

The variation that was seen was possibly due to the non-uniformity of the blend. The blend manufacture will therefore be altered in future runs.

5.4.3 Buoyancy testing

Three tablets from batch 1 were tested in the buoyancy apparatus to ascertain if a distinct difference could be seen between the tablet traces and the baseline results from the earlier work in Figure 10, page 35. The tablets were tested using the method outlined previously in section 3.8, page 33.

The results are shown graphically in Figure 26, page 76.

Figure 26 **A graph to show the resultant weight profiles of three tablets from blend 1**

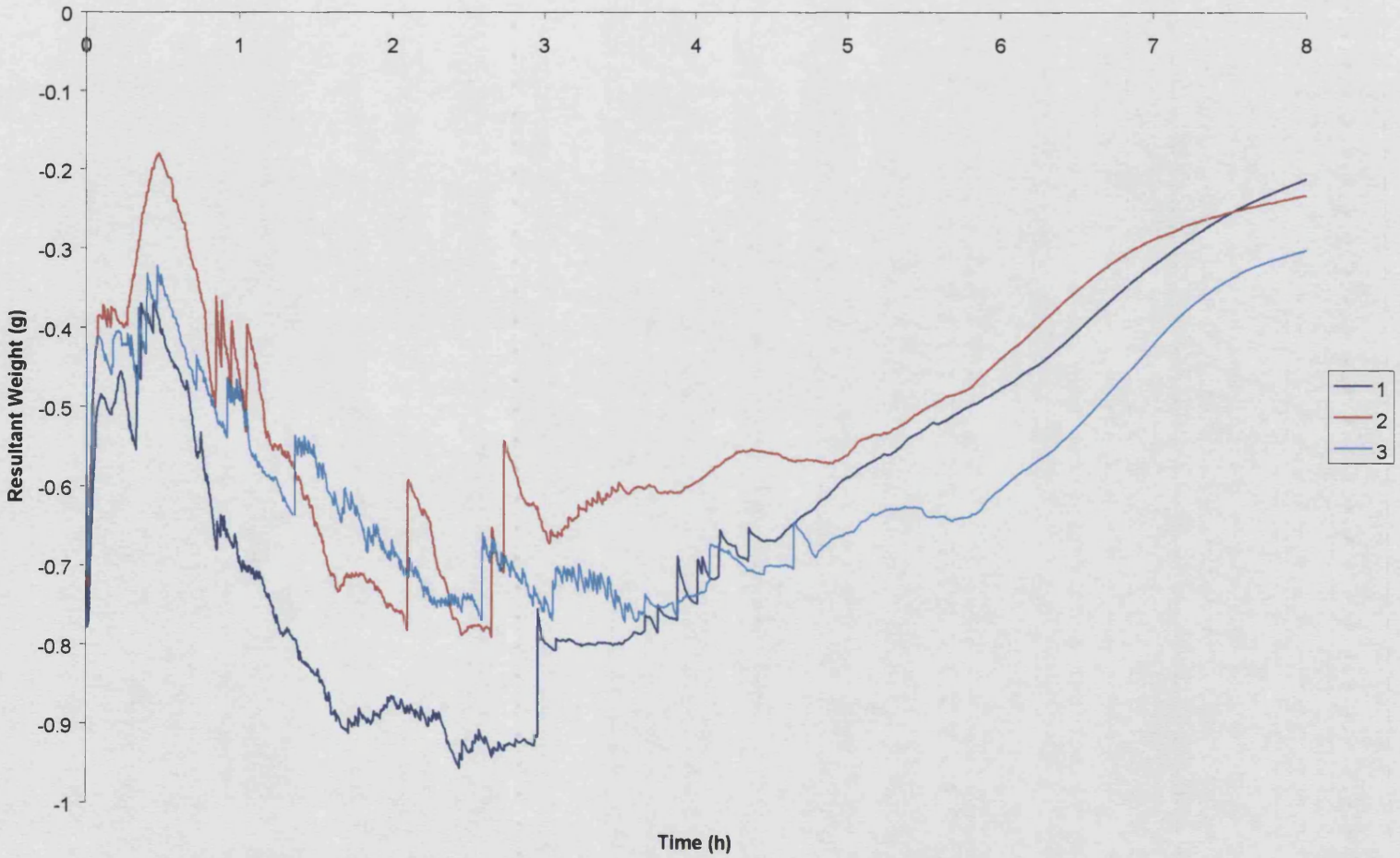

The buoyancy profiles produced for the three tablet runs were at least an order of magnitude different from the buoyancy seen due to water loss. This indicates that the apparatus is a suitable indicator of floating force, and that it can be used as a future tool for buoyancy comparisons.

The profiles produced all followed a very distinctive pattern over the course of the experiment, and although the magnitudes of the forces were not always identical, they were relatively close throughout the run.

The graphs show that all the tablets had an initial buoyancy period as soon as they were immersed in the medium. It is thought that this initial buoyancy is a combination of the polymers within the tablet swelling and gas production. The swelling of the tablet causes an increase in the buoyancy effect that is seen. This is due to a corresponding decrease in the density of the dosage form, caused by the increase in volume. The production of gas will also inevitably add to the buoyancy effect that is initially seen. Some of the gas that is produced as the bicarbonate reacts with the acid medium will get trapped within the polymer network of the tablet, therefore helping the tablet to float.

Following the initial buoyancy period the graphs exhibited a slow decrease in buoyancy up until approximately 30 minutes had elapsed. This period probably arises as the tablet has now swollen to its full capacity and the gas that had been generated, and initially trapped, slowly releases as the polymer matrix relaxes.

A second slower buoyancy increase then becomes apparent in all the traces. This increase continues until approximately 3 hours after the start of the experiment. It was thought that this second phase of buoyancy was due to erosion of the tablet front, resulting in an increase in the surface area to mass ratio within the tablet. Gas is still thought to be evolving from the tablet at this time, but it may now be more effectively trapped within the polymer network, resulting in a more buoyant system.

After 3 hours until the end of the tests, the buoyancy is seen to decrease. This is probably due to a reduction in gas evolution and the release of previously trapped gas from the matrix. However, all tablets were buoyant throughout the duration of the test.

At various points of the test all profiles exhibit a "jumping" effect where there is a sudden loss of buoyancy. This is thought to be due to bubbles of CO_2 escaping from the polymer matrix and therefore their contribution to buoyancy is lost. All of the various hypotheses can be further investigated using gas release and swelling studies.

5.4.4 Helium pycnometry and mercury porosimetry

To fully understand floating dosage forms it is vital to have the capability to characterise the formulation both before and during testing. Mercury porosimetry can be used to assess the pore structure of the dosage form before testing. It is possible that changing the pore size / structure within a dosage form may have a direct effect on the formulation's interaction with surrounding mediums, especially during the initial periods of wetting and subsequent swelling. It is already known that the degree of swelling will have an effect on the density of a dosage form, therefore it follows that variation of the pore size / structure may yield similar effects.

A second reading that can be taken during mercury porosimetry is bulk density. The initial bulk density of a floating dosage form is of importance as it dictates whether or not the formulation will float when placed into a medium. The bulk density will then change over time as the formulation interacts with the surrounding medium, however this change can be measured using the buoyancy apparatus described earlier.

Mercury porosimetry is therefore a powerful technique that can be used to help to further understand the mechanisms contributing towards the ability of a formulation to float. However, before the technique can be used to measure the tablets, the size and volume of the stem to use during the experiments must be decided. In order to do this it is necessary to first calculate the true density of the blend using helium pycnometry. The true density can then be used to calculate the rough porosity of the tablets, which will then help to decide which porosimetry equipment to use for future testing.

5.4.4.1 Helium pycnometry and calculations

Helium pycnometry was used to calculate the true density of the blend. An accupyc 1330 (Micromeritics, Norcross, USA) was used, and was set to take 10 density readings.

The average density of the blend was determined to be 1.5547 g/cm^3. From this true density value it is possible to calculate the rough porosity of the tablets. In order to do so the volume (1) and weight (2) of those tablets must be known and used to calculate the volume of powder in each tablet.

(1) The volume of the tablets was roughly calculated to be equal to:

21.5mm X 10mm X 8mm

= 1.72cm^3

(2) The weight of the tablets was known to be approximately 1.44g.

The volume of powder actually in each tablet can be determined by calculating:

Volume of powder in the tablet = Mass of tablet / True density of blend

= 1.44g / 1.5547g/cm^3

= 0.926cm^3

The rough porosity of the tablets can then finally be calculated as:

Rough porosity = Bulk volume of tablet - Volume of powder in the tablet

= 1.72cm^3 - 0.926cm^3

= 0.79cm^3

When performing mercury porosimetry, optimum results are achieved when the porosity of the tablet is between 25% and 90% of the mercury stem volume. A stem volume of **1.131cm^3** will be therefore be used in all future experiments with tablets of this kind.

5.4.4.2 Mercury porosimetry

Having decided which equipment to use, tablets were tested according to the protocol outlined in paragraph 2.3.1, page 14. The tablets were tested in triplicate to assess reproducibility on this occasion, as it was believed that some variation in tablet properties might have occurred during manufacture. See Table 7, page 80 for results.

Table 7 **A table to show the mercury porosimetry results for tablets made from blend 1**

	Run 1	Run 2	Run 3	Average
Intrusion volume ml/g	0.2163	0.2348	0.2309	0.2273
Median pore diameter (vol.) μm	0.1140	0.1239	0.1233	0.1204
Bulk density g/ml	1.1787	1.1730	1.0866	1.1461
Apparent density g/ml	1.5820	1.6189	1.4506	1.5505
Porosity %	25.49	27.54	25.09	26.04

The results were seen to be reproducible for the three tablets, despite the inherent weight variation present in the tablets. The technique will therefore be useful for future batches. The bulk of the pores detected were between 0.1μm and 0.2μm in diameter. It is possible that there may be some correlation between the pore size and initial wetting / swelling of the tablets. The bulk density of this set of tablets was 1.1461 g/ml, indicating that the tablets should sink when placed in the SGF medium, however the tablets interact with the medium such that they soon float.

All future blends will also be tested with the complementary technique of nitrogen adsorption in order to investigate the pore size distribution further.

5.5 Changes to blending methodology

Due to the inherent variation in basic tablet parameters seen with the previous manufacturing conditions, it was decided to alter the methodology in order to improve reproducibility.

The main problem encountered during tablet manufacture was the sticking of the blend to the punches and the capping that this produced. It was thought that this was a direct consequence of poor mixing of the blend, resulting in an uneven distribution of lubricant. In order to remedy this situation it was decided to alter three steps of the previous manufacturing method:

1 All magnesium stearate will be screened through a 60-mesh sieve using a sieve shaker (Octagon digital, Endecotts, London, UK) to deaggregate agglomerates. This step should ensure that the lubricant is able to disperse evenly throughout the blend once it has been added.

2 Pre-blend will now be initially screened through a 22-mesh sieve, rather than the 44-mesh screen used previously. An automated sieve shaker will again be used for this process. Some of the blend had been lost in the previous manufacture as the 44-mesh screen size had been too small.

3 Tablet punches will be wiped clean after each tablet has been produced, in order to limit the chances of tablet capping.

5.6 Formulation, manufacture and testing of blends

Having assessed the initial blending methodology and made the necessary alterations, a second blend, consisting of identical excipients (see Table 4, page 72), was made and tested. The methodology for the blending and tableting of this blend is shown below:

- All magnesium stearate was screened through a 60-mesh sieve using a sieve shaker (Octagon digital, Endecotts, London, UK) to deaggregate agglomerates.

- All excipients, excluding the intra-granular magnesium stearate, were weighed out onto a (A&D HF1200G, A&D instruments, Oxford, UK) balance and placed together into a glass jar. The jar was shaken by hand to roughly mix the excipients.
- The mix was then screened through a 22-mesh sieve (Endecotts, London, UK), using a sieve shaker, in order to break up any aggregates.
- The sieved mix was placed into a clean glass jar and blended on a low shear, turbula mixer (Glen Creston, Stanmore, UK) for 20 minutes at a rate of 20 rpm. The jar size was chosen so that the mixture occupied approximately half of the jar volume, leaving adequate space for mixing.
- The blend was then slugged using an F-press (Manesty, Liverpool, UK) equipped with 20mm tooling. The dye was hand filled and the F-press was manually operated.
- The slugs were dry-granulated through a 1mm-mesh screen (Frewitt, Fribourg, Switzerland)
- The inter-granular magnesium stearate was weighed out and added to the granular blend, which was then mixed in a glass jar for a further 10 minutes at 20rpm using the same turbula mixer.
- The blend was tabletted using an F-press that was equipped with specially made caplet tooling, measuring 21.5mm by 10mm. Using an A&D HM120 balance (Oxford, UK), approximately 1.446g of blend was weighed out onto a plastic weighing boat and transferred to the die. The punches were turned over by hand to compact the tablet. The punches were wiped clean after each compaction to avoid tablet capping.
- Each tablet was made to a hardness of approximately 18KPa.

Approximately 50 tablets were made, and there were no obvious problems during manufacture, which indicated that the alterations to the methodology were successful. The tablets were then tested for uniformity.

5.6.1 Weight variation

The tablets were assessed according to the method outlined in section 2.3.5, page 15. Results are shown below in Table 8, page 83.

Table 8 A table to show the weight variation in batch 2

Tablet no.	Weight (g)
1	1.4403
2	1.4425
3	1.4419
4	1.4434
5	1.4432
6	1.4401
7	1.4411
8	1.4401
9	1.4428
10	1.4415
Average	1.4417
Standard deviation	0.00127

The tablets had an average weight of 1.4417g and a standard deviation of 0.00127. This is an improvement on the results that were produced with blend 1 (Table 5, page 74). The improvement in the reproducibility of the tablet weight groupings was due to the improved blending methodology associated with this batch.

5.6.2 Hardness testing

The tablets were assessed according to the method outlined in section 2.3.4, page 15. The results are shown below in Table 9, page 84.

Table 9 A table to show the hardness variation in batch 2

Tablet no.	Hardness (KPa)
1	16.4
2	18.0
3	15.8
4	17.4
5	16.4
Average	16.8
Standard deviation	0.883

The tablets had an average hardness of 16.8KPa, with a standard deviation of 0.883. The standard deviation of this batch of tablets is again lower than for the previous batch. This was also thought to be due to the improvement in the blending methodology. The tighter grouping of the results indicates that the blend, and therefore the tablets, is more homogenous than before. This increase in homogeneity will inevitably result in more reproducible tablets that will, in turn, provide more reproducible results during later testing.

5.6.3 Buoyancy testing

Five tablets from blend 2 were tested in the buoyancy apparatus to see if an improvement in correlation could be determined after changes to the blend methodology. The tablets were tested using the method outlined previously in section 3.8, page 33. The results are shown graphically in Figure 27, page 85.

Figure 27 A graph to show the resultant weight profiles of five tablets from blend 2

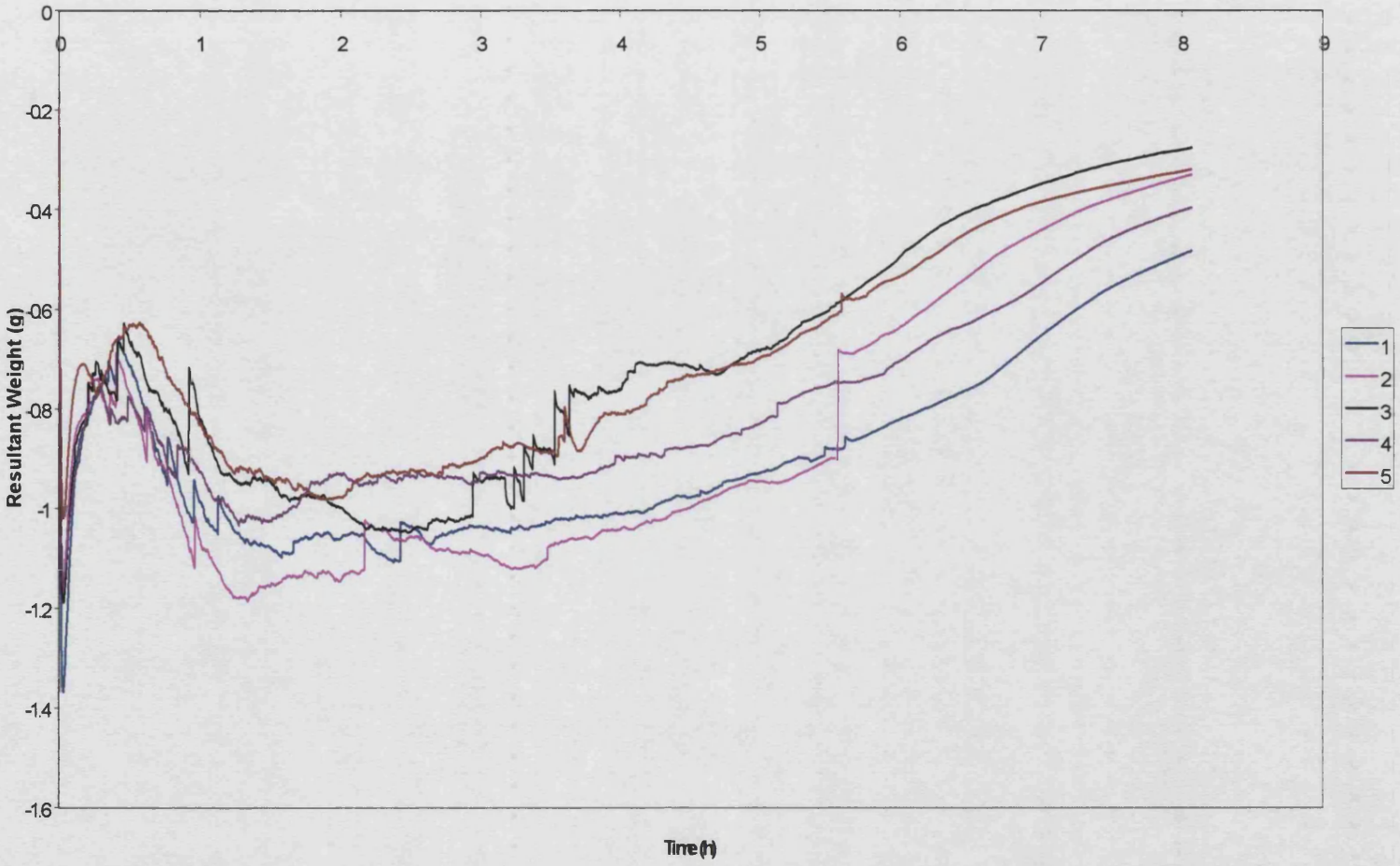

The buoyancy profiles produced for the five tablet runs were again an order of magnitude different from the buoyancy seen due to water loss previously.

The profiles produced all followed a distinctive, four-phase pattern over the duration of the experiment. The four distinct patterns have been described previously on page 77.

At various points of the test all profiles can still be seen to exhibit the "jumping" effect seen previously. This was again thought to be due to bubbles of CO_2 escaping from the polymer matrix and therefore their contribution to buoyancy suddenly being lost. All of the "jumps" show a loss of buoyancy, which would have been the case if gas were being lost from the system.

The graphs were assessed for reproducibility by measuring the area above each individual curve, as this area is a direct measurement of the buoyancy force exhibited by each tablet throughout the duration of the experiment. This method of integration was chosen as a quantitative technique due to the complex nature of the graphs. All buoyancy force data will be shown in gram hours (gh) for ease of comparison. Peakfit 4.06 for Windows was used to analyse the data sets and to produce the buoyancy force data shown in Table 10, page 86. The tablets showed a mean buoyancy force of 6.381gh during the experiment, with a standard deviation of 0.714.

Table 10 A table to show the buoyancy force data for blend 2

Tablet Number	Buoyancy Force (gh)
1	7.204
2	6.925
3	5.672
4	6.466
5	5.635
Mean	6.381
Standard Deviation	0.714

5.6.4 Pressure vessel testing

Five tablets from blend 2 were tested in the pressure vessel to assess the rate of carbon dioxide production from the formulation. The tablets were tested using the method outlined previously in section 4.9.1, page 58, with the tablet being added to the release mechanism before the vessel was sealed, and the tablet released into the medium after re-zeroing of the pressure vent.

Results of the five tablet runs are shown in Figure 28, page 88. The graph shows the data sets from the re-zero point onwards until the end of the tests. The five runs show a similar profile of carbon dioxide release throughout the duration of the test. It can be seen that CO_2 is still being released even after 7 hours of testing in all of the profiles. All tablets also show the most rapid phase of CO_2 release to be immediately after immersion into the SGF. This is to be expected as the large surface area of the tablet hydrates, causing the sodium bicarbonate in the formulation to react with the hydrochloric acid in the medium. This burst of CO_2 lasts for only a matter of minutes before subsiding for the subsequent 20-minute period. This 20 minute resting period is thought to be caused by a gel like barrier being formed on the outside of the tablet which slows down the penetration of the acidic SGF medium into the tablet core. Any fluid that does penetrate this gel layer may well have already been neutralised by the bicarbonate reaction that has taken place, resulting in a slowing of the CO_2 reaction. Following this 20-minute period, CO_2 is again slowly released until the end of the test. The rate of release initially increases before slowing from this point onwards. This was thought to be because the acid medium started to react with the tablet core, therefore re-initiating the production of CO_2 gas. The rate of gas production decreases until the end the test due to the reduction of the surface area available for interaction as the tablet undergoes constant erosion in the vessel. Figure 29, page 89, shows the average pressure accumulated in the vessel for the five tablet runs. Also shown is the rate of pressure build up during consecutive 1.5-minute periods. The graph has been normalised so that the results can be plotted onto the same axis. The graph proves the initial hypothesis, that the peak gas release rate was during the first few minutes of the test. The rate of release then slows dramatically, before slowly peaking again after approximately 1-hour. The gas release rate then slows down continuously until the end of the test.

Figure 28 **A graph to show the carbon dioxide release rate for five blend 2 tablets**

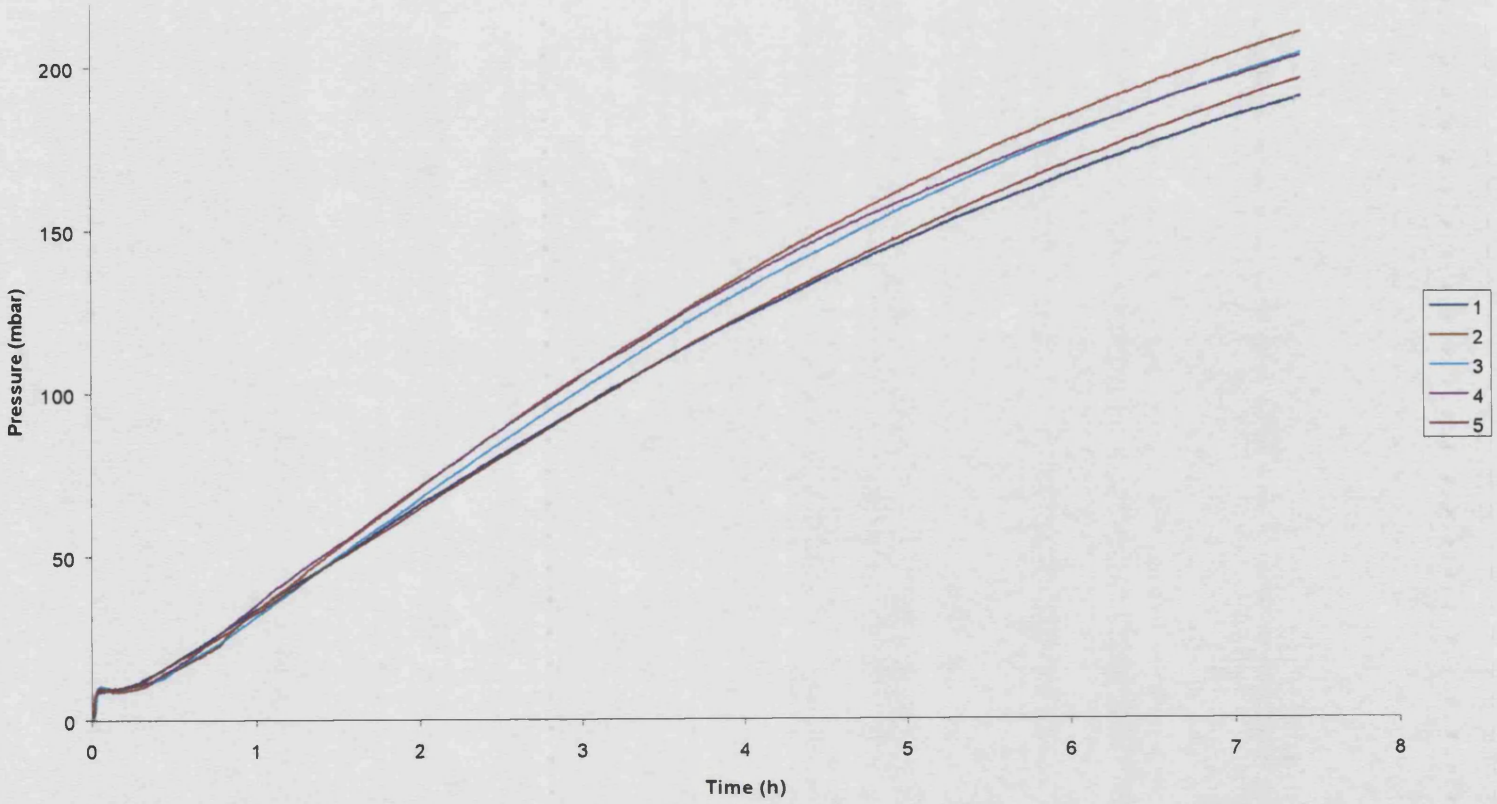

Figure 29 **A graph to show the rate of gas release during consecutive 1.5-minute periods for blend 2**

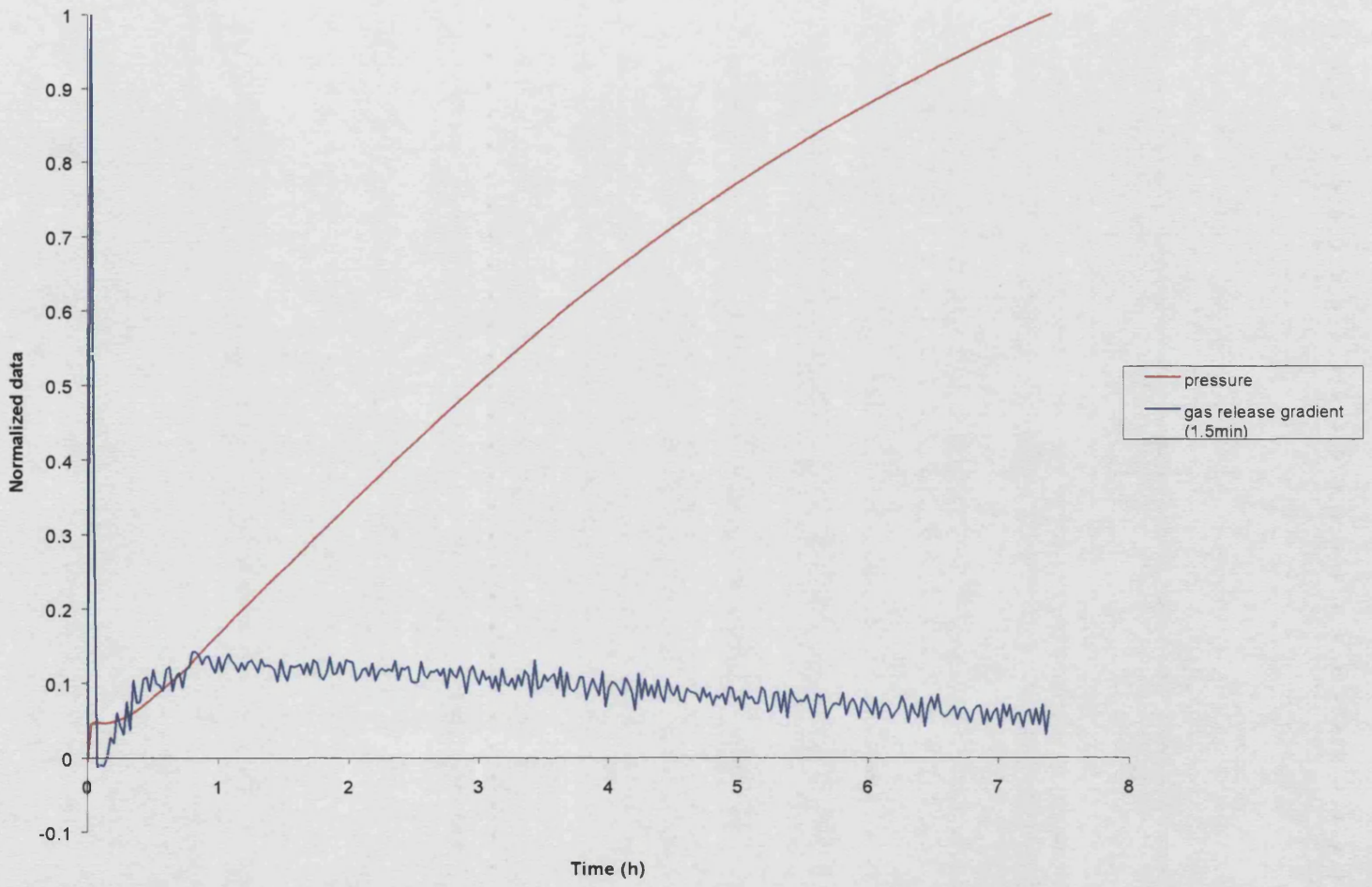

Table 11, page 90, shows a summary of the data. It can be seen from the table that all the tablets generated between 190 and 210 mbar of pressure over the 7.4-hour test duration. The small variation in results is simply due to the slightly different interaction of each individual tablet with the SGF as the experiment progresses. The average pressure generated per hour has also been calculated so that this batch can be compared with future formulations. The average pressure generated per hour for blend two varied between 25.72 – 28.37 mbar.

Table 11 CO_2 release data for the five blend 2 tablets

Tablet number	Maximum pressure generated (mbar)	Run time (h)	Average pressure generated per hour (mbar)
1	190.32	7.4	25.72
2	209.91	7.4	28.37
3	203.43	7.4	27.49
4	202.73	7.4	27.40
5	195.84	7.4	26.46

5.6.5 Mercury porosimetry

Runs were performed under the conditions discussed in 5.4.4, page 79, and tablets were tested according to the protocol outlined in paragraph 2.3.1, page 14. The tablets were tested in duplicate to assess reproducibility. See Table 12, page 91 for results.

Table 12 **A table to show the mercury porosimetry results for tablets made from blend 2**

	Run 1	Run 2	Average
Intrusion volume ml/g	0.2113	0.1967	0.2040
Median pore diameter (vol.) μm	0.1251	0.1256	0.1254
Bulk density g/ml	1.1633	1.1693	1.1663
Apparent density g/ml	1.5424	1.5186	1.5305
Porosity %	24.58	23.00	23.79

The results were seen to be reproducible for the two tablets. The bulk of the pores detected were between 0.1μm and 0.2μm in diameter, which correlated with the results seen previously for blend one. The bulk density of this set of tablets was 1.1663 g/ml, which indicates the tablets should have sunk when placed into the SGF medium, however the previous buoyancy data has shown that the tablets float upon immersion due to their immediate interaction with the gastric medium. Future blends will also be investigated using this technique to see if initial bulk density and pore size distribution has any affect on floating properties.

5.6.6 Nitrogen adsorption

The specific surface area of tablets is a parameter of interest when looking to characterise floating dosage forms. Specific surface areas can be measured using gas adsorption techniques, which depend on the ability to predict the number of adsorbate molecules required to exactly cover the surface of a material with a single molecule layer of inert gas (Brittain et al, 1991). One such technique is surface area analysis using nitrogen adsorption. This technique measures surface area and pore size based on the adsorption and desorption of nitrogen on the surface and into the pores of solids. An imbalance of atomic forces on the surface of a clean, evacuated solid attracts gas

molecules. When these molecules collide with the surface, they either bounce off or adsorb. The period of time taken for a gas molecule to adsorb on to the surface of the solid depends on the energetics of the surface with which it collides, the physical and chemical nature of the sample and the gas, and the temperature of the sample. When molecules leave the bulk of the gas to adsorb onto the surface of a sample, the average number of molecules in the gas decreases; therefore, the pressure decreases. A pressure transducer within the apparatus detects this change in pressure and determines the number of molecules adsorbed from the gas. The instrument also measures the temperature of the gas and the volume of the container used, so that the data can be used to calculate the surface area and the pore size of the material being tested. The sorption isotherms produced are interpreted using the equation developed by Brunauer, Emmett and Teller (BET) (Brunauer and Emmett, 1937). The BET equation (Equation 4, page 92) is applied over the linear range of the P/P^0 graph.

Equation 4

$$\frac{P}{V(P_0 - P)} = \frac{1}{V_m C} + \frac{(C-1)P}{V_m C P_0}$$

where V is the volume of gas adsorbed at pressure P, P is the partial pressure of nitrogen, V_m is the volume of nitrogen adsorbed in the monolayer, P_0 is the saturation pressure of nitrogen and C is a constant exponentially related to the heat of adsortion of the nitrogen gas on the sample. The surface area was determined as a product of the number of molecules in a completed monolayer and the effective cross-sectional area of nitrogen (Equation 5, page 93).

Equation 5

$$S_t = \frac{V_m N_0 A_{cs}}{M}$$

where S_t is the total surface area, N_0 is Avogadro's number, A_{cs} is the cross sectional area of nitrogen ($0.1620nm^2$) and M is the mass of the sample.

Three tablets from blend 2 were tested using the protocol outlined in section 2.3.2. The results for are shown below in Table 13, page 93.

Table 13 Results from BET surface area analysis on blend 2

Sample weight before outgassing (g)	Sample weight after outgassing (g)	BET surface area (m^2/g)
4.3259	4.2298	3.1134

The BET value of 3.1134 m^2/g that was recorded is a low value typical of many pharmaceutical excipients (Brittain et al, 1991). This value is lower than that predicted using mercury porosimetry, however this is expected as in pharmaceutical samples such as powders and tablets, total surface area values obtained with mercury porosimetry have been historically higher than those obtained with the gas adsorption method (Van Brakel et al, 1981). The existence of ink-bottle pores explains this phenomenon, as the narrow opening of the pores allows them only to be filled at the higher pressures present in mercury porosimetry. Another reason for the discrepancy is the different measurement ranges of the two techniques, with the gas adsorption technique looking at the smaller pore range (3-200nm). It is therefore necessary to use both techniques when analysing the surface area properties of tablets, so that all pore ranges can be assessed. Future blends will therefore be tested using both techniques to see whether surface area is affected by changes in the formulation. It will then be possible to see how important the initial pore size, structure and surface area are when trying to determine the floating characteristics of a dosage form.

When dealing with materials that have a low surface area it is usually prudent to use as much material as possible so as to improve correlation (Newman, 1995). However,

increasing the amount of material being tested leads to a direct increase in the time needed to outgas the sample prior to testing. In the case of the tablets made from blend 2, the outgassing already took over 12 hours to complete, thus any increase in sample size would cause problems with the length of analysis time. It is possible to reduce analysis time by heating the sample during outgassing, but increased temperatures, especially under vacuum, can change the properties of organic materials (Newman, 1995). It was therefore decided to use this set of parameters for all future tests.

5.6.7 Development of an apparatus capable of quantifying tablet swelling

5.6.7.1 Introduction

The extent with which an excipient or formulation interacts with the medium surrounding it can have a direct effect on the ability of a dosage form to float, as well as having an effect on drug release. Density is inversely proportional to the volume of a dosage form, therefore if a tablet swells when immersed in medium, so the density of that dosage form will decrease correspondingly – assuming that the mass of the system remains constant. The thickness of the gel that the swelling process produces will also have an effect on gas-powered floating dosage forms, as it would be preferential, for optimal floating, if the gel was capable of trapping gas in order to facilitate buoyancy. An *in vitro* method capable of measuring the swelling of a floating dosage form would therefore be of use to the formulator. The data from such a test could be used in conjunction with the data from previous experiments when trying to predict *in vivo* results. It is also necessary to be sure that a dosage form does not swell too much and hence potentially form a blockage *in vivo*.

A number of methods have been used to measure the swelling of floating dosage forms, including gravimetric (Gerogiannis et al, 1993) and photographic techniques. Talukdar and Kinget (1995) described one such test that had been designed to measure the swelling of dosage forms. Their work describes a technique for measuring both the axial and radial swelling of tablets. The radial swelling was measured by immersing the tablet into a beaker of 500ml of medium, underneath which was placed a piece of graph paper. At defined time intervals, the increase in tablet diameter was determined using the divisions printed on the graph paper. This technique is flawed in terms of accuracy as the method necessitates looking through the test medium in order to see how much the tablet

had swollen. Obviously the medium will have a refractive index that will alter the accuracy of the results obtained. It would also not be a suitable method for floating dosage forms due to the distance that would be present between the tablet and the graph paper, adding to the inaccuracy of the system.

The method used for axial swelling was also inappropriate. It involved the use of a dial indicator placed on top of the tablet, however the indicator inhibited the swelling seen due to the force it exhibited on the polymer system.

It was therefore decided to produce a method capable of measuring the radial swelling of floating dosage forms accurately over the course of an 8-hour period (approximate gastric residence time *in vivo*).

5.6.7.2 Original apparatus design

One litre of simulated gastric fluid (SGF) was produced according to Formula 1, page 33, and was then degassed by bubbling helium through the mixture for 1 hour to remove any dissolved gasses. The SGF was then transferred to a glass vessel, situated on a Heidolph heated plate (Schwabach, Germany), and heated to 37°C. The temperature of the medium was controlled using a feedback control directed through a thermometer in the medium, linked to the hot plate. In the centre of the glass container was placed a smaller, blacked out, plastic vessel to house the tablet. The plastic vessel was weighed down using magnetic stirrers attached to the bottom of the structure. The plastic was blacked out to improve the contrast seen in the digital photographs that were to be produced. The plastic housing was machined to such a height that its peak was just underneath the meniscus of the SGF in the vessel. The diameter of the plastic housing was such that it would not restrict the swelling of a tablet, but small enough that the tablet would be unable to float out of view of the camera.

To measure the degree of swelling a wire mesh was added to the top of the plastic housing, so that the floating tablet would sit underneath the mesh. The mesh would then provide a grid like structure through which the size of the tablet could be easily measured.

A digital camera (Fujifilm DX7, Tokyo, Japan) was suspended, by a series of clamp stands, above the SGF so that the plastic housing and floating tablet could be clearly seen in the viewer. The camera was directly linked to a P.C., so that all pictures could be instantly downloaded and analysed on screen.

5.6.7.3 Results from original apparatus

A digital photograph of the plastic housing and mesh prior to addition of a tablet can be seen in Figure 30, page 96. A tablet manufactured from blend 2 was then placed into the SGF and photographs were taken at 30-minute intervals for a period of 2 hours. Two photographs from this series can be seen in Figure 31, page 97. It can be seen from the photographs that the mesh worked well initially, both containing the floating tablet and acting as a useful measuring tool for swelling analysis. However, in the later photographs as the floating tablet breaks up, definition of the tablet boundary is lost, making analysis of swelling impossible. This brought the accuracy of the technique into question, so it was decided to remove the mesh from the plastic housing.

Figure 30 A digital photograph of the housing structure and mesh

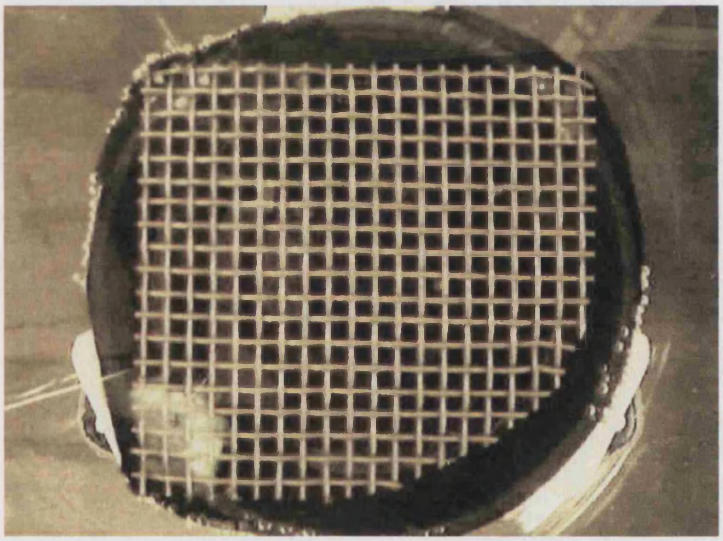

Figure 31 Two digital photographs showing the swelling of a blend 2 tablet

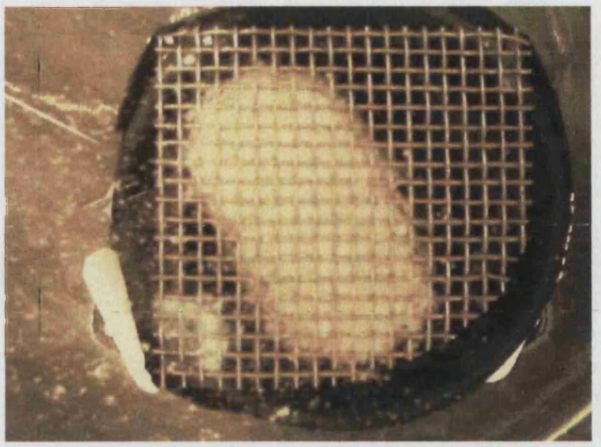

0 minutes

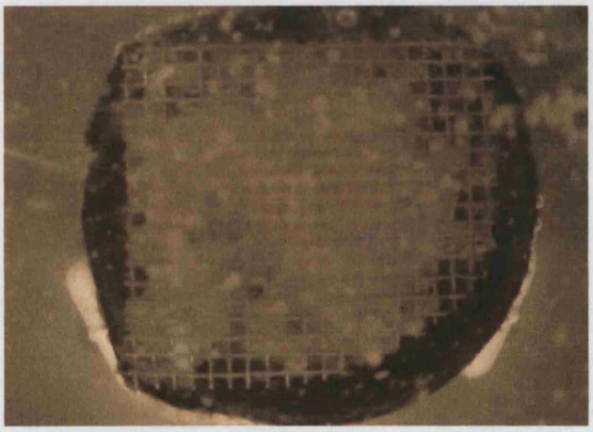

120 minutes

5.6.7.4 Modifications to the apparatus

Due to the removal of the meshwork, swelling could be no longer be measured by simple grid occlusion. To overcome this problem it was decided to use the technique of image analysis.

Image analysis is a technique whereby the cross sectional area of the tablet can be measured directly from a digital photograph. Image analysis has previously been shown to be useful for measuring the bubble formation within an alginate raft preparation (Johnson et al, 1998). To ensure that accuracy of the technique is maintained it is necessary to

calibrate the analyser prior to each calculation. To do this two perpendicular measurement gauges were integrated into the apparatus so that calibrated scales would appear on each digital photograph. The scales could then be used as a calibration tool for the image analyser. Before using the technique it was first necessary to calibrate the analyser both horizontally and vertically, before manually selecting the outside border of the swollen tablet. The image analyser then accurately calculated the cross-sectional area of the swollen tablet image.

5.6.7.5 Final methodology

- One Litre of SGF was produced according to Formula 1, page 33. Helium was then bubbled through the SGF for 1 hour in order to remove all dissolved gasses.
- The degassed SGF was transferred to the glass vessel and heated to 37°C.
- The camera assembly and plastic housing were placed into position and the time set to zero.
- A tablet from blend 2 was placed into the medium using a spatula and left to react with the medium.
- Digital Photographs of the tablet were taken after 1, 15, 30, 45, 60, 90, 120, 150, 180, 240, 300, 360, 420 and 480 minutes.
- The photographs were subjected to image analysis to determine the cross-sectional area of the swollen tablet and therefore the radial swelling.
- Tests were repeated in triplicate in order to assess reproducibility.

5.6.7.6 Results from blend 2

Sample digital photographs are shown below in Figure 32, page 99. Table 14, page 100 shows the results of the image analysis for each run, along with average values. The data for time zero was taken by subjecting a dry control tablet to the image analysis process.

The data can be seen graphically in Figure 33, page 101. From the data we can see that all three runs show similar profiles. As expected the runs do not follow identical traces. This is because each individual tablet has a slightly different interaction profile with the SGF medium, despite all tablets being made to similar specifications initially.

The overall profile of the three traces does, however, show similarities. Four distinct phases of interaction can be seen.

i. Initial rapid burst of swelling as the tablet begins to interact with the SGF in the first minute of the test.
ii. A prolonged decrease in the size of the tablet which continues up until the two and a half-hour period.
iii. A stabilisation of the tablet size that lasts until the four-hour mark.
iv. Further degeneration of the tablet that continues until the end of the test run.

Figure 32 Sample digital photographs of tablet swelling process

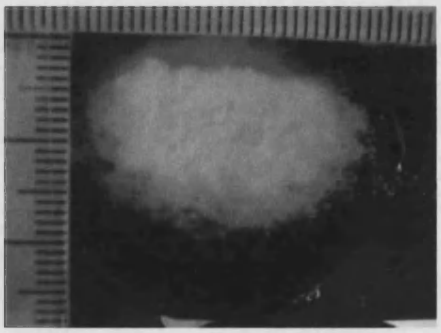

1 minute

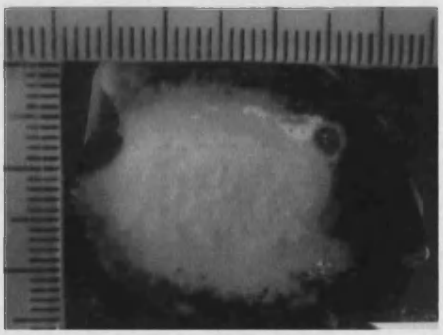

60 minutes

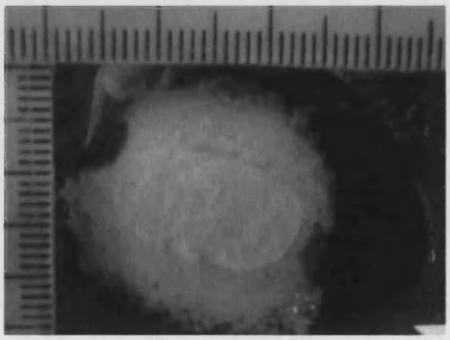

240 minutes

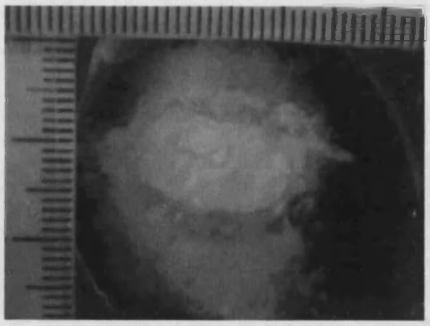

480 minutes

Table 14 Cross-sectional area data for blend 2

Time (min)	Tablet 1 area (cm^2)	Tablet 2 area (cm^2)	Tablet 3 area (cm^2)	Average area (cm^2)	Standard Deviation
0	2.1711	2.1711	2.1711	2.1711	0.0000
1	2.5799	2.3106	2.7151	2.5352	0.2059
15	2.2729	2.0343	2.3579	2.2217	0.1678
30	1.9789	2.0054	2.2307	2.0717	0.1384
45	1.8978	1.7680	1.9276	1.8645	0.0849
60	1.7610	1.6993	1.8617	1.7740	0.0820
90	1.6367	1.5461	1.7563	1.6464	0.1054
120	1.5807	1.4500	1.7063	1.5790	0.1282
150	1.5197	1.3942	1.6335	1.5158	0.1197
180	1.5139	1.3757	1.6032	1.4976	0.1146
240	1.4924	1.3386	1.5856	1.4722	0.1247
300	1.4178	1.3008	1.4116	1.3767	0.0658
360	1.1910	1.1745	1.2348	1.2001	0.0312
420	1.1893	1.0459	1.0689	1.1014	0.0770
480	1.0701	0.9846	0.9973	1.0173	0.0461

Figure 33 A graph to show the image analysis data for blend 2

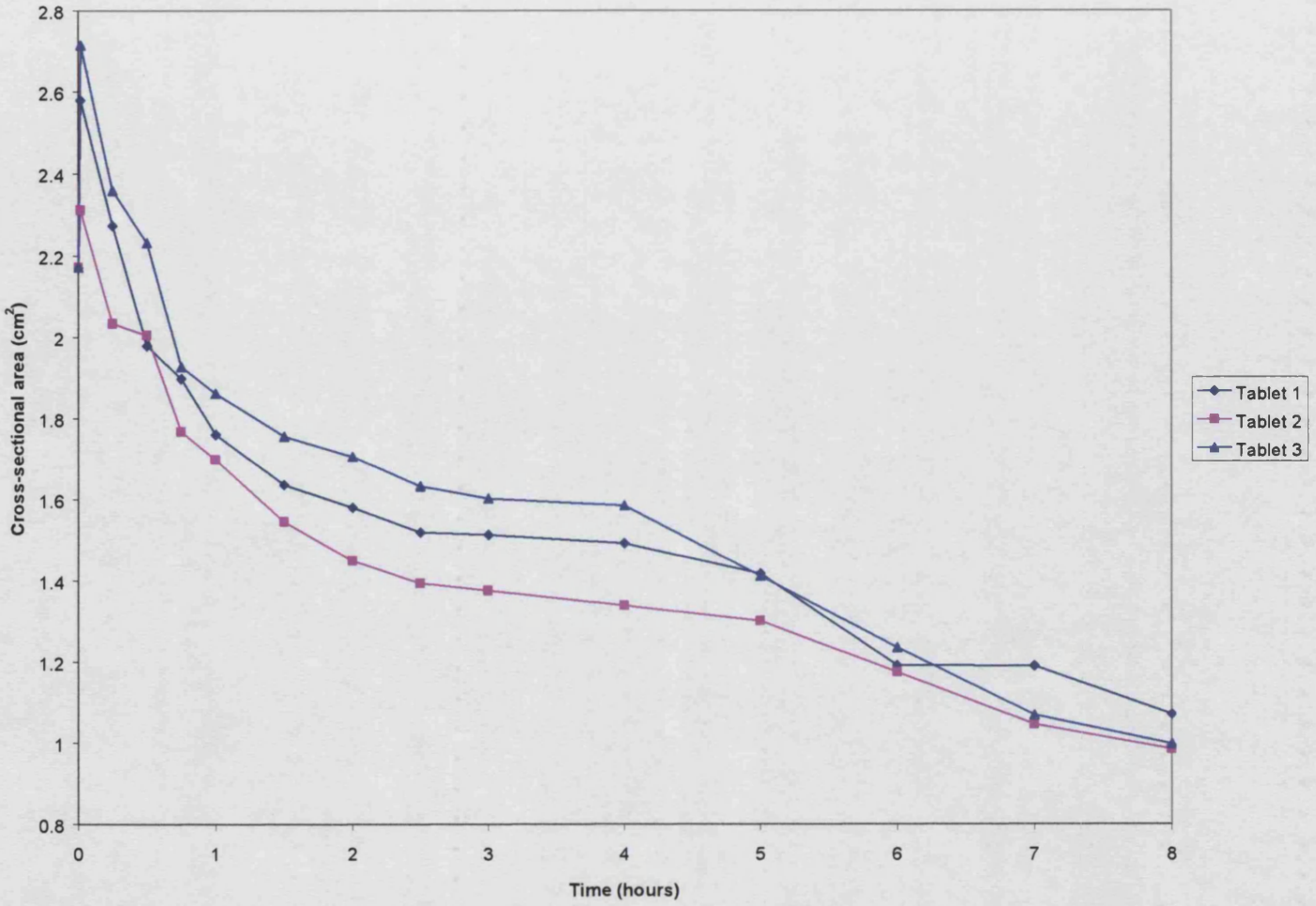

Phase i. of the graph, as described above, is due to the initial interaction of the dry tablet with the SGF. The outside of the tablet swells rapidly as the polymers in the matrix hydrate and the sodium bicarbonate interacts with the SGF to produce carbon dioxide. The carbon dioxide acts as a disintegrant and forces the tablet to expand to accommodate the gas. Some of the carbon dioxide escapes from the matrix, whilst some is thought to remain trapped in the polymer network. It is the combination of these effects that cause the initial burst of swelling as the dry tablet is submerged.

Phase ii. of the graph is seen as the tablet extremes begin to erode away from the tablet core, perhaps partly due to the disintegrant effect. The polymer matrix becomes looser and detaches from the bulk of the tablet. A shrinking effect is therefore seen.

Phase iii. of the graph can be described as a regeneration phase. It occurs when the initial layer of swollen matrix has been eroded from the core, and a second layer of dry matter begins to interact with the SGF medium. This second swelling phase is, however, countered by the constant erosion that is occurring, which produces this static phase of "growth".

Phase iv. is the final phase of degeneration that occurs as the erosion becomes quicker than the swelling phase and the tablet begins to shrink. This phase then continues until the entire tablet has disintegrated.

5.6.8 Discussion of blend 2 characteristics

Each test has so far been discussed in isolation, however it is the integration of all the tests to produce a complete overview that is the aim of this project. This section will attempt to bring together the data amassed so far, in order to explain the behaviour of blend 2 as a floating dosage form. This data will enable us to assess the specific details that enable blend 2 to float successfully for a duration of 8-hours. It will also enable us to see if the assembled barrage of *in vitro* tests yield enough information to identify the various factors that lead to the development of a floating dosage form.

The tests that have been conducted fall into two main categories:

1) Initial dry tablet characterisation
2) Dynamic wet tablet characterisation

The dry characterisation tests were essential to ensure that the tablets produced for blend 2 were as similar as possible. Both weight variation and hardness testing were

chosen as standard parameters for tablet processing quality control. The aim was to produce tablets with a weight of 1.44g and an approximate hardness of 17-18KPa. The tablets that were produced had an average weight of 1.4417g, with a standard deviation of 0.00127, and an average hardness of 16.8KPa, with a standard deviation of 0.883. These values were deemed more than adequate for the purposes of this study.

The second part of the dry testing was concerned with the surface area and pore size distribution of the tablets. Mercury porosimetry and nitrogen adsorption techniques were utilised to derive this information. The available surface area and pore size distribution may be important in determining the speed with which dosage forms interact with the SGF in the dynamic tests. It was discovered, however, that the surface areas present in the blend 2 tablets were small, which is in correlation with many other pharmaceutical products. The problem with pre-measuring the surface area and pore size of these tablets is highlighted by the dynamic changes that the tablets undergo when submerged in the SGF. The tablets undergo a dramatic change in structure that is likely to be more due to the blend formulation than the initial pore size / surface area. The relationship between initial surface area, pore size and buoyancy will be discussed in a future chapter after further formulations have been assessed. It is likely however, that the only way to assess whether varying surface area and / or pore size has an effect on initial buoyancy results, would be to produce tablets with the same formulation but varying surface areas. This is not within the scope of this project, but we will continue to utilise the mercury porosimetry and nitrogen adsorption results as a means of quality control.

The dynamic stage of testing is obviously the most pertinent to this work. Three different tests were performed to study the factors that lead to buoyancy. These were the resultant weight, the rate of gas production and the continuous swelling of the dosage form. By choosing these three parameters we are able to combine the results to try to understand why the formulation floats with a different force at particular stages of its interaction with SGF. This information will then enable understanding as to why particular formulations float for longer than others *in vivo*, enabling a better understanding of the results of previous *in vivo* work.

It is perhaps the profile of the graphs that are produced which tell us most about the dynamic changes occurring within the tablet during testing. Figure 34, page 106, shows the average data from all three dynamic tests. The data sets have been normalised in order to show the data on the same axis. The buoyancy graph shows positive data, e.g. the average resultant weight exhibited by the tablets. The swelling data is simply the average

data for the five tablets, whilst the pressure data shows the average normalised gradient (e.g. the normalised rate of gas release) of the pressure build up in the pressure vessel. The pressure gradient was calculated using 90-second intervals throughout the duration of the test.

It is seen that, as expected, the buoyancy graph can be fully explained from the swelling and rate of gas release graphs. As discussed before the buoyancy profile of the tablets can be broken down into four main sections:

1. An initial peak buoyancy period as soon as the tablets are immersed in the SGF medium.
2. After the initial buoyancy period, a rapid decrease in buoyancy until approximately 30 minutes has passed.
3. A second, slower buoyancy increase then becomes apparent in the trace. This increase continues until approximately 1-1.5 hours after the start of the experiment.
4. After 3 hours, until the end of the test, the resultant weight is seen to decrease steadily.

These four distinct sections of the buoyancy profile occurred reproducibly for all tablets tested. It is possible to use the dynamic testing data to fully explain this distinctive profile. Below is a summary of the changes that the tablet undergoes during the floating process, with each step being used to explain to the four sections of buoyancy that are seen:

1. It can be seen from the graphs that the initial buoyancy peak is a combination of the polymers within the tablet swelling and CO_2 gas production. Swelling of the tablet possibly increases buoyancy due to a corresponding decrease in the density of the dosage form, caused by the increase in volume. The gas production also inevitably adds to the buoyancy effect seen initially as some of the gas produced when the bicarbonate reacts with the acid medium is trapped within the polymer network of the tablet, therefore helping the tablet to float.

2. This period comes about as the tablet, having swollen to its peak size, begins to undergo erosion in the SGF. Though the tablet is still producing gas, the rate of production has also slowed dramatically during this period. This loss of gas production inevitably results in a loss of buoyancy to the tablet. The gas previously generated, and trapped, is slowly released as the polymer matrix relaxes, and as the rate of gas

evolution has slowed, there is no more gas to replace the lost CO_2. The release of this gas therefore causes the density of the tablet to increase, reducing the buoyancy effect.

3. The second phase of buoyancy increase is directly correlated to the second increase in gas production rate (see Figure 34, page 106). This increase in CO_2 release is possibly due to the erosion of the initial tablet front. As the tablet erodes, acid in the SGF is able to react with previously stable sodium bicarbonate, causing an increase in gas production from the blend. Some of this gas will again be trapped in the polymer matrix of the tablet causing a decrease in the density of the dosage form.

4. The final phase starts with a stabilisation of buoyancy followed by a decrease until completion of the test. The stabilisation phase is due to the size of the tablet remaining constant during this period. There is a slight decrease in buoyancy, caused by the slowing down of gas evolution, which is seen until the end of the test. This is due to the tablet again eroding away, in conjunction with the constant slowing of gas production. During this period more gas will be escaping from the matrix of the tablet, with less and less gas being produced to replace it. However, all tablets were buoyant throughout the duration of the test.

Following the development of the dynamic *in vitro* testing methodology and utilisation of the equipment to produce results capable of explaining the behaviour of a floating dosage form, it was decided to test the ability of the apparatus to detect small changes in tablet formulation. It was decided to produce two blends similar to blend two for testing purposes, and to investigate the effect on buoyancy that altering the blend formulation had. It will also test the robustness of the methodology, as the dosage forms will still be quite similar in their make up. The next section will also attempt to rationalise the findings and hypothesise on what changes should be made to the formulation to improve *in vivo* floating capacity.

Figure 34 **A graph to show the normalised dynamic testing data sets for blend 2**

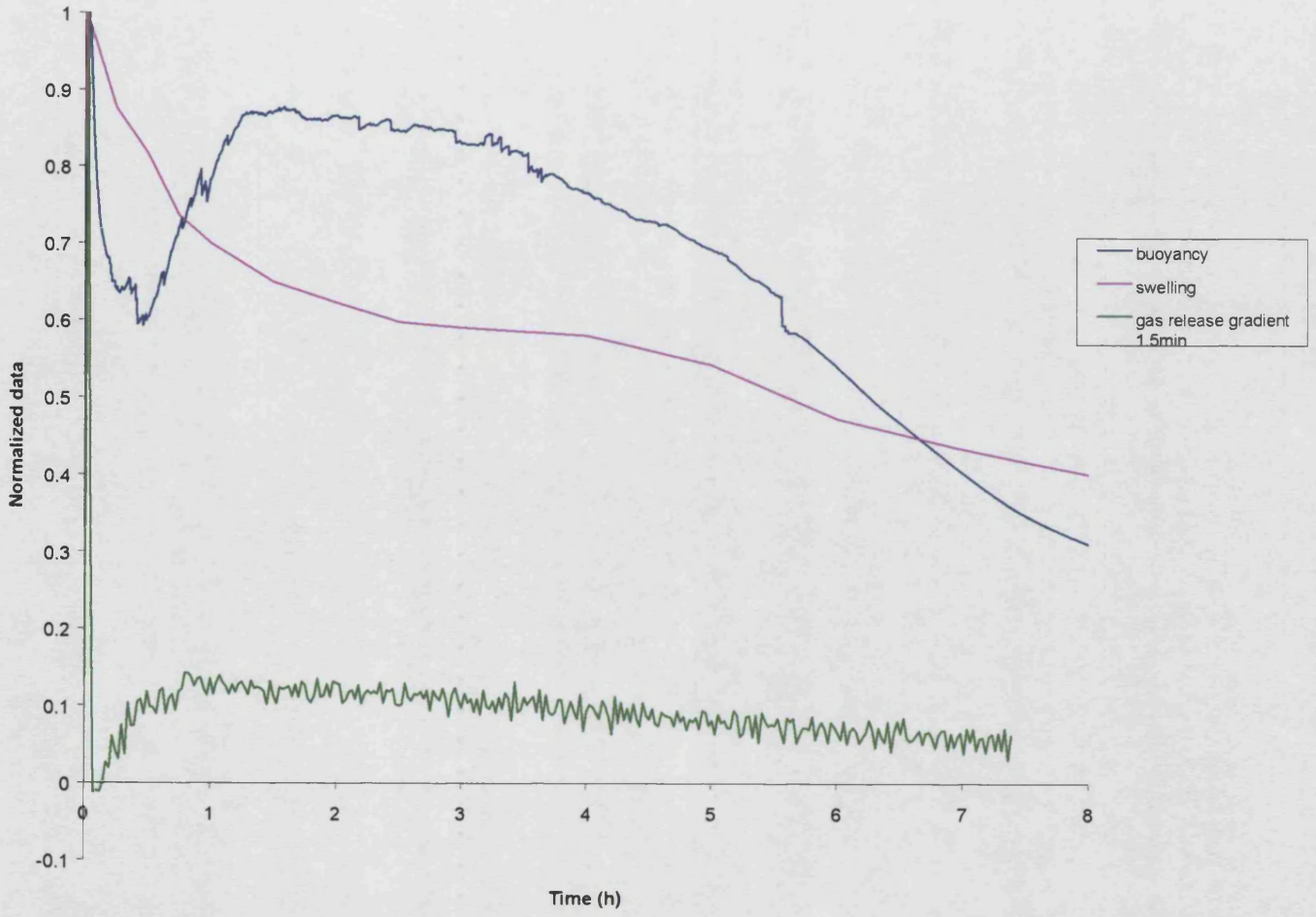

5.7 Formulation and testing of secondary blends

It was decided to test two further blends to assess if the apparatus were capable of distinguishing between similar formulations. It was also necessary to assess these dosage forms to ensure that the dynamic testing methodologies could provide accurate information capable of explaining the individual floating profiles shown by specific formulations.

Blend 2 was used as the control around which the new formulations were developed. It was decided that one of the most important components of the floating formulation was the inclusion of sodium bicarbonate. The sodium bicarbonate would therefore make an ideal parameter for alteration within the new blends. Using blend 2 as the reference point, it was decided to use twice as much sodium bicarbonate in blend 3 (400mg per tablet) and half as much in blend 4 (100mg per tablet).

It was felt that it would be important to keep the weight of the tablets, and the ratio of excipients, equal throughout the testing protocols, therefore it was also necessary to change another constituent of the blends in an equal and opposite way to that of the sodium bicarbonate. The parameter that was thought to be contributing least to the floating process was the active ingredient (ciprofloxacin) in the blend. The ciprofloxacin was therefore reduced in such a way as to keep the weight of the tablets in blends 3 and 4 equal to those in blend 2. The formulation of blends 3 and 4 are shown in Table 15, page 107.

Table 15 Blend constituents of formulations 3 and 4

Excipient	Blend 3 (mg per tab)	Blend 4 (mg per tab)
Ciprofloxacin	800	1100
Sodium Alginate	5	5
Xanthan Gum	15	15
Sodium Bicarbonate	400	100
XL PVP	177	177
Magnesium Stearate		
Intra-granular	26	26
Inter-granular	7	7
Talc	10	10
Total Weight	1440	1440

In the next section the blends will be assessed individually using the dynamic testing mechanisms and basic tablet testing theories, used for blend 2. The formulations will then be compared to assess both the robustness of the testing regimes, and the effect that changing the amount sodium bicarbonate in the blend has on floating. It should also be possible to explain how the alterations to the blend have affected the buoyancy profile, and to suggest how the current blend could be improved for future use.

5.7.1 Results from blend 3

The formulation of blend 3 is shown in Table 15, page 107. The blend was prepared and made into tablets using the protocol outlined in Section 5.6., page 81. As before, approximately 150g of the blend was made and tabletted. No obvious problems were encountered during manufacture. The tablets were then tested for uniformity.

5.7.1.1 Weight variation

The tablets were assessed according to the method outlined in section 2.3.5, page 15. Results are shown below in Table 16, page 109.

Table 16 A table to show the weight variation in batch 3

Tablet no.	Weight (g)
1	1.4422
2	1.4426
3	1.4430
4	1.4414
5	1.4430
6	1.4429
7	1.4413
8	1.4415
9	1.4427
10	1.4429
Average	1.4424
Standard deviation	0.000698

The tablets had an average weight of 1.4424g and a standard deviation of 0.000698. The tablet weights from this batch were closely grouped and deemed appropriate for the study.

5.7.1.2 Hardness testing

The tablets were assessed according to the method outlined in section 2.3.4, page 15. The results are shown below in Table 17, page 110.

Table 17 A table to show the hardness variation in batch 3

Tablet no.	Hardness (KPa)
1	17.5
2	18.2
3	17.9
4	18.4
5	17.7
Average	17.94
Standard deviation	0.365

The tablets had an average hardness of 17.94KPa, with a standard deviation of 0.365. The standard deviation of this batch of tablets is again low. The tight grouping of the results indicates that the blend and therefore the tablets are homogenous. This homogeneity will help to provide reproducible results during dynamic testing.

5.7.1.3 Buoyancy testing

Five tablets from blend 3 were tested in the buoyancy apparatus to ascertain the effect of changing the levels of sodium bicarbonate in the tablets. Five tablets were tested to further assess the reproducibility of the apparatus and testing methodology. The tablets were tested using the method outlined previously in section 3.8, page 33.

The results are shown graphically in Figure 35, page 111.

Figure 35 A graph to show the resultant weight profiles of five tablets from blend 3

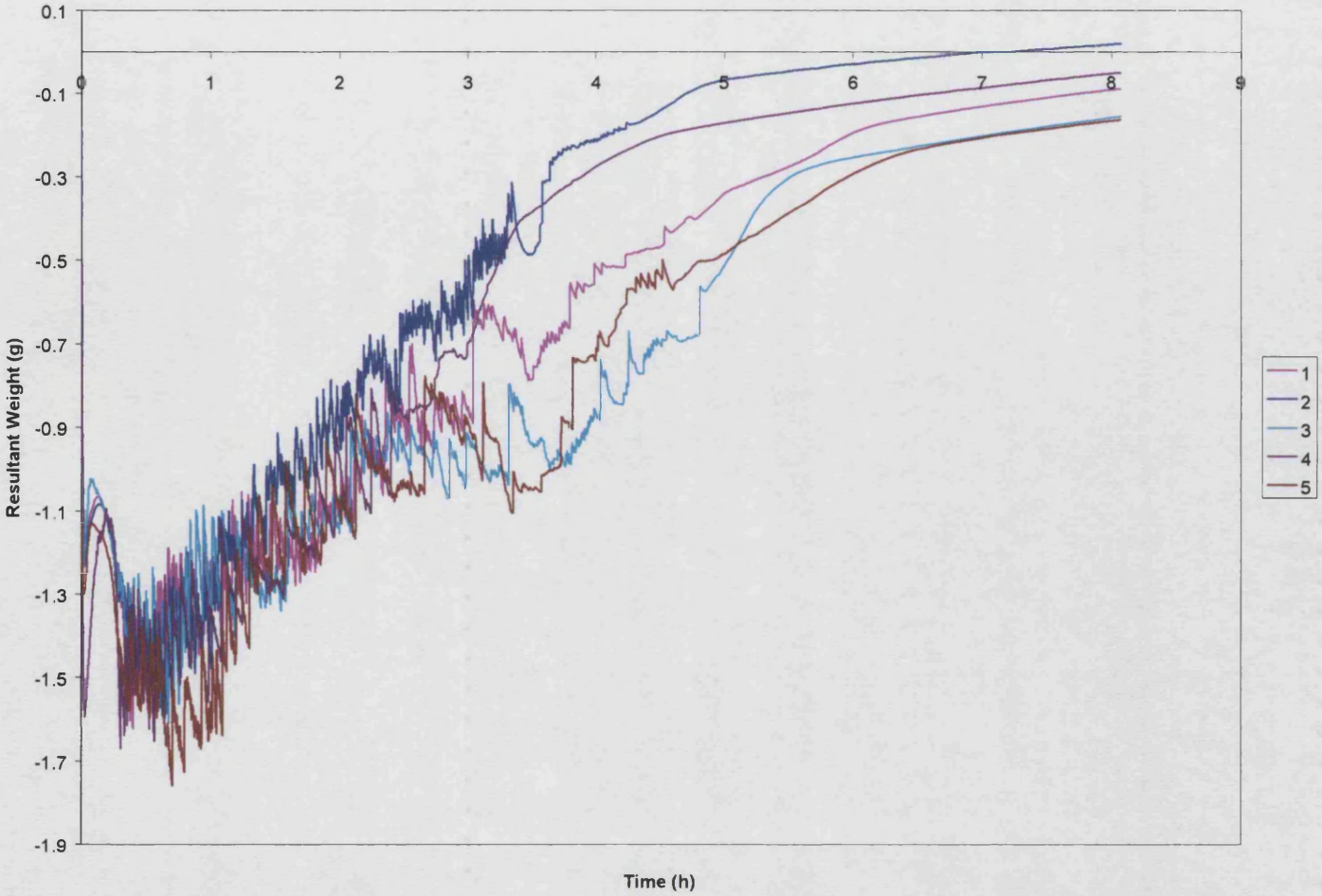

The profiles produced all followed the distinctive, four-phase pattern over the duration of the experiment. The four-phase pattern has been described previously on page 77. However, the duration of each phase differed from previous blends. It can be seen from the graphs that tablets from blend 3 begin to enter phase four after only 1 hour has passed, compared with the 3 hours seen with blend 2 tablets. It is possible that the phase time has been reduced due to the increase in sodium bicarbonate content in the blend 3 tablets.

It can also be seen from the graph that the peak buoyancy, which occurs during the first few minutes of the test, is greater when using this set of tablets. Again this is thought to be due to the increase in the sodium bicarbonate content reacting with the acid medium and driving the tablet upwards through its buoyant effect. After 8 hours, the graph shows that the 5 tablet runs are all exhibiting less buoyancy than that seen with blend 2 tablets. This decrease does not correlate with the increased quantity of sodium bicarbonate present in the tablets, as it would be expected that more CO_2 would be released throughout the test, which should aid buoyancy. However, it seems in this case that most of the sodium bicarbonate has already reacted before the test has finished.

Throughout the test all profiles exhibit a wildly fluctuating buoyancy reading. This fluctuation is greater than that of the previous blend. This was again thought to be due to bubbles of CO_2 escaping from the polymer matrix and therefore their contribution to buoyancy suddenly being lost, however, as we expected the rate of CO_2 to increase with this blend, this should come as no surprise. All of the "jumps" are once again showing a loss of buoyancy which is what we would expect if gas were being lost from the dosage form.

The graphs were assessed for reproducibility by measuring the area above each individual curve, as this area is a direct measurement of the buoyancy force exhibited by each tablet throughout the duration of the experiment. Peakfit 4.06 for Windows was again used to analyse the data sets and to produce the buoyancy force data shown in Table 18, page 113. The tablets showed a mean buoyancy force of 4.987gh during the experiment, with a standard deviation of 0.981.

Table 18 A table to show the buoyancy force data for blend 3

Tablet Number	Buoyancy Force (gh)
1	5.057
2	3.646
3	5.856
4	4.410
5	5.966
Mean	4.987
Standard Deviation	0.981

5.7.1.4 Pressure vessel testing

Five tablets from blend 3 were tested in the pressure vessel to assess the rate of carbon dioxide production from the formulation. The tablets were tested using the method outlined previously in section 4.9.1, page 58, with the tablet being added to the release mechanism before the vessel was sealed, and the tablet released into the medium after re-zeroing of the pressure vent.

Results of the five tablet runs are shown in Figure 36, page 115. The graph shows the data sets from the re-zero point onwards until the end of the tests. The five runs show a similar profile of carbon dioxide release throughout the duration of the test. The rate of CO_2 release for this blend is greater than for blend 2, which is what would have been expected due to the increased percentage of sodium bicarbonate present in blend 3. In fact, the amount of CO_2 released by the tablets soon exceeds the internal calibration limits of the pressure vessel. The limit is exceeded 1.5 – 2 hours after the tests started. The gas release rate for this batch can therefore only be measured for the length of time that the pressure remains within the calibration limits of the vessel.

All tablets still show the most rapid phase of CO_2 release to be immediately after immersion into the SGF. This is due to the large surface area of the tablet rapidly hydrating, causing the sodium bicarbonate near to the surface of the tablet to react with the hydrochloric acid in the medium. The resulting burst of CO_2 lasts for only a couple of minutes before subsiding for the subsequent 20-minute period. The 20 minute resting

period is thought to be due to a gel barrier being formed on the outside of the tablet which slows down the penetration of the acidic SGF medium into the tablet core. After this 20-minute period, CO_2 again begins to be released until the end of the test. The rate of release increases initially before slowly decreasing from this point onwards. This phase of gas release is thought to be due to the acid medium reacting with the previously shielded core of the tablet, therefore re-initiating the production of CO_2 gas. The rate of gas production decreases until completion of the test due to the diminishing size of the surface area available for interaction with the medium as the tablet undergoes constant erosion.

Figure 37, page 116, shows the average pressure accumulated in the vessel for the five tablet runs. Also shown is the rate of pressure build up during consecutive 1.5-minute periods. The graph has been normalised so that the results can be plotted onto the same axis. The graph confirms that the peak gas release rate was during the first couple of minutes of the test. The rate of release then slows dramatically, before peaking again after approximately half an hour. The gas release rate then slows down continuously until the end of the test. Each phase of the gas release follows the same profile as blend 2, however blend 3 undergoes each phase over a shorter period of time.

Table 19, page 117, shows a summary of the data. It can be seen from the table that all tablets easily generated 210 mbar of pressure, the maximum pressure that the vessel could accurately measure. Each tablet took a slightly different time to achieve this pressure; the variation in time being due to the slightly different dynamic interaction of each tablet with the simulated gastric fluid. It should be noted that the maximum pressure generated by this set of tablets was determined by the calibration restriction of the pressure vessel, not by the amount of CO_2 being produced by the tablets. If the vessel had been able to measure higher pressures, then it would have shown that these tablets produced pressures in excess of 210 mbar. The average pressure generated per hour has therefore been calculated in order to enable the rate of gas release for this batch to be compared with other batches. The average pressure generated per hour for blend three varied between 99.45 – 141.88 mbar.

Figure 36 A graph to show the carbon dioxide release rate for five blend 3 tablets

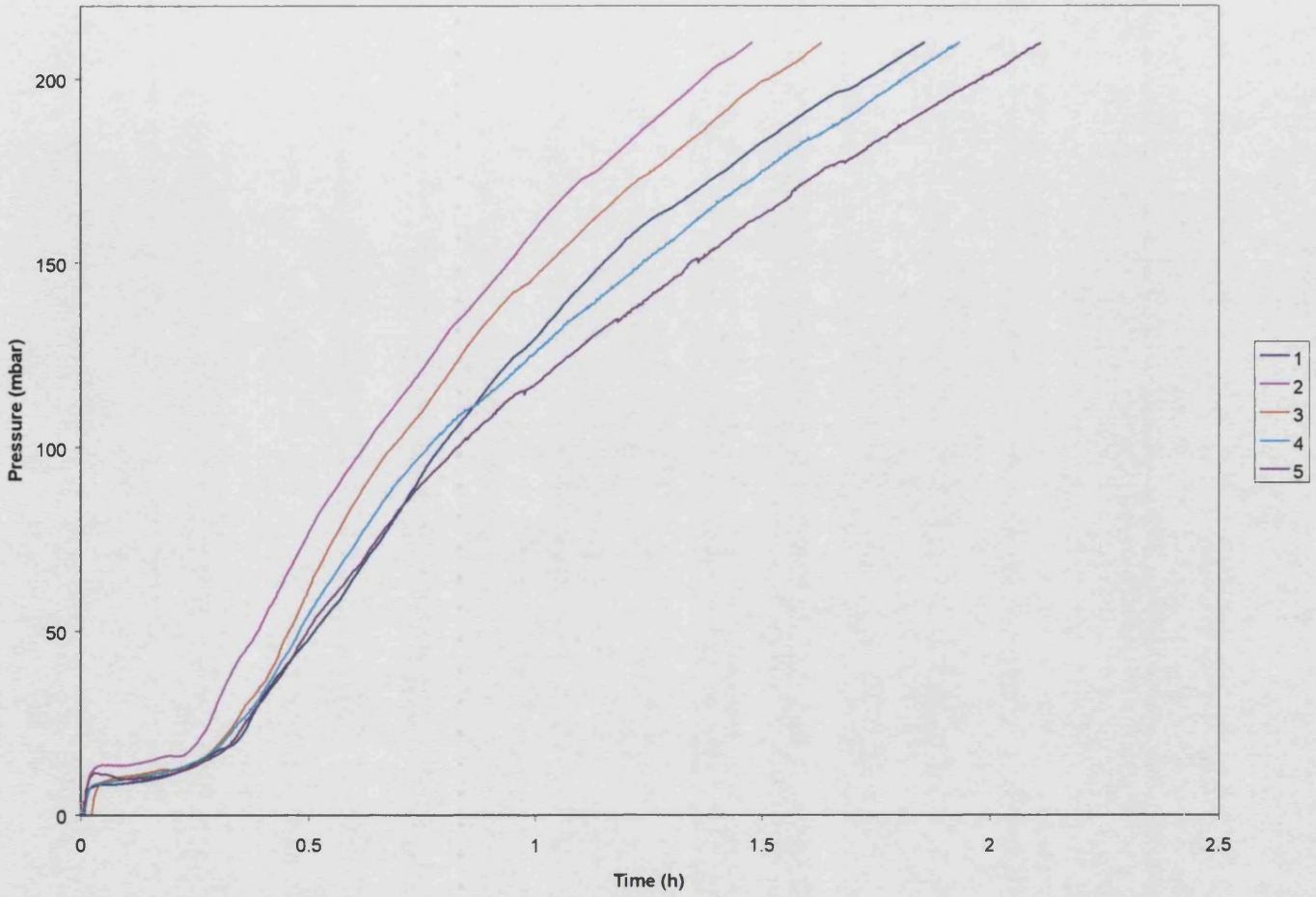

Figure 37 **A graph to show the rate of gas release during consecutive 1.5-minute periods for blend 3**

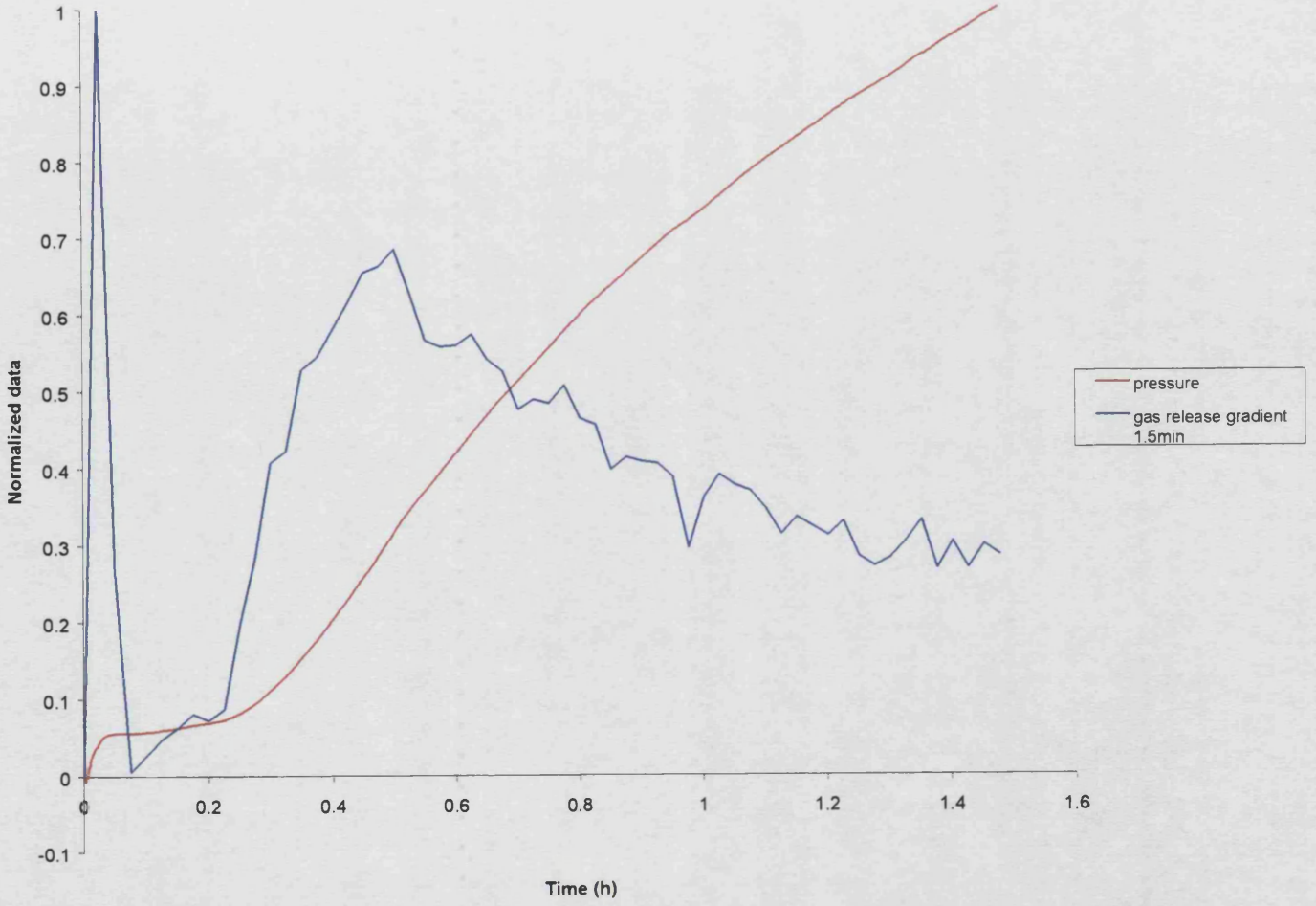

Table 19 CO_2 release data for the five blend 3 tablets

Tablet number	Maximum pressure generated (mbar)	Run time (h)	Average pressure generated per hour (mbar)
1	209.99	1.86	112.90
2	209.98	1.48	141.88
3	209.89	1.63	128.77
4	209.97	1.93	108.79
5	209.83	2.11	99.45

5.7.1.5 Mercury porosimetry

Runs were performed under the conditions discussed in 5.4.4, page 79, and tablets were tested according to the protocol outlined in paragraph 2.3.1, page 14. The tablets were tested in duplicate to assess reproducibility. See Table 20, page 118 for results.

The results for the two tablets were seen to be reproducible, as expected. The bulk of the pores detected were between 0.1μm and 0.2μm in diameter, which correlated with the results seen previously when analysing blend 2. The bulk density of this set of tablets was 1.2827g/ml, which indicates the tablets should again sink when they are placed into SGF medium. We have already seen from the buoyancy data that the tablets float almost as soon as they are immersed into the SGF medium, which indicates the overriding factor for floating is the dynamic interaction rather than the initial specifications.

Table 20 **A table to show the mercury porosimetry results for tablets made from blend 3**

	Run 1	Run 2	Average
Intrusion volume ml/g	0.1682	0.1693	0.16875
Median pore diameter (vol.) μm	0.1066	0.1122	0.1094
Bulk density g/ml	1.2815	1.2839	1.2827
Apparent density g/ml	1.6337	1.6406	1.63715
Porosity %	21.56	21.74	21.65

5.7.1.6 Nitrogen adsorption

Three tablets from blend 3 were tested using the protocol outlined in section 2.3.2. The results for are shown below in Table 21, page 119.

The BET value of 6.1691 m^2/g that was recorded is again a low value that is typical of pharmaceutical excipients. This value is lower than the value determined using mercury porosimetry. The existence of ink-bottle pores has been one explanation for this phenomenon. However, the main reason for the discrepancy is the different measurement ranges of the two techniques, with the gas adsorption technique looking only at the smaller pore range (3-200nm).

Table 21 Results from BET surface area analysis on blend 3

Sample weight before outgassing (g)	Sample weight after outgassing (g)	BET surface area (m^2/g)
4.3246	4.2112	6.1691

The results from the gas sorption study show that the surface areas of the tablets from blend 3 are similar to those of blend 2. The results both show that a pore network is available within the tablets, despite the compression necessary to initially compact the tablets. This pore network should allow the tablets to rapidly hydrate upon immersion into the simulated gastric fluid. We have already seen from the buoyancy studies that this is the case, however it is hard to assess how much of this is down to the pore networks, as the tablets rapidly change their characteristics as they dynamically interact with surrounding medium. We can therefore only use these characterisation studies to measure initial bulk characteristics and to ensure that all blends have similar profiles before testing.

5.7.1.7 Swelling studies

Tablets from blend 3 were tested according to the protocol outlined in section 5.6.7.5, page 98.

Sample digital photographs from the study are shown below in Figure 38, page 120. Table 22, page 121 shows the results of the image analysis for each run, along with average values. The data for time zero was taken by subjecting a dry control tablet to the image analysis process.

The data can be seen graphically in Figure 39, page 122. From the data we can see that all three runs show similar profiles. As expected the runs do not follow identical traces, due to each individual tablet having a slightly different interaction profile with the SGF medium. The overall profiles of the three traces do, however, show similarities. Three distinct phases of interaction can be seen.

i. Initial rapid burst of swelling as tablet begins to interact with the SGF within the first minute of the test.

ii. A rapid decrease in the size of the swelling that continues up until the three-hour mark.

iii. A further, slower degeneration of the tablet that continues until the end of the 8-hour test run.

Figure 38 Sample digital photographs of tablet swelling process

1 minute

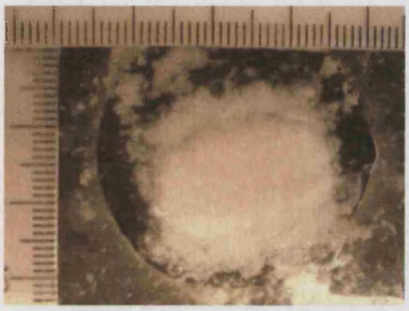

60 minutes

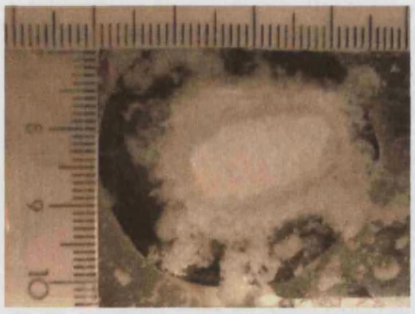

240 minutes

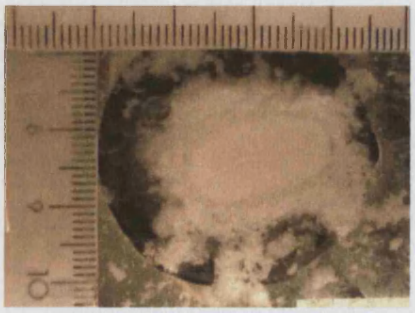

480 minutes

Table 22 Cross-sectional area data for blend 3

Time (min)	Tablet 1 area (cm^2)	Tablet 2 area (cm^2)	Tablet 3 area (cm^2)	Average area (cm^2)	Standard Deviation
0	2.1711	2.1711	2.1711	2.1711	0.0000
1	2.8493	2.8260	2.9028	2.8593	0.0394
15	2.7788	2.6544	2.6645	2.6992	0.0691
30	2.7485	2.6330	2.5003	2.6272	0.1242
45	2.5233	2.6131	2.3117	2.4827	0.1547
60	2.3746	2.3211	2.2911	2.3289	0.0423
90	2.2380	2.2257	2.1343	2.1993	0.0567
120	1.9243	1.8892	2.0401	1.9512	0.0790
150	1.8263	1.6028	1.8321	1.7537	0.1307
180	1.7486	1.5486	1.6974	1.6648	0.1039
240	1.6046	1.3898	1.6391	1.5445	0.1351
300	1.5509	1.3030	1.5877	1.4805	0.1548
360	1.4005	1.2705	1.534	1.4016	0.1318
420	1.3549	1.2594	1.5025	1.3722	0.1225
480	1.3202	1.2017	1.4672	1.3297	0.1330

Phase i. of the graph, as described above, is due to the rapid, initial interaction of the dry tablet with the SGF. The polymers in the matrix hydrate making the outside of the tablet swell rapidly, and the sodium bicarbonate also interacts with the SGF to produce carbon dioxide. The carbon dioxide produced acts as a partial disintegrant and forces the tablet to expand to accommodate the gas. Some of the carbon dioxide is lost from the matrix, whilst remains trapped in the polymer network. It is the combination of these effects that cause the initial burst of swelling.

Phase ii. of the graph is seen as the outside of the tablet begins to erode away from the tablet core, perhaps partly due to the power of the disintegrant effect. The polymer matrix becomes looser and detaches from the bulk of the tablet. A rapid shrinking effect is therefore seen.

Phase iii. is the final phase of degeneration that occurs after the swelling phase has completely stopped, and the tablet begins to simply erode away slowly.

Figure 39 A graph to show the image analysis data for blend 3

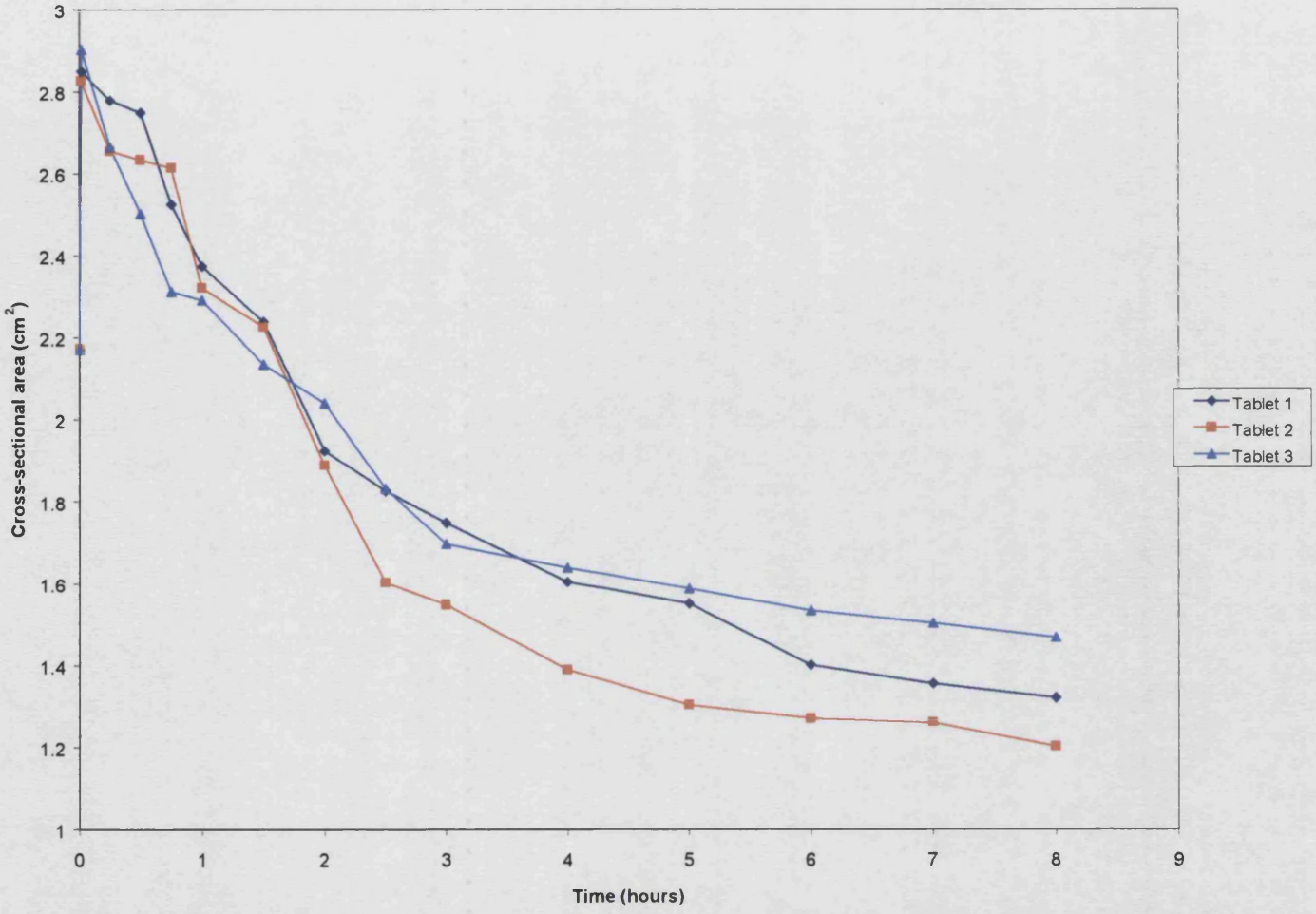

5.7.2 Discussion of blend 3 characteristics

Thus far the characteristics of the tablets from blend 3 have been investigated and discussed on an individual test basis, however it is the aim of this work to utilise these results to elucidate the mechanisms of a tablets *in vitro* floating properties. This section will attempt to bring together the data amassed so far, in order to explain the behaviour of blend 3 as a floating dosage form. The data will enable us to assess the combination of features that allow blend 3 to float successfully for an 8-hour period.

As discussed previously the tests that have been conducted fall into two main categories:

1) Initial dry tablet characterisation
2) Dynamic wet tablet characterisation

The initial dry characterisation tests were an important section of the work. The tests ensure that the tablets that had been produced from blend 3 were as similar to each other as possible. Both weight variation and hardness testing were chosen as standard parameters for tablet processing quality control, as these parameters are used throughout the pharmaceutical industry.

The aim was to produce tablets with an average weight of 1.44g and an approximate hardness of between 17-18KPa. The tablets that were produced had an average weight of 1.4424g, with a standard deviation of 0.00070, and an average hardness of 17.9KPa, with a standard deviation of 0.365. These ranges were deemed to be appropriate for the studies.

The second part of the dry testing was concerned with the surface area and pore size distribution of the tablets. Mercury porosimetry and nitrogen adsorption techniques were again utilised to derive this information. The available surface area and pore size distribution may be of importance in determining how quickly the dosage forms interact with the surrounding gastric medium during dynamic testing. The tests showed that the tablets from blend 3 had a relatively small surface area. It is thought, therefore, that the relationship between initial surface properties and dynamic properties are not very strong, due to the rapid changes that the tablets undergo once they are submerged in SGF. The tablets undergo a dramatic change in structure that is likely to be due more to the blend formulation than the initial pore size / surface area.

The dynamic stage of testing is obviously the most relevant to this work. Three different tests were performed to study the factors that lead to buoyancy, the resultant weight, the rate of gas production and the continuous swelling of the dosage form. By choosing these parameters it is possible to study the results, and the relationship between them, to try to understand why the formulation exhibits a particular floating force at particular stages of its interaction with SGF. This information will allow an understanding as to why some formulations float for longer than others *in vivo*, which will enable a better understanding of the results from previous *in vivo* work.

In order to totally understand the dynamic changes that occur within the tablet during testing, it is necessary to study the profile of the graphs that have been produced from the multiple runs. Figure 40, page 126, shows the average data from all three dynamic tests. The data sets have been normalised in order to show the data on the same axis. The buoyancy graph shows the average resultant weight exhibited by the tablets. The swelling data is the average data for the five tablets, whilst the pressure data shows the average normalised gradient (e.g. the normalised rate of gas release) of the pressure build up in the pressure vessel. The pressure gradient was calculated using 90-second intervals throughout the duration of the test. The data for the gas release is only shown for the first 90 minutes of testing as the amount of gas released was exceeded the calibration limits on the pressure vessel.

It is seen, as expected, that the buoyancy graph can be fully explained from the swelling and rate of gas release graphs. As discussed previously the buoyancy profile of the tablets can be broken down into four main sections:

1. An initial peak buoyancy period once the tablets are immersed in the SGF medium.
2. After the initial buoyancy period, a rapid decrease in buoyancy until approximately 10 minutes has passed.
3. A second, rapid buoyancy increase then becomes apparent. This increase continues until approximately 25 minutes after the start of the experiment.
4. After 25 minutes, until the end of the test, the resultant weight decreases steadily.

These four distinct phases of the buoyancy profile occurred reproducibly for all tablets tested. It is possible to use the dynamic testing data to fully explain this distinctive profile. Below is a summary of the changes that the tablets undergo during the floating process, with each step being used to explain to the four sections of buoyancy profile that are seen:

1 The graphs show the initial peak of buoyancy is a combination of the polymers within the tablet swelling and CO_2 gas production. The tablet swelling inevitably results in an increase in the buoyancy effect due to the relationship present between volume and density. Gas production also adds to the buoyancy effect as some of the gas produced by the bicarbonate reacting with the acid medium will be trapped within the polymer network of the tablet, ultimately helping the tablet float. The gas release rate and the degree of swelling are both at their highest level during the first few minutes of the test, which explains why the initial buoyancy of the tablets is so strong.

2 At this point the tablet is still producing gas, but the rate has slowed dramatically. This loss of gas production inevitably results in a direct loss of tablet buoyancy. Gas generated, and trapped in the polymer matrix, begins to be slowly released as the matrix relaxes. This loss of carbon dioxide from the polymer system results in a density increase, reducing its buoyancy in the SGF. The tablet is also undergoing a degree of erosion as the initial swelling begins to subside, adding to the increase in density.

3 The secondary phase of buoyancy increase directly correlates to the second increase in gas production rate. This increase in CO_2 release is due to erosion of the swollen tablet front. As the tablet erodes the acid in the SGF can react with previously protected sodium bicarbonate, causing an increase in gas production from the blend. Some of this gas again gets trapped within the new polymer matrix front of the tablet and increases the buoyancy of the dosage form. During this phase the tablets continued to erode steadily in the vessel, but the rapid increase in gas production was more than enough to overcome this effect.

4 The last phase shows a continuous decrease in buoyancy until completion of the test. Again there is correlation with a decrease in gas production rate. Unfortunately it was not possible to monitor the evolution of the gas until the end of the test due to the pressure vessel calibration limitations. It can however be seen that the tablets continued to erode, indicating that any gas previously trapped in the polymer network will have been slowly released into the SGF medium. Despite this, all tablets were buoyant for at least 7-hours of testing.

Figure 40 A graph to show the normalised dynamic testing data sets for blend 3

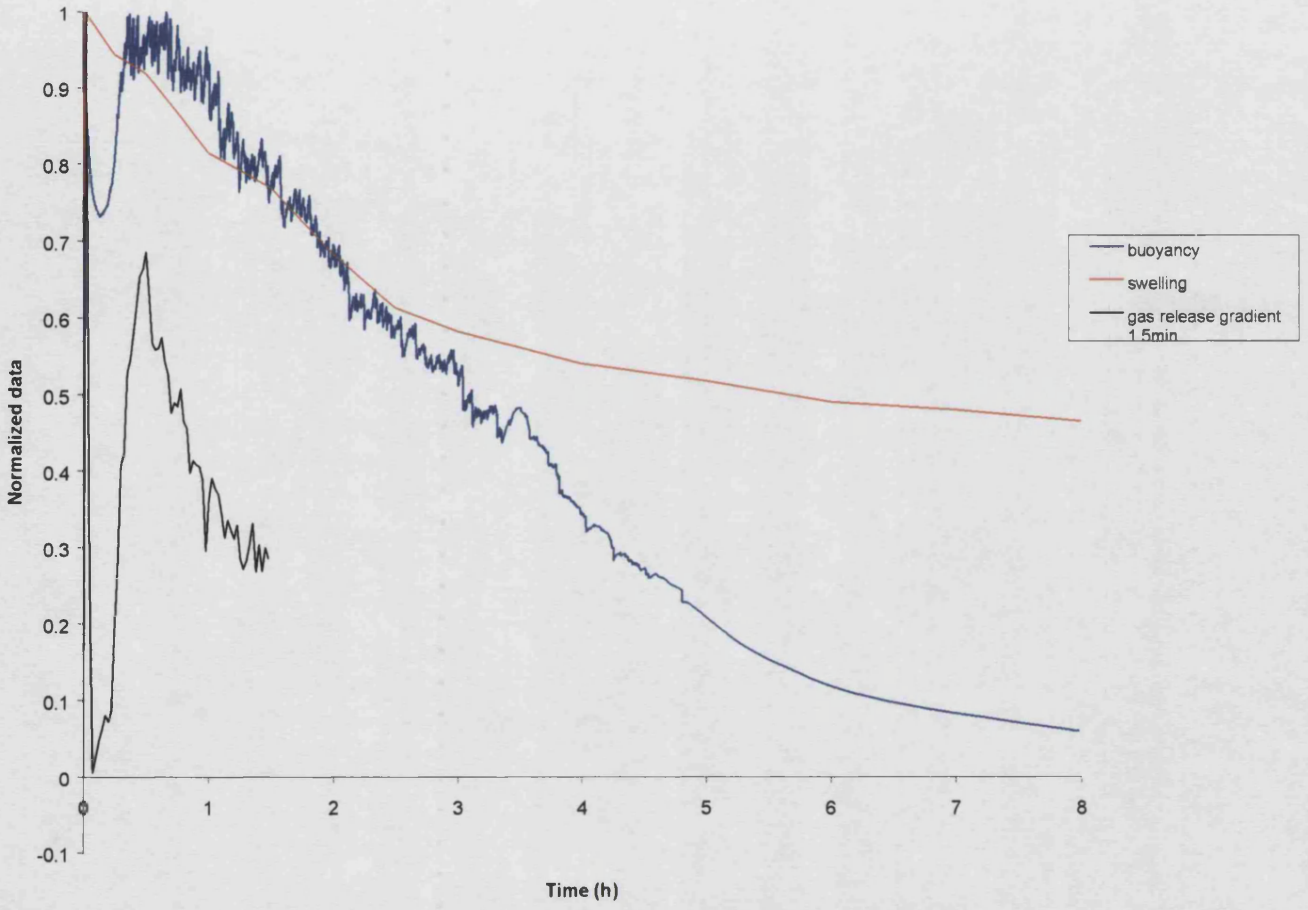

5.7.3.2 Hardness testing

The tablets were assessed according to the method outlined in section 2.3.4, page 15. The results are shown below in Table 24, page 128.

Table 24 A table to show the hardness variation in batch 4

Tablet no.	Hardness (KPa)
1	19.2
2	18.4
3	18.8
4	17.8
5	19.0
Average	18.64
Standard deviation	0.555

The tablets had an average hardness of 18.64KPa, with a standard deviation of 0.555. The standard deviation of this batch of tablets is again low. The tight grouping of the results indicates that the tablets are homogenous, which should lead to reproducible results during dynamic testing.

5.7.3.3 Buoyancy testing

Five tablets from blend 4 were tested in the buoyancy apparatus to further assess the effect of changing the levels of sodium bicarbonate in the tablets. The tablets were tested using the method outlined previously in section 3.8, page 33.

The results are shown graphically in Figure 41, page 129.

5.7.3 Results from blend 4

The formulation of blend 4 is shown in Table 15, page 107. The blend was prepared and made into tablets using the protocol outlined in Section 5.6., page 81. As before, approximately 150g of the blend was made and tabletted. No obvious problems were encountered during manufacture. The tablets were tested for uniformity.

5.7.3.1 Weight variation

The tablets were assessed according to the method outlined in section 2.3.5, page 15. Results are shown below in Table 23, page 127.

Table 23 A table to show the weight variation in batch 4

Tablet no.	Weight (g)
1	1.4388
2	1.4382
3	1.4405
4	1.4379
5	1.4413
6	1.4377
7	1.4379
8	1.4387
9	1.438
10	1.4397
Average	1.4389
Standard deviation	0.001236

The tablets had an average weight of 1.4389g and a standard deviation of 0.001236. The tablet weights from this batch were closely grouped and deemed appropriate for the study.

Figure 41 **A graph to show the resultant weight profiles of five tablets from blend 4**

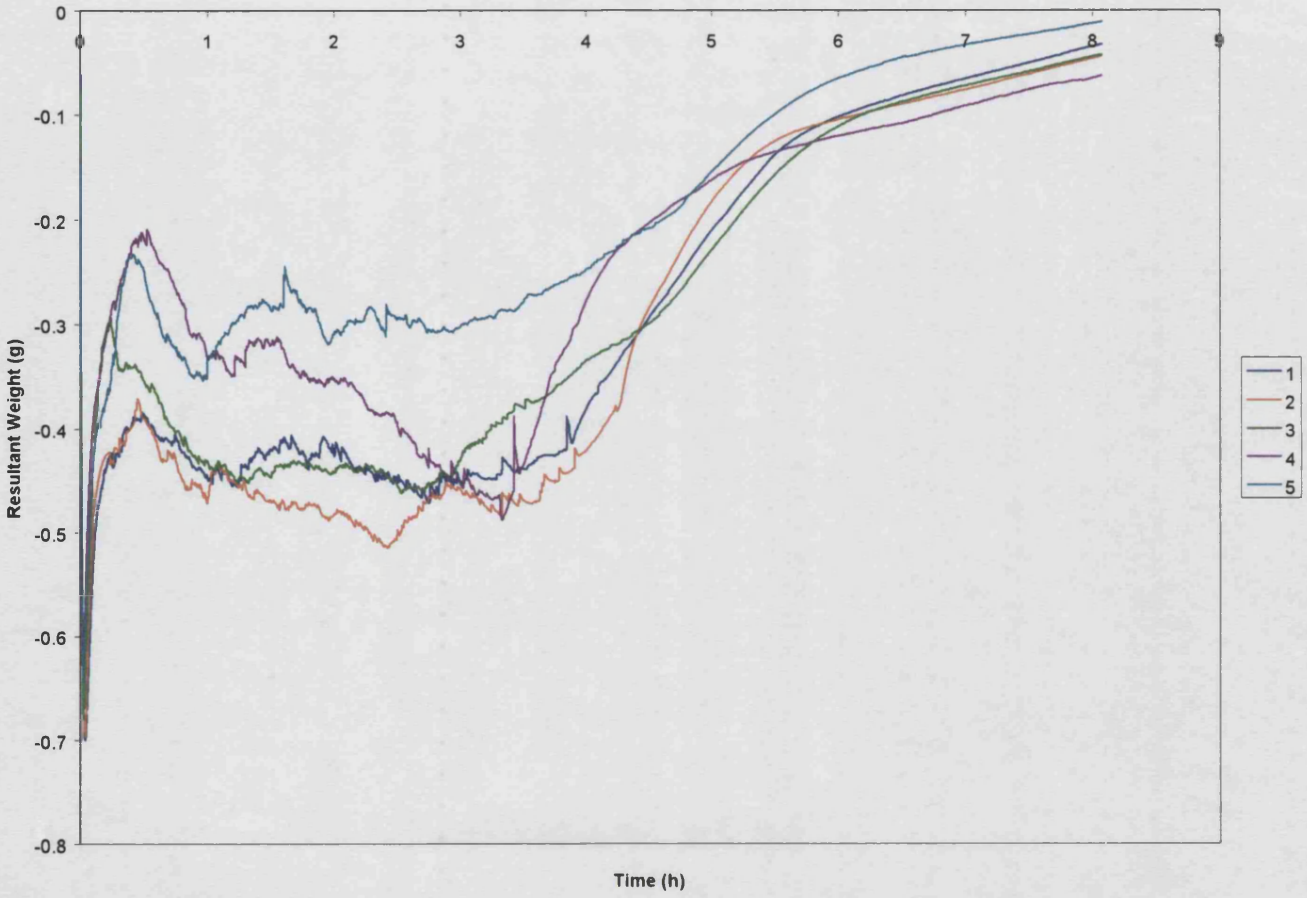

The profiles produced followed the distinctive, four-phase pattern, which has been present in all blends, over the duration of the experiment. The four-phase pattern has been described previously on page 77. However, as with blend 3, the duration of each phase lasted for a different time. The graph shows that tablets from blend 4 begin to enter phase four after approximately 4 hours have passed, compared with the 3-hour period seen with the blend 2 tablets. It is likely this phase time has been increased due to the reduction in sodium bicarbonate content in the blend 4 tablets.

It can also be seen that the peak buoyancy, which still occurs during the first few minutes of the test, is reduced when using this set of tablets. Again this is due to the decrease in the sodium bicarbonate content resulting in a reduced reaction with the acid medium therefore decreasing the buoyant effect. After 8 hours, the graph shows that the 5 tablets are all still exhibiting a buoyant effect. The buoyancy seen at this time is similar to that of the blend 3 tablets, but less than that of the blend 2 tablets

There is less fluctuation in the buoyancy readings throughout this test than in previous runs. This was thought to be due to fewer bubbles of CO_2 escaping from the polymer matrix, which previously resulted in their contribution to buoyancy being suddenly lost. This had been expected due to the decrease in the sodium bicarbonate content of the blend.

The graphs were assessed for reproducibility by measuring the area above each individual curve, as a direct measurement of the buoyancy force exhibited by each tablet throughout the duration of the experiment. Peakfit 4.06 for Windows was once again used to analyse the data sets and to produce the buoyancy force data shown in Table 25, page 131. The tablets showed a mean buoyancy force of 2.111gh during the experiment, with a standard deviation of 0.3432.

Table 25 A table to show the buoyancy force data for blend 4

Tablet Number	Buoyancy Force (gh)
1	2.317
2	2.434
3	2.257
4	1.966
5	1.580
Mean	2.111
Standard Deviation	0.3432

5.7.3.4 Pressure vessel testing

Five tablets from blend 4 were tested in the pressure vessel to assess the rate of carbon dioxide production from the formulation. The tablets were tested using the method outlined previously in section 4.9.1, page 58, with the tablet being added to the release mechanism before the vessel was sealed, and the tablet released into the medium after re-zeroing via the pressure vent.

Results of the five tablet runs are shown in Figure 42, page 133. The graph shows the data sets from the re-zero point onwards until the end of the tests. The five runs show a similar profile of carbon dioxide release throughout the duration of the test. The rate of CO_2 release for this blend is slower than for the previous blends, which is what was expected due to the decreased percentage of sodium bicarbonate present in the blend.

The most rapid phase of gas release is still immediately after immersion into the SGF. This is again due to the large surface area of the tablet hydrating rapidly, causing the sodium bicarbonate near the surface to react with the hydrochloric acid in the SGF medium. The resulting burst of CO_2 lasts for only a short period before subsiding for the subsequent 20-minute period. The 20 minute resting period is thought to due to the formation of a gel barrier on the outside of the tablet slowing the penetration of the acidic SGF medium into the tablet core. After this 20-minute period, CO_2 is again released until the end of the test. The rate of release increases initially before slowly decreasing from this point onwards. This phase of gas release is attributed to the acid medium reacting with

the previously shielded tablet core, therefore re-initiating CO_2 production. The rate of gas production then decreases until the end the test due to the diminishing size of the surface area available for interaction with the medium as the tablet undergoes constant erosion.

Figure 43, page 134, shows the average pressure that accumulated in the vessel for the five tablet runs. Also shown is the rate of pressure build up during consecutive 1.5-minute periods. The graph has been normalised such that the results can be plotted onto the same axis. The graph confirms the peak gas release rate was during the first couple of minutes of the test. The rate of release then slows dramatically, before peaking again after approximately half an hour. The gas release rate then stabilises for the next 3 hours before gradually decreasing towards the end of the test. Each phase of the gas release follows the same profile as previous blends.

Table 26, page 132, shows a summary of the data. It can be seen that the tablets generated between 102.2 and 112.5 mbar of pressure throughout the duration of the experiment. The variation in pressure is due to the slightly different interactions of each tablet with the simulated gastric fluid. The average pressure generated per hour has also been calculated to enable the rate of gas release for this batch to be compared with other batches. The average pressure generated per hour for blend 4 varied between 13.67 – 15.03 mbar.

Table 26 CO_2 release data for five blend 4 tablets

Tablet number	Maximum pressure generated (mbar)	Run time (h)	Average pressure generated per hour(mbar)
1	107.02	7.48	14.31
2	112.44	7.48	15.03
3	110.02	7.48	14.71
4	106.68	7.48	14.26
5	102.20	7.48	13.67

Figure 42 A graph to show the carbon dioxide release rate for five blend 4 tablets

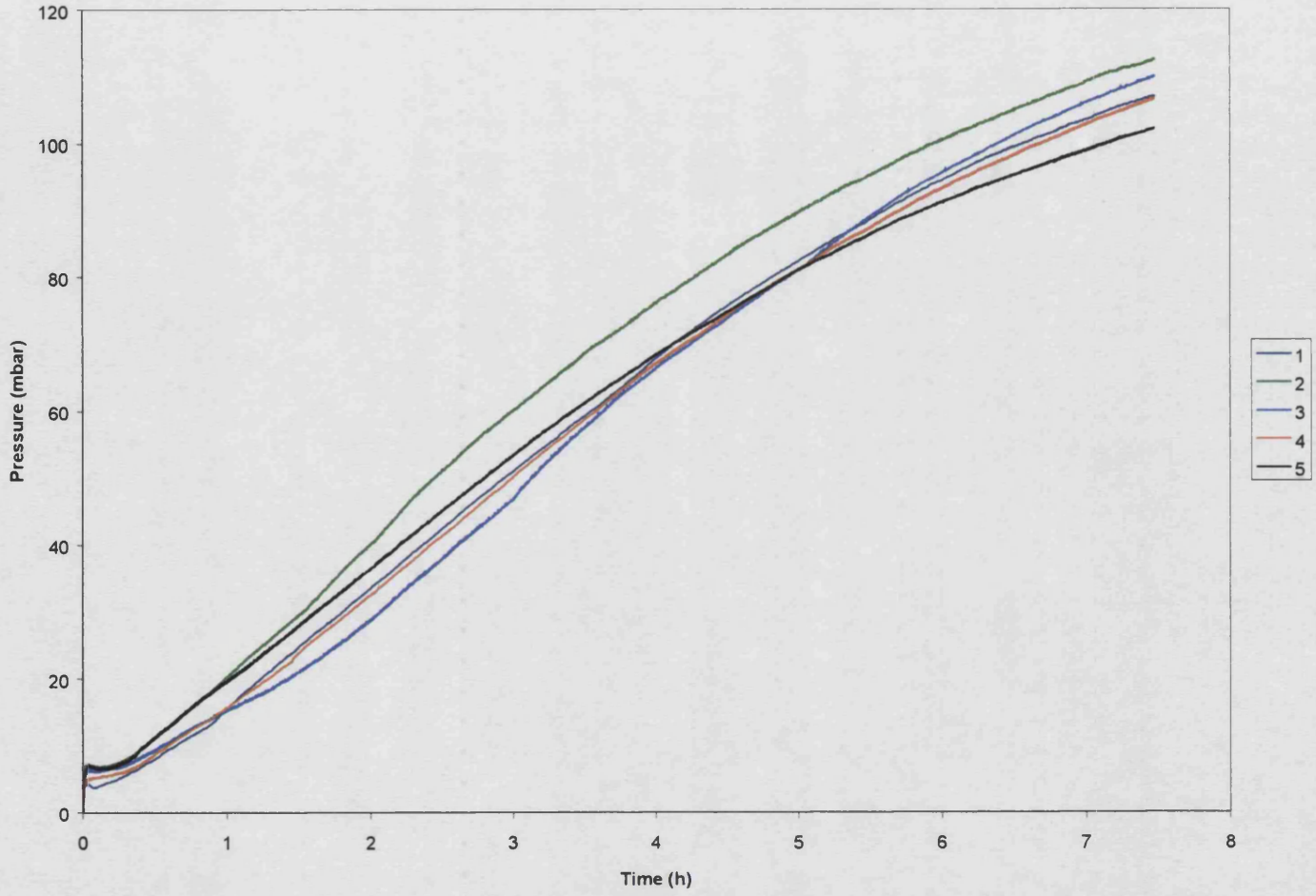

Figure 43 **A graph to show the rate of gas release during consecutive 1.5-minute periods for blend 4**

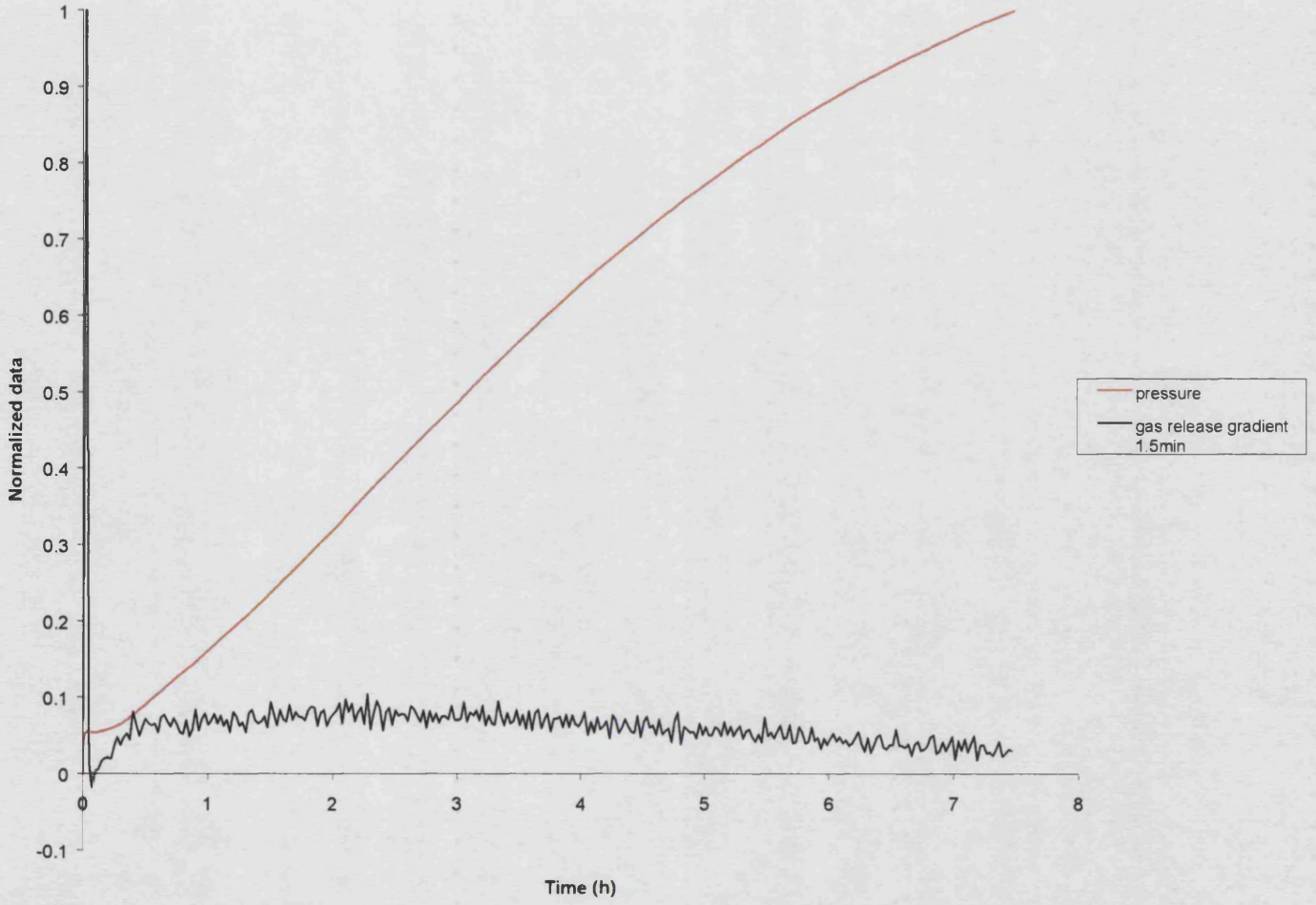

5.7.3.5 Mercury porosimetry

Runs were performed under the conditions discussed in 5.4.4, page 79, and tablets tested according to the protocol outlined in paragraph 2.3.1, page 14. The tablets were tested in duplicate to assess reproducibility. See Table 27, page 135 for results.

Table 27 A table to show the mercury porosimetry results for tablets made from blend 4

	Run 1	Run 2	Average
Intrusion volume ml/g	0.1949	0.1927	0.1938
Median pore diameter (vol.) μm	0.1065	0.1036	0.10505
Bulk density g/ml	1.1608	1.1656	1.1632
Apparent density g/ml	1.5002	1.5031	1.50165
Porosity %	22.62	22.46	22.54

The results for the two tablets were seen to be reproducible, as expected. The bulk of the pores detected were between 0.1μm and 0.2μm in diameter, which correlated with previous blends. The bulk density of this set of tablets was 1.1632g/ml, which indicates that the tablets should again sink are placed into SGF medium. We have already seen from the buoyancy data that the tablets float almost as soon as they are immersed into the SGF medium, indicating that the overriding factor for floating is the dynamic interaction rather than the initial specifications.

5.7.3.6 Nitrogen adsorption

Three tablets from blend 4 were tested using the protocol outlined in section 2.3.2. The results for are shown below in Table 28, page 136.

Table 28 Results from BET surface area analysis on blend 4

Sample weight before outgassing (g)	Sample weight after outgassing (g)	BET surface area (m^2/g)
4.3263	4.2147	6.0185

The BET value of 6.0185 m^2/g was again lower than the value determined using mercury porosimetry, due to the different measurement ranges of the two techniques.

The results from the gas sorption study show that the surface areas of the tablets from blend 4 are similar to those of the two previous blends. As discussed previously these characterisation studies are only being used to measure initial bulk characteristics and to ensure that all blends have similar profiles before dynamic testing.

5.7.3.7 Swelling studies

Tablets from blend 4 were tested according to the protocol outlined in section 5.6.7.5, page 98.

Sample digital photographs from the study are shown below in Figure 44, page 137. Table 29, page 138 shows the results of the image analysis for each run, along with average values. The data for time zero was taken by subjecting a dry control tablet to the image analysis process.

The data can be seen graphically in Figure 45, page 139. From the data we can see that all three runs show similar profiles. As seen with previous blends, the runs do not follow identical traces, due to the different interaction profile of each tablet with the SGF medium. The overall profile of the three traces does, however, show similarities. Three distinct phases of interaction can be seen.

i. Small burst of swelling as the tablet begins to interact with the SGF within the first minute of the test.
ii. A rapid decrease in the size of the tablet that continues for the first hour of the test.
iii. A further, slower degeneration of the tablet that continues until the end of the 8-hour test run.

Figure 44 Sample digital photographs of tablet swelling process

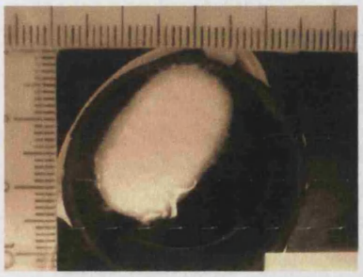

1 minute

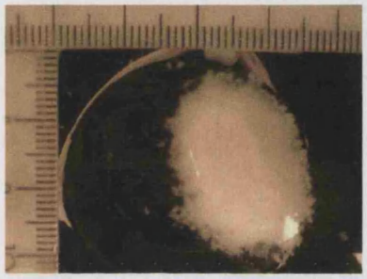

60 minutes

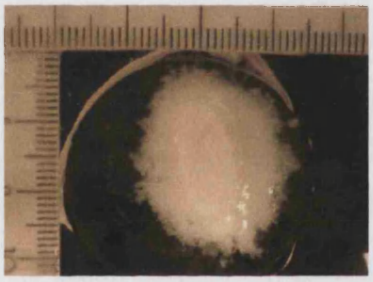

240 minutes

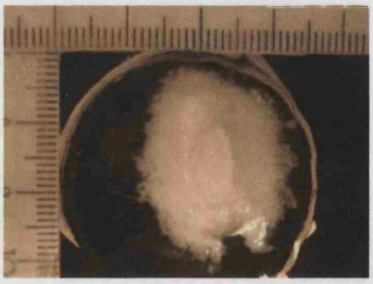

480 minutes

Table 29 Cross-sectional area data for blend 4

Time (min)	Tablet 1 area (cm^2)	Tablet 2 area (cm^2)	Tablet 3 area (cm^2)	Average area (cm^2)	Standard Deviation
0	2.1711	2.1711	2.1711	2.1711	0.0000
1	2.1435	2.1855	2.2727	2.2006	0.0659
15	1.9623	1.9628	1.919	1.9480	0.0251
30	1.7756	1.8530	1.726	1.7849	0.0640
45	1.6417	1.5761	1.5345	1.5841	0.0540
60	1.5169	1.4824	1.4329	1.4774	0.0422
90	1.3988	1.3633	1.2996	1.3539	0.0503
120	1.2511	1.2052	1.1392	1.1985	0.0563
150	1.1388	1.1492	0.9765	1.0882	0.0968
180	1.0695	1.0815	0.9103	1.0204	0.0956
240	0.9157	0.9279	0.7457	0.8631	0.1018
300	0.8024	0.7630	0.6707	0.7454	0.0676
360	0.7180	0.6932	0.5916	0.6676	0.0669
420	0.5417	0.6257	0.5044	0.5573	0.0621
480	0.4569	0.5324	0.3958	0.4617	0.0685

The mechanisms involved in the swelling process have been discussed previously on page 121. However, the swelling is less pronounced than in previous blends, which was expected due to the reduced quantity of sodium bicarbonate present.

Figure 45 A graph to show the image analysis data for blend 4

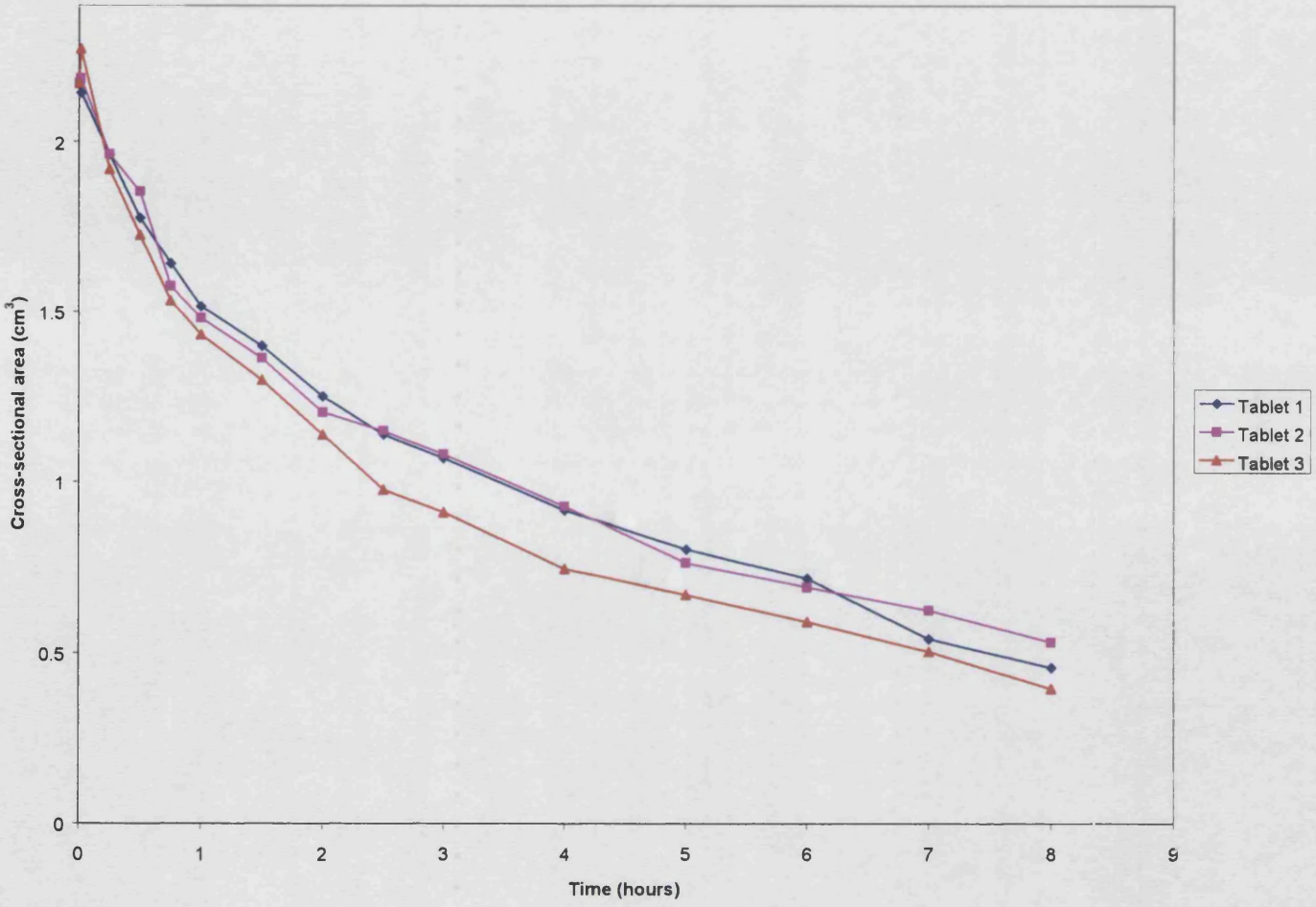

5.7.4 Discussion of blend 4 characteristics

So far the characteristics of the tablets from blend 4 have been investigated and discussed on an individual test basis. This section aims to compile these results to explain the mechanisms of the tablets *in vitro* floating properties, in order to understand the behaviour of blend 4 as a floating dosage form. The data will enable assessment of the importance of the individual features that allow blend 4 to float successfully for the 8-hour period.

As discussed previously the tests that have been conducted fall into two main categories:

1) Initial dry tablet characterisation
2) Dynamic wet tablet characterisation

The aim was to produce tablets with an average weight of 1.44g and an approximate hardness of between 17-18KPa. The tablets that were produced had an average weight of 1.4389g, with a standard deviation of 0.0012, and an average hardness of 18.64KPa, with a standard deviation of 0.555. These ranges were deemed to be appropriate for the studies.

The second part of the dry tablet characterisation was concerned with the surface area and pore size distribution of the tablets. The tests showed that the tablets from blend 4 had a relatively small surface area. It is thought that the relationship between initial surface properties and dynamic properties in this blend are not very strong, due to the rapid changes that the tablets undergo once they are submerged in SGF. The tablets undergo a dramatic change in structure that is more due to the blend formulation than the initial pore size / surface area.

The dynamic stage of testing is the most relevant to this work. Three different tests were performed to study the factors that lead to buoyancy; the resultant weight, the rate of gas production and the continuous swelling of the dosage form.

In order to fully understand the dynamic changes that are occurring within the tablet during testing, it is necessary to study the profile of the graphs that have been produced from the multiple runs. Figure 46, page 142, shows the average data from the three dynamic tests. The data sets have been normalised in order to show the data on the same axis. The buoyancy graph shows the average resultant weight exhibited, the swelling

data shows the average for the five tablets, whilst the pressure data shows the average normalised gradient of the pressure built up in the pressure vessel. The pressure gradient was calculated using 90-second intervals throughout the duration of the test.

As expected, the buoyancy graph can be explained using the swelling and rate of gas release graphs. As discussed before the buoyancy profile of the tablets can be broken down into four main sections:

1. An initial peak buoyancy period as soon as the tablets are immersed in the SGF medium.
2. After the initial buoyancy period, a rapid decrease in buoyancy until approximately 30 minutes has passed.
3. A second buoyancy increase then becomes apparent in the trace. This increase continues until approximately 3.5 hours after the start of the experiment.
4. After 3.5 hours, until the end of the test, the resultant weight is seen to decrease steadily.

These four distinct sections within the buoyancy profile occurred reproducibly for all tablets tested. The principles have been described previously for blend 2 and 3.

Having discussed the properties of each of the individual profiles created by blend 4, the next section will go on to discuss the comparison seen between the three blends that have been made.

Figure 46 A graph to show the normalised dynamic testing data sets for blend 4

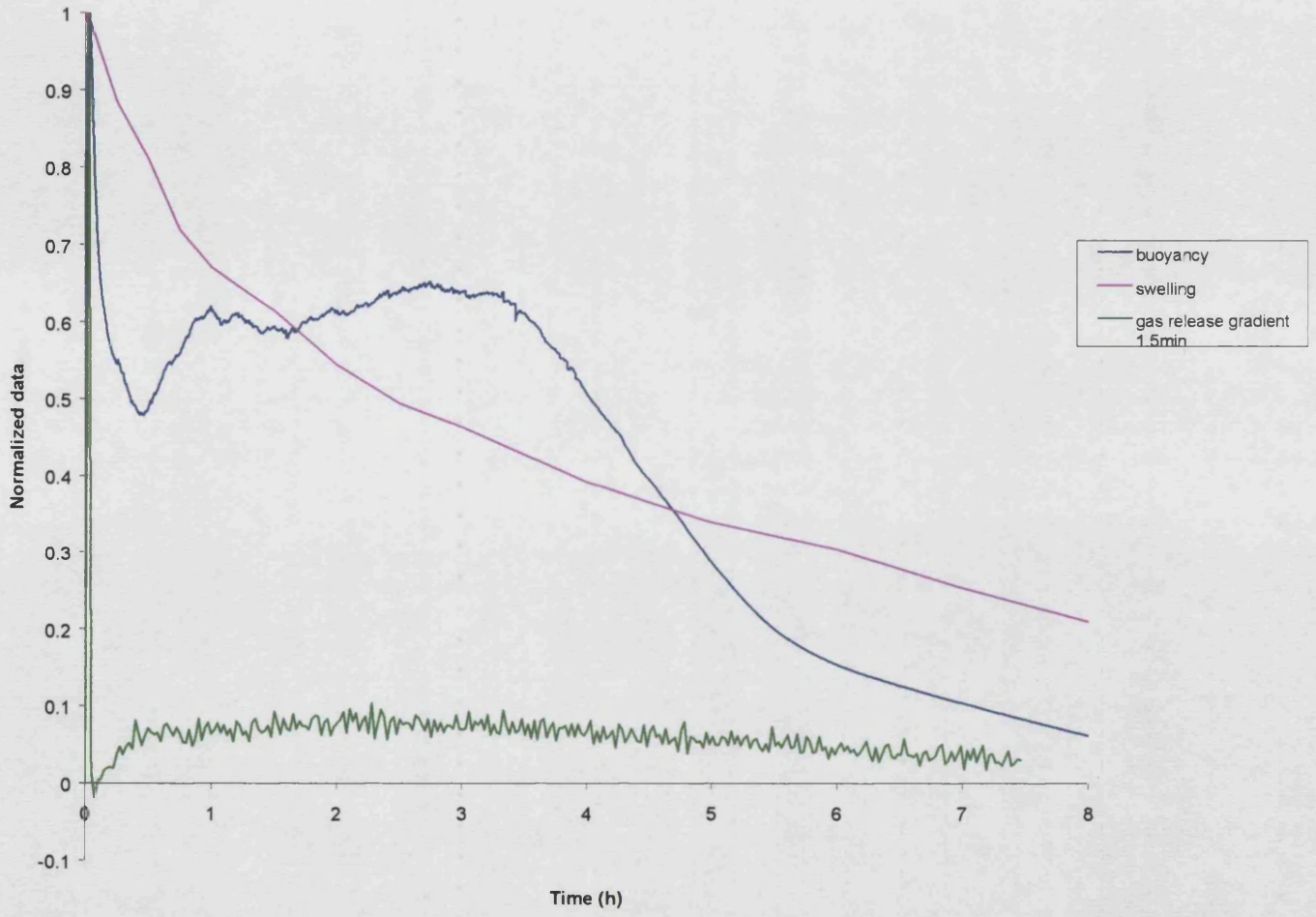

5.8 Blend comparisons

Three similar blends have been produced and analysed using the developed barrage of testing techniques. It has been shown that the techniques developed are capable of explaining the buoyancy effects of a particular dosage form. This section will compare the three blends to see if the dynamic methods are capable of distinguishing between tablets produced with slightly different blend excipients. The constituents of each blend are shown below in Table 30, page 143.

Table 30 Comparison of blend constituents

Excipient	Blend 2 (mg per tab)	Blend 3 (mg per tab)	Blend 4 (mg per tab)
Ciprofloxacin	1000	800	1100
Sodium Alginate	5	5	5
Xanthan Gum	15	15	15
Sodium Bicarbonate	200	400	100
XL PVP	177	177	177
Magnesium Stearate			
Intra-granular	26	26	26
Inter-granular	7	7	7
Talc	10	10	10
Total Weight	1440	1440	1440

5.8.1 Comparison of buoyancy results

The three blends that were tabletted consisted of varying levels of sodium bicarbonate in the formulation, at the expense of ciprofloxacin. The ciprofloxacin was removed from the formulation to accommodate the extra sodium bicarbonate because it was thought that the drug itself had the least effect of all tablet constituents on the floating properties of the formulation.

Each formulation was tested five times in the buoyancy apparatus and the average buoyancy profile for each formulation was calculated. The average profiles are shown in comparison in Figure 47, page 146. It can be seen from the graph that all the formulations produced a similar buoyancy profile and all floated for the duration of the 8-hour test period. Common characteristics of the buoyancy profile were:

1. A sudden rapid increase in buoyancy during the first few minutes of testing.
2. A decrease in buoyancy which occurred between the 10-30 minute period.
3. A second increase in buoyancy, culminating in a peak between the 30-90 minute period (less marked for blend 4).
4. A slow decrease in buoyancy that lasts until the end of the 8-hour test.

We can see from the profiles that the blend with the least sodium bicarbonate (blend 4) also yields the lowest resultant weight at all times during the test. This is to be expected due to the direct link between gas generated and trapped within the polymer network and density. When the amount of sodium bicarbonate is doubled in the formulation (blend 2) it yields more than a 2-fold increase in buoyancy effect throughout the duration of the test. This increase in buoyancy would lead to the dosage form being more likely to float in a more viscous medium. As *in vivo* the viscosity of the stomach contents will vary depending on food content it is more likely that blend 2 will stay afloat on the contents on the human stomach than blend 4.

In blend 3 the amount of sodium bicarbonate has again been doubled, however this does not result in a 2-fold increase in buoyancy over blend 2 on this occasion. It can be seen in Figure 47 that blend 3 does exhibit an increased buoyancy effect during the first three phases of the profile. However, it is also noticeable that these three phases occur over a shorter time period than for the other blends. After approximately 2-hours of the run it is seen that blend 3 actually becomes less buoyant than blend 2, despite having a higher bicarbonate content. It appears this is a direct result of the formulation breaking up due to the increased bicarbonate level exhibiting a greater disintegrant action.

We can therefore say that blend 2 would be the optimum blend if a formulator was looking to achieve floating *in vivo* over an 8-hour period, whilst if a shorter floating period was needed then blend 4 may be the formulation of choice.

It is also noticeable from the graphs that as the amount of bicarbonate in the formulations is increased, so the degree of fluctuation in the average traces increases. This

fluctuation is a result of gas bubbles escaping from the polymer matrix of the tablet, and buoyancy suddenly being lost.

It has been shown that the buoyancy apparatus developed is capable of distinguishing the differences between similar formulations. The apparatus could therefore be used in future work to assess *in vivo* candidates prior to testing. It would also be possible to study previous work in order to investigate explanations for *in vivo* failures. Further to this the apparatus could be used to optimise the floating properties of a particular floating formulation.

Figure 47 A graph to show the comparison of resultant weight profiles for the three test blends

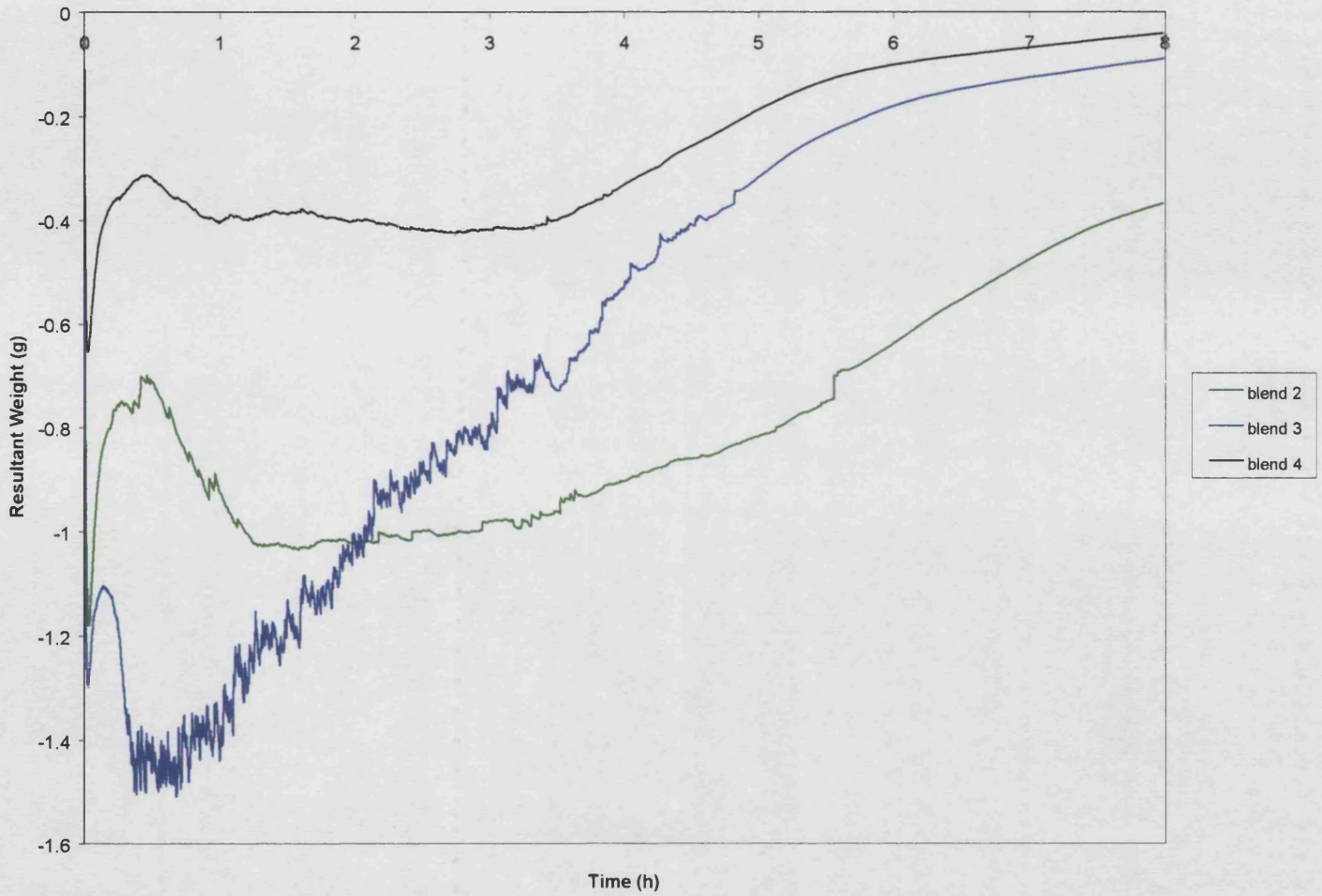

5.8.2 Comparison of pressure vessel results

Each formulation was tested five times in the pressure vessel and the average pressure profile for each formulation was calculated. The average profiles are shown in comparison in Figure 48. All profiles are characterised by a rapid gas release during the first minutes of testing as the tablets initially react with the simulated gastric medium. There then follows a momentary pause in gas release as the tablets stabilise in the medium, prior to a secondary phase of gas release that continues until the end of the test.

It can be seen from the profiles that the formulation with the least sodium bicarbonate (blend 4) exhibits the slowest rate of gas release, as expected. In fact the rate of gas release increases in direct correlation with increasing levels of sodium bicarbonate content in the formulation.

The blend with the most sodium bicarbonate present (blend 3) released gas so rapidly that the calibration limits of the pressure vessel were soon exceeded. In order to assess the rates of gas release further the pressure generated per hour was calculated for each blend. The results are shown below in Table 31. One way ANOVA performed on the original average pressure generated per hour data indicated that the sample means were significantly different.

The pressure generated for blend 2 is approximately twice that of blend 4, which was expected before the test. However the rate of gas production for blend 3 is more than twice that of blend 2. This is because the blend 3 tablets exhibit their optimum gas release during the first 2 hours of testing, as seen in the buoyancy graphs. If the pressure release could have been monitored for the entire 8-hour period it would have been expected that the rate of gas release for blend 3 would have decreased dramatically.

It has been shown though that the apparatus is capable of reproducibly detecting the differences between formulations produced with varying levels of excipients. The rate of gas release and total gas production exhibited by a formulation has been shown to be vitally important when assessing the intrinsic properties of floating dosage forms. This apparatus can therefore be used to assess future candidates for gas-powered floating dosage forms in order to optimise their *in vivo* floating properties. The results of these tests can be used in conjunction with the buoyancy testing results to assess the effect that variations in gas release rate have on buoyancy over extended periods.

Figure 48 A graph to show the comparison of gas release profiles for the test blends

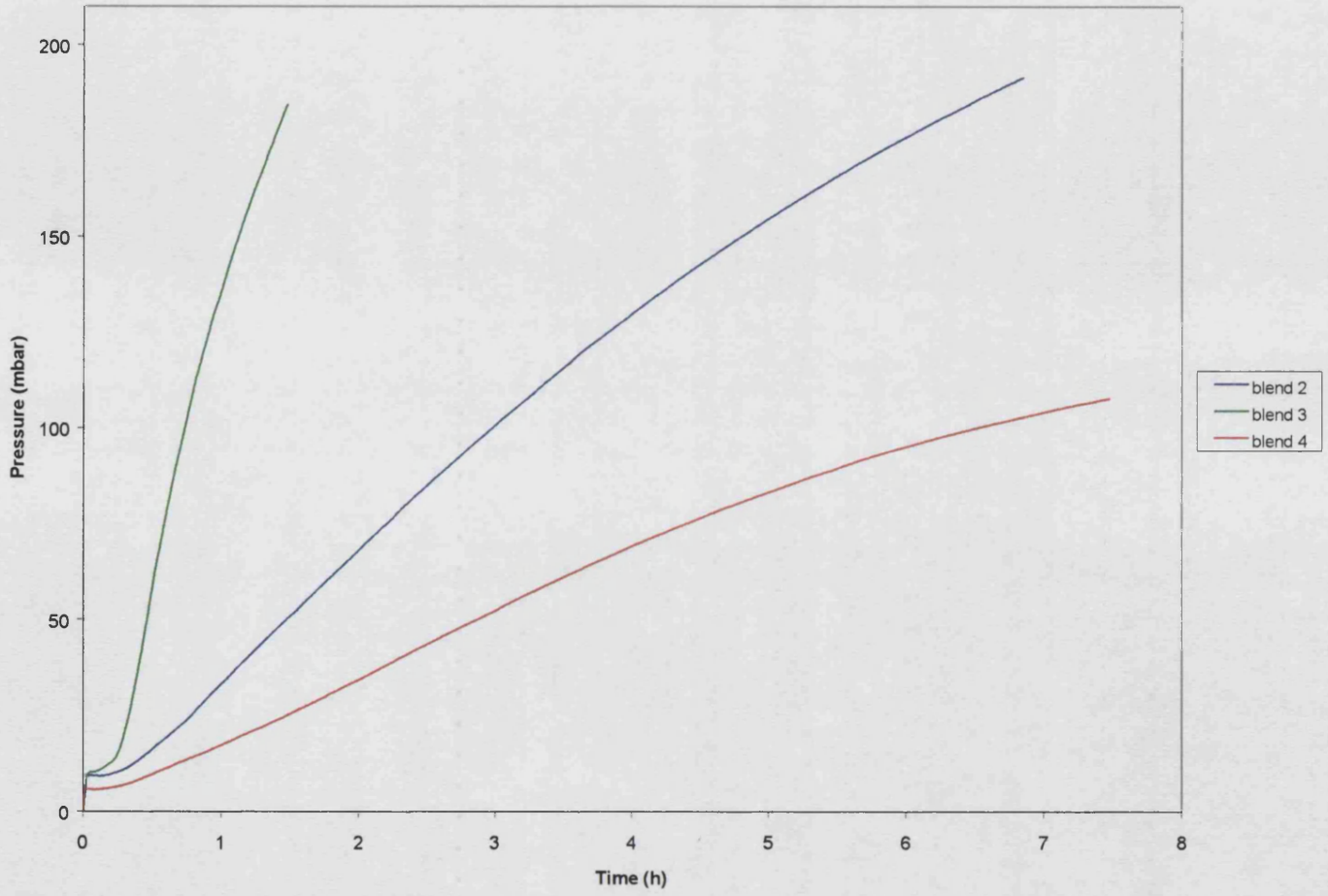

Table 31 Average pressure generated per hour for test blends

	Blend 2	Blend 3	Blend 4
Average pressure generated (mbar/h)	27.01	118.36	14.40

5.8.3 Comparison of swelling results

Each formulation was tested three times in the swelling apparatus and the average swelling profile for each formulation was calculated. The average profiles are shown in comparison in Figure 49. All profiles follow a distinctive pattern whereby the peak swelling is achieved in the first minute of testing. The tablets then erode away until the end of the test. The peak mean swelling size for each blend is shown in Table 32, page 151.

The profiles show that the blend with the least sodium bicarbonate (blend 4) also exhibits the least swelling. This was expected, as the extra bicarbonate in the blend acts as a disintegrant for the tablets, therefore increasing the surface area. This also helps explain why the buoyancy for blend 4 is reduced, as a decreased surface area will lead to an increased density.

Blend 3 (maximum sodium bicarbonate content) exhibits the most swelling, however it can be seen after approximately 2.5 hours, until the end of the test, the difference between blend 3 and blend 2 is minimal. This would help to explain why the buoyancy of blend 3 is at its peak during the first 2 hours of testing.

One way ANOVA was performed on the mean peak swelling size data, which indicated that there was a significant difference between all data sets.

It has been shown therefore that the swelling apparatus is capable of distinguishing between blends made from similar excipients, and that the results can be used to explain the floating properties of the formulations. The apparatus could be used along with the buoyancy apparatus and the swelling vessel to assess the effect of changing excipient parameters on buoyancy. Once the effect of different parameters are understood it is possible to change the contents of a blend to provide optimal floating properties over a predetermined time period.

Figure 49 A graph to show the comparison of swelling profiles for the test blends

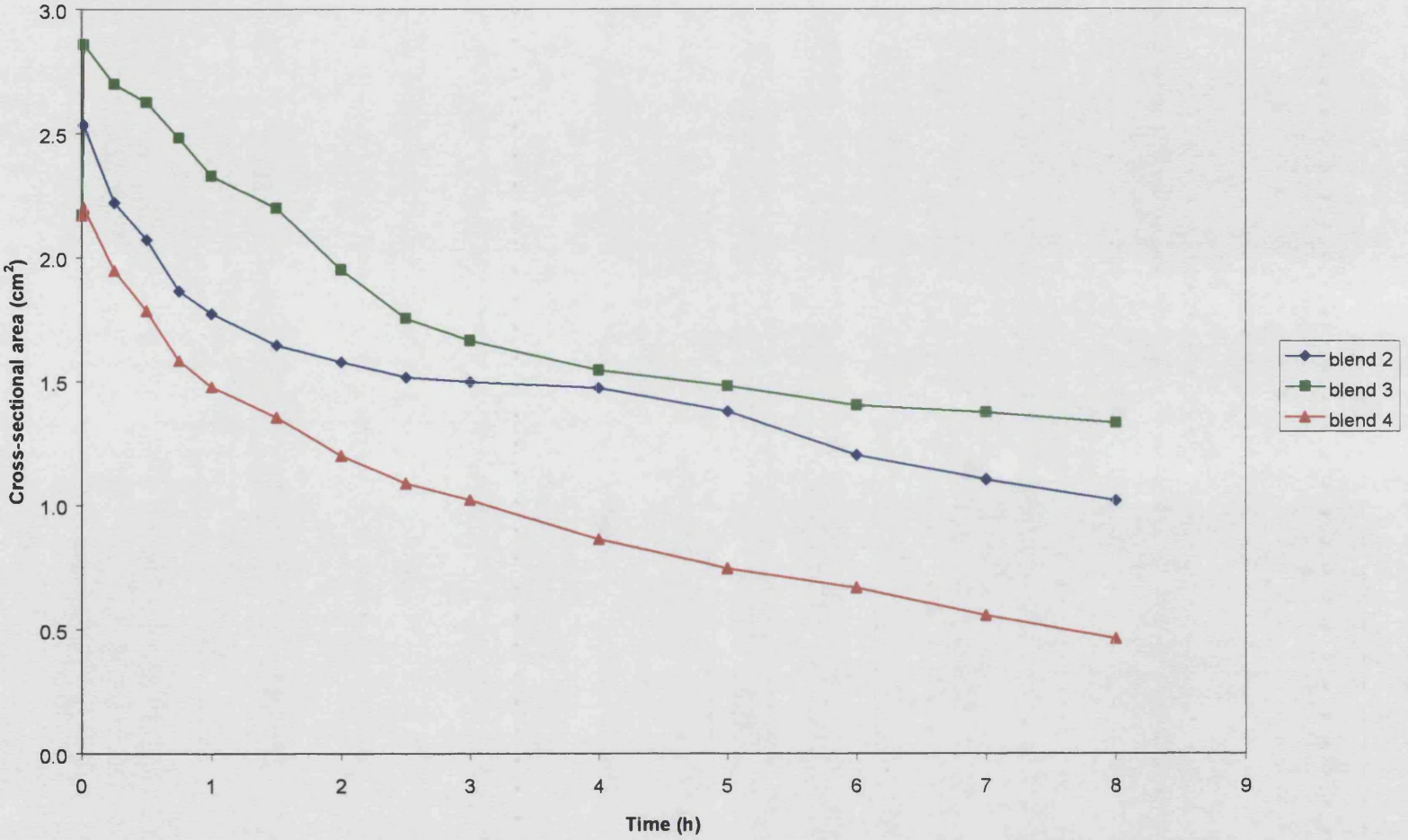

Table 32 Peak swelling size comparison for test blends

	Blend 2	Blend 3	Blend 4
Mean Peak Swelling Size	2.535	2.859	2.201

5.9 Summary

Three methods and apparatus have been developed capable of identifying and quantifying the parameters associated with gas-powered floating dosage forms.

A buoyancy test has been developed that enables constant assessment of buoyancy over a predetermined test period. The test allows determination of the dynamic interactions occurring between the dosage form and the test fluid.

A method and apparatus capable of quantifying the amount of gas released from a dosage form over a period of time has also been developed. The pressure vessel has been shown to be capable of distinguishing between similar formulations. It has also been shown that the pressure vessel results can be used to partly explain the results seen in the buoyancy apparatus.

A further technique has been developed that enables assessment of the swelling of a dosage form. The swelling of floating tablets has been shown to be of importance when trying to establish why a dosage form exhibits particular buoyant properties.

The amount of sodium bicarbonate is of importance for floating dosage forms. However, an increase in the amount of bicarbonate does not always result in increased buoyancy. The three dynamic methodologies could however be used to optimise the amount of bicarbonate required in a formulation in order to achieve a desired floating profile.

It is possible that the three methodologies can also be used in unison to assess previous *in vivo* test results in order to explain previous discrepancies.

CHAPTER 6

CASE STUDY OF A FLOATING SYSTEM (1)

A study was conducted to assess whether the developed apparatus were capable of testing a non-tablet formulation. All previous work had thus far been conducted using tablets that generated a significant amount of carbon dioxide in order to achieve their buoyancy. This case study looks at an aerogel capsule system that had been developed to have a density of less than that of water, and which will therefore, once swallowed, float on the contents of the stomach for a prolonged period of time (Patent number WO 0110419). Carvedilol was used as an example of a low-dose drug that has site-specific absorption in the small intestine.

6.1 Manufacture of the aerogel system

The aerogel capsules were manufactured according to the qualitative composition in Table 33, page 153.

Table 33 Qualitative composition of aerogel capsules

Material	Manufacturer	Batch number
Carvedilol	Cadila healthcare	9CD003
Glucidex 40D	Rouquette	65081
Xanthan gum	Monsanto	8J0370K
Emcocel 90M	Mendell	9S6005
Ammonium bicarbonate	BDH	-
Calcium carbonate (heavy)	BDH	-
Lubritab	Mendell	666812603

Method:

1. Emcocel 90M, glucidex and xanthan gum are sifted through a 40-mesh sieve and mixed for 30 minutes in a turbula mixer.
2. The Carvedilol and calcium carbonate are passed through a 40-mesh sieve and the ammonium bicarbonate and lubritab are passed through an 85-mesh sieve. These components are then mixed with the blend from step 1 for another 30 minutes using a turbula mixer.

3. The blend was then left overnight, before being filled into size 0 gelatine capsules.
4. The capsules were treated at 80°C for 35 minutes before being cooled to room temperature.

6.2 Buoyancy testing

Five capsules were tested in the buoyancy apparatus to assess the floating force properties of the aerogel system. The capsules were tested using the method outlined previously in section 3.8, page 33.

The results are shown graphically in Figure 50, page 155. The graphs show that all the aerogel capsules floated for the duration of the 8-hour test. The resultant weight generated by the capsules varied between 0.5 and 0.15g. All capsules showed a similar buoyancy profile, with a slight variation between the maximum buoyancy achieved. It was thought that this slight variation was due to small variations in the quantity of ammonium bicarbonate present in the capsules. In previous experiments fluctuations in the resultant weight have been seen that were thought to be the escape of gas from the formulation leading to a sudden loss of buoyancy. When using aerogel capsules the degree of rapid fluctuation is much reduced and only seen at the start of some capsule runs. This is due to the reduced sodium bicarbonate content of this formulation, with the "jumps" occurring due to the escape of gas from the inside of the capsule, as it begins to degenerate.

The average buoyancy profile is shown below in Figure 51, page 156. The profile shows that the average initial buoyancy of the capsules is approximately 0.2g. As soon as the capsules are submerged into the simulated gastric fluid, an increase in buoyancy is seen that reaches a peak after approximately 25-minutes of almost 0.4g. The resultant weight was then constant until 4-hours of the test had passed. After approximately 4-hours a decrease in the resultant weight is seen that continues until the end of the test.

Figure 50 A graph to show the resultant weight profile of five aerogel capsules

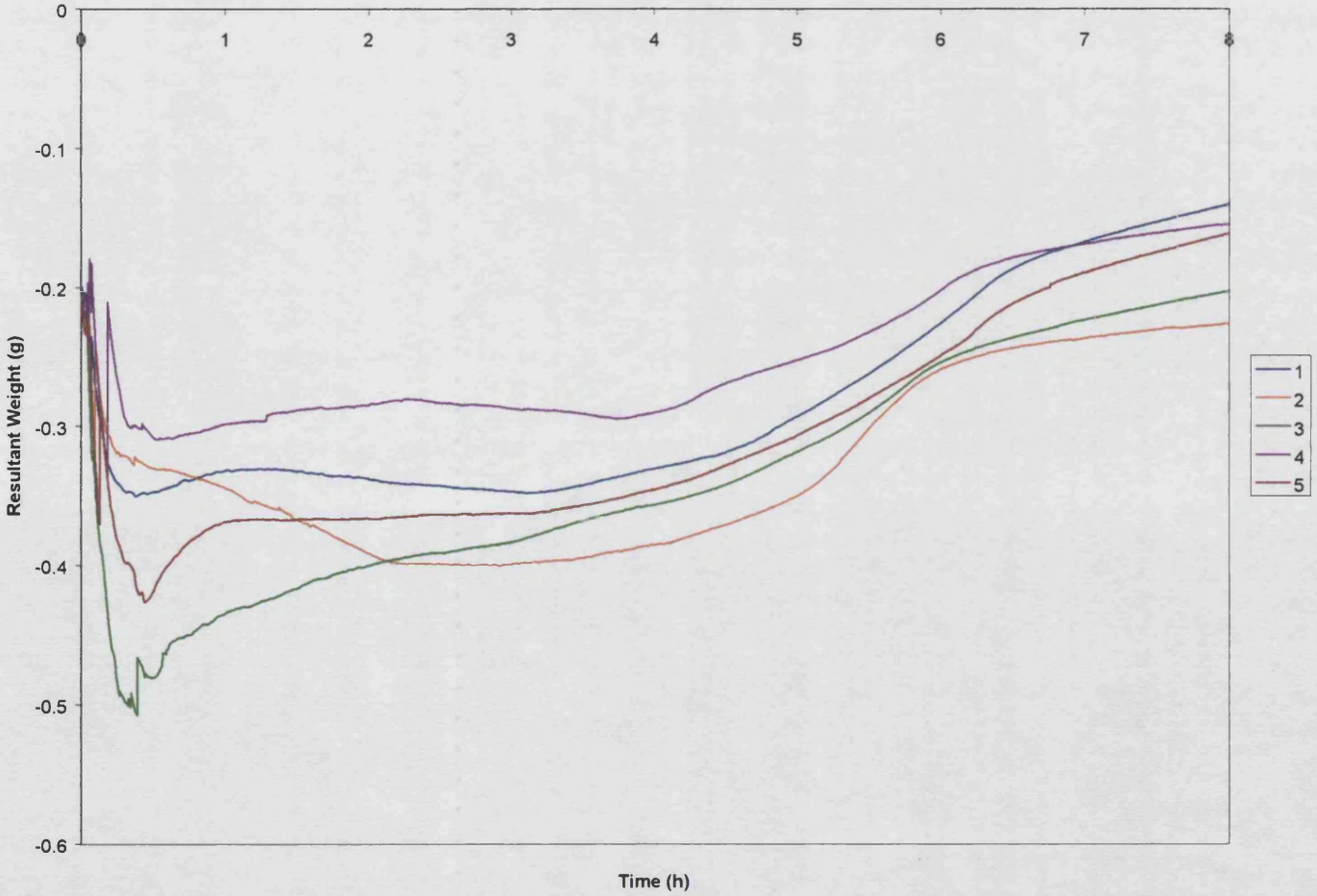

Figure 51 A graph to show the average resultant weight profile for the aerogel capsules

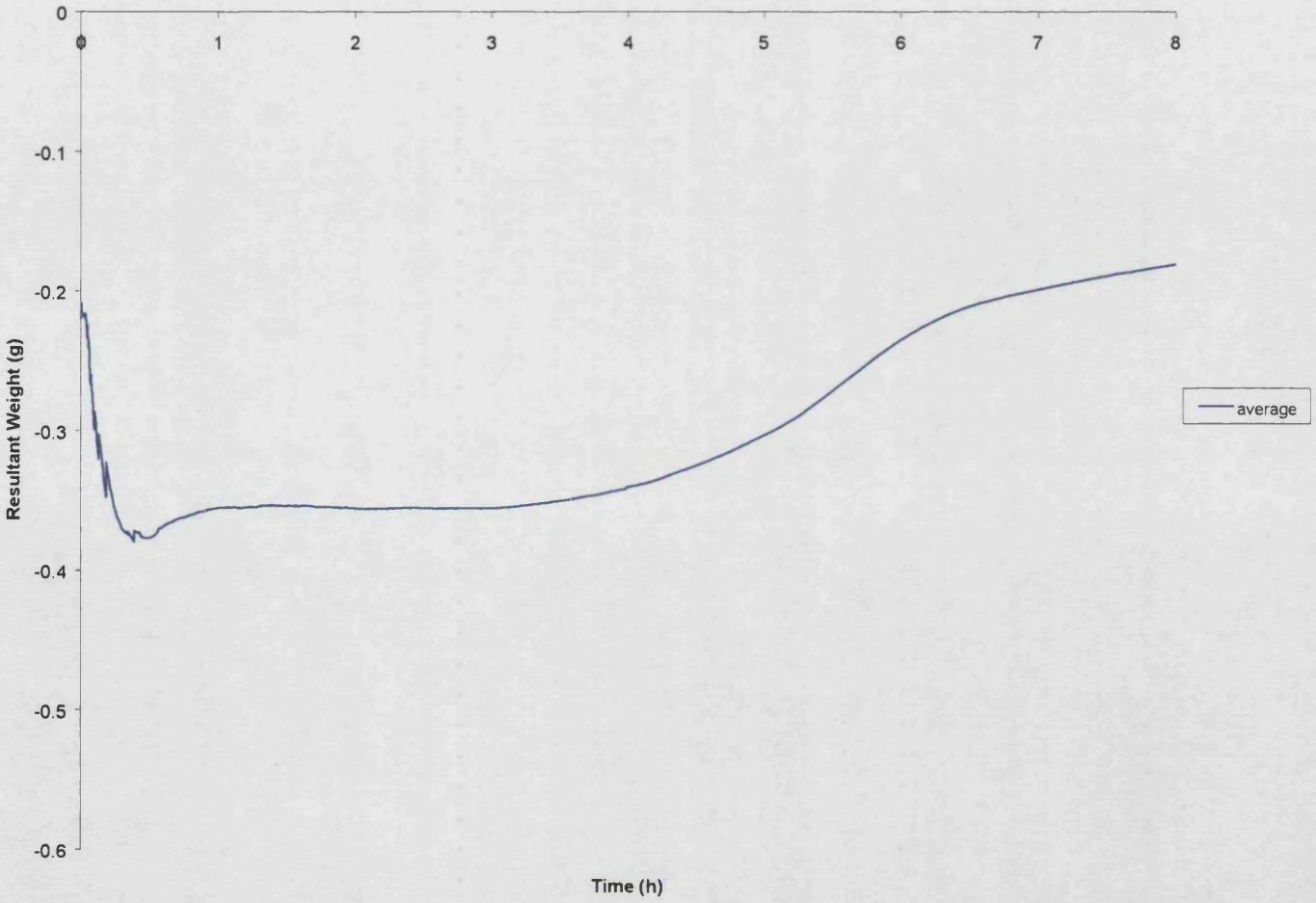

The graphs were assessed for reproducibility by measuring the area above each individual curve, as a measurement of the buoyancy force exhibited by each capsule throughout the duration of the experiment. Peakfit 4.06 for Windows was used to analyse the data sets and to produce the buoyancy force data shown in Table 34, page 157. The capsules showed a mean buoyancy force of 2.4190gh during the experiment, with a standard deviation of 0.28569. These values were deemed to be within the desired range for the purposes of the test.

Table 34 A table to show the buoyancy force data for aerogel capsules

Capsule number	Buoyancy force (gh)
1	2.2750
2	2.6438
3	2.7059
4	2.0060
5	2.4671
Mean	2.4190
Standard Deviation	0.28569

6.3 Pressure vessel testing

Five aerogel capsules were tested in the pressure vessel to assess the rate of carbon dioxide production from the formulation. The capsules were tested using the method outlined previously in section 4.9.1, page 58, with the capsule being added to the release mechanism before the vessel was sealed, and the capsule released into the medium after re-zeroing via the pressure vent.

Results of the five capsule runs are shown in Figure 52, page 159. The graph shows the data sets from the re-zero point onwards until the end of the test. The five runs show a similar profile of carbon dioxide release throughout the duration of the test. There is a small variation in the total gas released from each capsule, but this is to be expected

due to the inherent variability in the manufacturing procedure. However, all graphs follow the same reproducible profile.

Immediately after immersion no gas is produced from the capsules, as a direct consequence of the protective coating forming a barrier around the active formulation. After a few minutes this coating begins to erode away and allowing the gastric fluid access to the bicarbonate present in the aerogel blend. The result of the interaction is a burst of CO_2, which then continues to be produced throughout the test. After the initial burst, the rate of gas production slows slightly until approximately an hour has passed. After the first hour of the test the rate of gas production then increases again, before continually slowing until the test has been completed. The rate of gas production decreases until the end the test due to the diminishing stable bicarbonate content in the formulation. Figure 53, page 160 shows the average rate of gas release for the aerogel capsules.

Table 35, page 161, shows a summary of the data. It can be seen from the table that the capsules generated between 24.4 and 30.1 mbar of pressure throughout the duration of the experiment. The variation in pressure is due to the slightly different dynamic interaction of each capsule with the simulated gastric fluid, along with the inherent variation present in the formulation. The average pressure generated per hour for the aerogel capsules varied between 3.34 – 4.11 mbar.

Figure 52 A graph to show the carbon dioxide release rate for five aerogel capsules

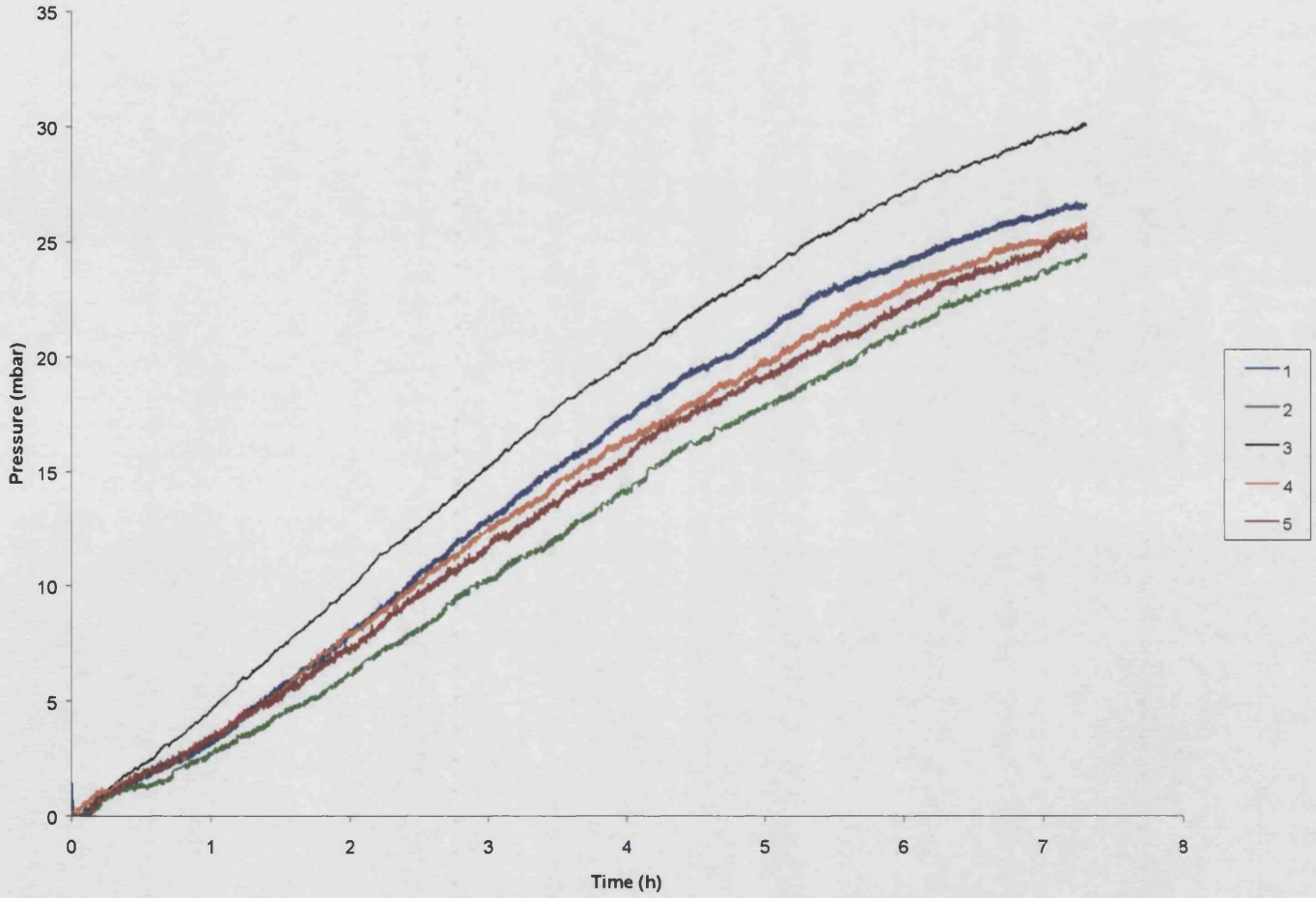

Figure 53 A graph to show the average rate of gas release for the aerogel capsules

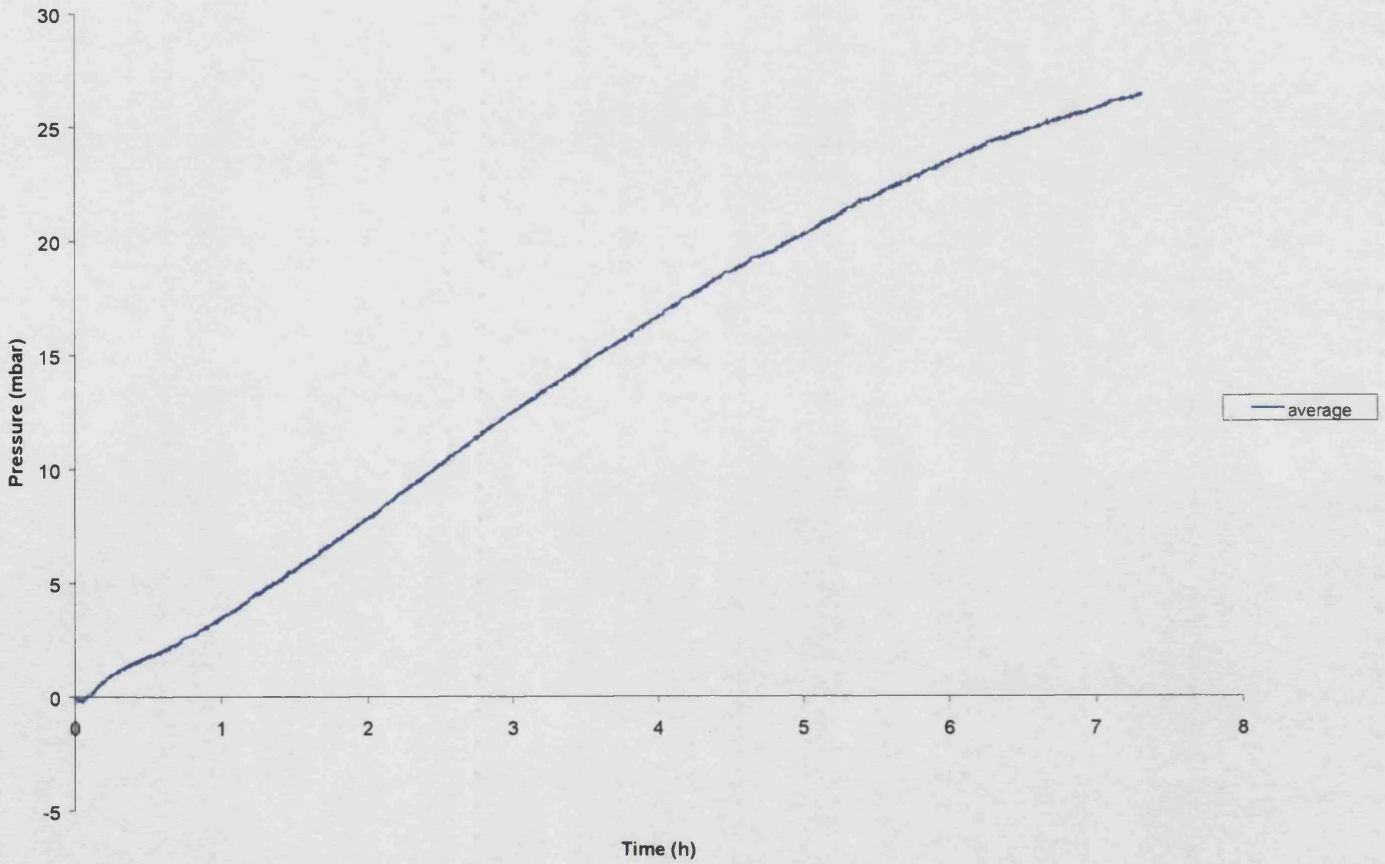

Table 35 CO_2 release data for five aerogel capsules

Capsule number	Maximum pressure generated (mbar)	Run time (h)	Average pressure generated per hour(mbar)
1	26.59	7.31	3.64
2	24.41	7.31	3.34
3	30.06	7.31	4.11
4	25.60	7.31	3.50
5	25.29	7.31	3.46

6.4 Swelling studies

Three aerogel capsules were tested according to the protocol outlined in section 5.6.7.5, page 98.

Sample digital photographs from the study are shown below in Figure 54, page 162. Table 36, page 163 shows the results of the image analysis for each run, along with average values. The data for time zero was taken by subjecting a dry control capsule to the image analysis process.

The data can be seen graphically in Figure 55, page 164. From the data it can be seen that all three runs show similar profiles. The runs do not follow identical traces, as each individual capsule has a slightly different interaction profile with the SGF medium. The overall profile of the three traces does, however, show similarities.

It can be seen from the graphs that initially the capsules shrink slightly, this is due to the initial interaction of the gelatine capsule with the SGF, which causes the gelatine to contract around the formulation as it begins to dissolve.

The capsules then swell rapidly until the 2-hour point. This swelling occurs once the gelatine capsule has been dissolved and ruptured, allowing the gastric fluid direct access to the previously dry formulation. The polymers in the formulation then hydrate rapidly making the capsule swell, whilst the sodium bicarbonate also interacts with the SGF to produce carbon dioxide. The carbon dioxide produced acts as a partial disintegrant and forces the tablet to expand to accommodate the gas.

The swelling process slows continuously from this point as the gastric fluid begins to erode away the capsule front. After six hours the capsule eventually starts to shrink as

the rate of erosion of the capsule overtakes any further swelling. This erosion continues until the end of the test.

Figure 54 Sample digital photographs of the capsule swelling process

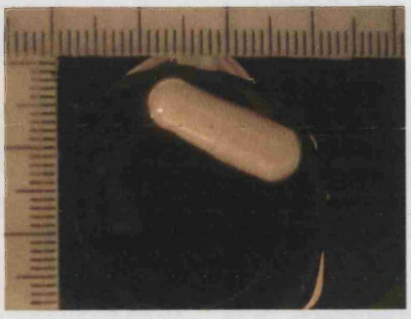

1 minute

60 minutes

240 minutes

480 minutes

Table 36 Cross-sectional area data for the aerogel capsules

Time (min)	Capsule 1 area (cm^2)	Capsule 2 area (cm^2)	Capsule 3 area (cm^2)	Average area (cm^2)	Standard Deviation
0	1.1256	1.1256	1.1256	1.1256	0.00000
1	1.0849	1.0707	1.0729	1.0762	0.00764
15	1.4297	1.4515	1.5395	1.4736	0.05813
30	1.5854	1.6973	1.7567	1.6798	0.08698
45	1.6564	1.8642	1.8971	1.8059	0.13051
60	1.9740	1.9193	1.9661	1.9531	0.02957
90	2.0525	2.1356	2.0991	2.0957	0.04165
120	2.2053	2.2441	2.2548	2.2347	0.02604
150	2.2260	2.4455	2.2564	2.3093	0.11893
180	2.3190	2.5130	2.2670	2.3663	0.12965
240	2.5026	2.6232	2.3252	2.4837	0.14990
300	2.6944	2.6105	2.3846	2.5632	0.16023
360	2.6343	2.6088	2.4128	2.5520	0.12119
420	2.5030	2.4228	2.3809	2.4356	0.06204
480	2.4869	2.2863	2.3555	2.3762	0.10190

Figure 55 A graph to show the image analysis data for the aerogel capsules

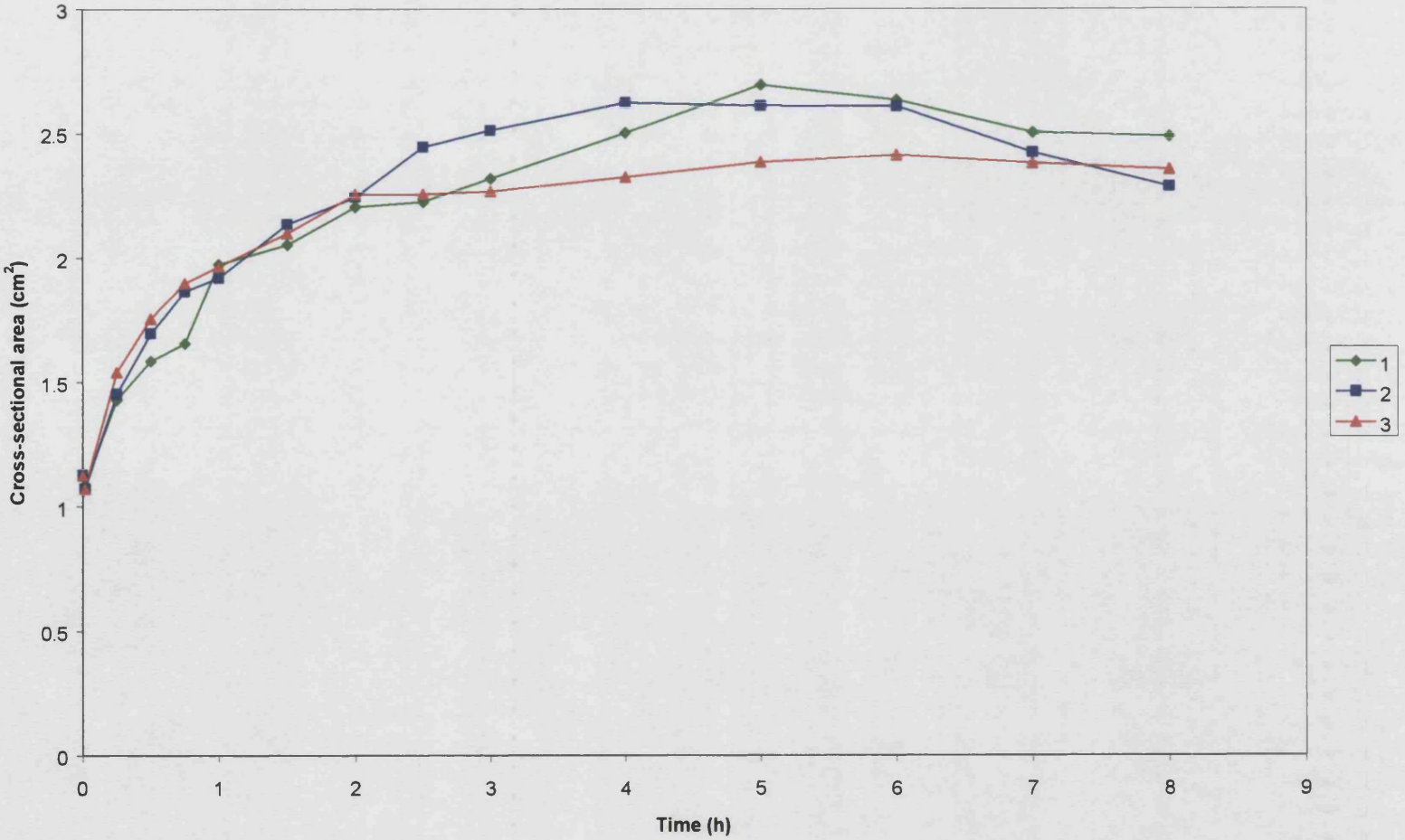

6.5 Discussion of the aerogel capsule characteristics

The characteristics of the aerogel capsules have been investigated and discussed on an individual test basis. This section aims to compile these results together so that the mechanisms of the *in vitro* floating properties can be explained, in order to understand the behaviour of the capsules as a floating dosage form. The data will enable us to assess the importance of individual features that allow the formulation to float successfully for an 8-hour period.

The three different tests were performed to study the factors that lead to buoyancy; the resultant weight, the rate of gas production and the continuous swelling of the dosage form. These tests have previously been shown to be useful when analysing a gas-powered floating dosage form.

In order to fully understand the dynamic changes occurring within the tablet during testing, it is necessary to study the profile of the graphs that have been produced from the multiple runs.

Before looking at all the data together it is first necessary to assess the gas release data set. Figure 56, page 166, shows the normalised gas release data for the aerogel capsules. The pressure data shown is the average normalised gradient of the pressure built up in the pressure vessel (e.g. the normalised rate of gas release). The pressure gradient was calculated using 6-minute intervals throughout the duration of the test. A polynomial trend-line has been added to the graph in order to smooth the results and aid analysis.

Figure 57, page 169, shows the average normalised data from all the experiments. The data has been normalised so that all the data can be shown against the same axis. The buoyancy graph shows positive data, e.g. the average resultant weight exhibited by the tablets. The swelling data shows the average data for the five tablets, whilst the pressure data shows the polynomial line of best fit described in Figure 56.

Figure 56 A graph to show the normalised data for gas release from aerogel capsules

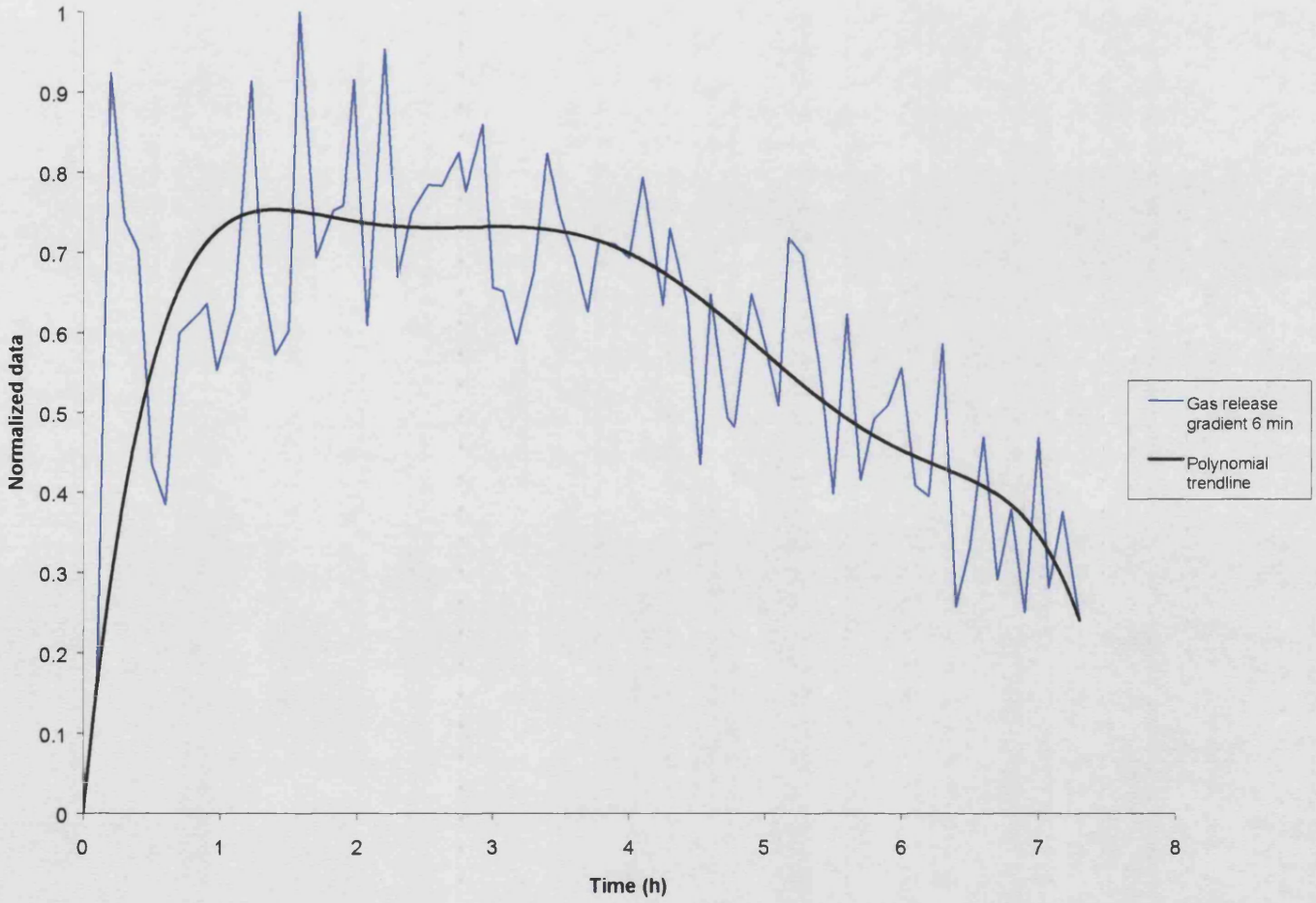

As expected, the buoyancy graph can be explained using the swelling and rate of gas release graphs. The buoyancy graph can be broken down into three main sections:

1. An initial increase in buoyancy during the first 30-minutes of the following immersion of the capsules in the SGF medium
2. After the initial buoyancy period, an equilibrium period is found that enables the resultant weight to remain approximately constant until four hours have elapsed.
3. After four hours the buoyancy of the aerogel capsules begin to decrease. This decrease continues until the end of the test.

These three distinct sections within the buoyancy profile occurred for all capsules tested. Listed below is an explanation of the changes the capsules undergo during the floating process, with each step being used to explain the three sections of the buoyancy profile that are seen:

1. The graphs show that the initial buoyancy increase is a combination of capsule swelling and gas production. Capsule swelling leads to an increase in buoyancy due to the intrinsic relationship present between volume and density. Gas production adds to the buoyancy increase because some of the gas produced will remain trapped within the polymer network of the capsule. As the aerogel capsule swells however, it is expected that some of the intrinsic buoyancy effect conveyed by the initial aerogel structure will lessen.

2. After about an hour the rate of gas release from the capsule becomes approximately constant. During this time the capsule continues to swell due to a combination of the polymers continuing to hydrate and the CO_2 forcing the capsule to expand. During this time the buoyancy of the capsules is seen to remain constant. It is thought that the gas being released is enough to sustain the buoyancy that is partially lost through the destruction of the aerogel structure.

3. The final phase on the graph shows a continuous decrease in buoyancy until the end of the test. We can see during this phase that the rate of gas production is also starting to decrease proportionally. We can also see that the capsules have stopped swelling and

are actually beginning to erode. It is the combination of these negative factors that result in the decrease in buoyancy that is seen. It should be noted that the capsules are still buoyant until the end of the 8-hour test period despite the decreasing trend.

It has been shown in the discussion above that the combination of methods used is an effective means of understanding the buoyancy profile of the capsules. It has also been shown that the developed methods can be used for either tablets or capsules.

The main difference between the aerogel capsules and the previous tablet formulations is the effect that swelling had on the buoyancy profile. This is due to the inherent difference between the initial properties of the formulations. The tablets relied on the generation of gas and an increase in volume to achieve buoyancy, whereas the aerogel capsules were formulated to be buoyant before any interaction with the SGF had taken place. This results in the buoyancy of the aerogel capsule formulation being, at times, adversely affected by swelling. It was thought this was due to the buoyant aerogel structure being partially damaged by the swelling process.

Figure 57 A graph to show the normalised dynamic testing data sets for the aerogel capsules

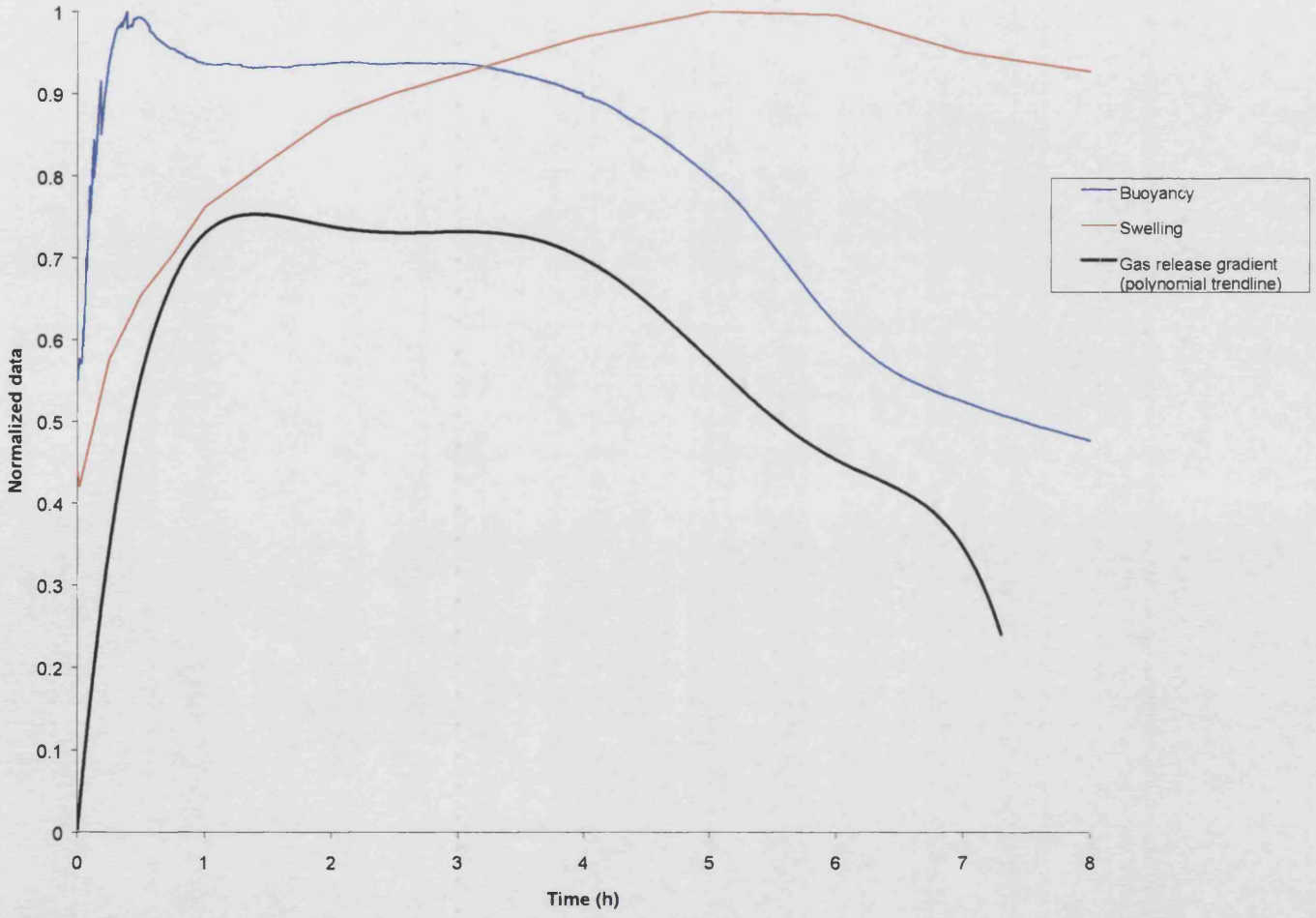

CHAPTER 7

CASE STUDY OF A FLOATING SYSTEM (2)

Studies have previously shown unexpected discrepancies between *in vivo* and *in vitro* results when using floating dosage forms. Due to the lack of *in vitro* testing mechanisms available, the exact reasons for some *in vivo* failures occur have not been determined. This study will look at an omeprazole capsule formulation that was shown to have unexpected *in vivo* results, before trying to establish the reason for the discrepancy.

7.1 Discussion of in vivo results

The omeprazole capsules (Ranbaxy, India) being tested (European patent number 0960620) were formulated as a generic equivalent to Losec 20mg capsules (Astra-Zeneca, London, UK). Omeprazole is a proton pump inhibitor that is degraded by the acid conditions found in the stomach. It is therefore necessary for an omeprazole system to have some degree of enteric coating that protects the drug from the acidic conditions of the stomach. Both of the formulations in the study utilise enteric coating, but in different ways. The generic capsule (Ranbaxy) enteric coating covers the entire capsule, whilst the Losec capsule (Astra-Zeneca, London, UK) enteric coating covers many individual microcapsules within the main capsule surround.

The previous *in vitro* work on the generic capsules had centred on achieving bio-equivalence with the Losec capsules. The dissolution results shown below in Table 37, page 171 were conducted using a USP 2 method at 100rpm and a pH of 6.8. The capsules were all pre-tested for 2-hours in 0.1M HCl to ensure the stability of the enteric coatings.

Table 37 Comparative dissolution results for Omeprazole formulations

Time (min)	0	15	30	45
% released (Losec)	0	80.4	85.2	86.9
% released (Generic)	0	29.0	87.0	92.0

The results show that the enteric coating protects the drug from the 0.1M HCl in both formulations. The results also show that over 85% of omeprazole had been released after only 30 minutes of testing in the 6.8pH medium. This indicated that once the capsules passed the stomach *in vivo* the formulations would display similar release profiles, leading to bio-equivalence.

The capsules were then tested in an *in vivo* study, using 23 people (Study number 100/98, Ranbaxy, India). All participants were under fasting conditions so that the stomach was empty during testing. Table 38, page 172 shows the results of the *in vivo* study.

Table 38 Comparative *in vivo* Cmax values of omeprazole formulations

	Cmax (ng/ml)
Geometric mean (Losec)	454.6
Geometric mean (Generic)	371.7
Cmax ratio (Generic/Losec)	81.76

The results of the study show that the Cmax of the generic formulation was much lower than that of the Losec formulation. This result was unexpected after the previous equivalent dissolution results. It is possible that some of the generic capsules were being retained in the stomach for longer than expected and therefore undergoing degradation in the acid conditions as the enteric coating fails. In order to test this theory, the capsules were tested in the buoyancy apparatus.

7.2 In vitro buoyancy results

Five generic capsules were tested in the buoyancy apparatus to assess the floating force properties of the aerogel system. The capsules were tested using the method outlined previously in section 3.8, page 33.

The results are shown graphically in Figure 58, page 173.

Figure 58 A graph to show the resultant weight profiles for the generic capsules

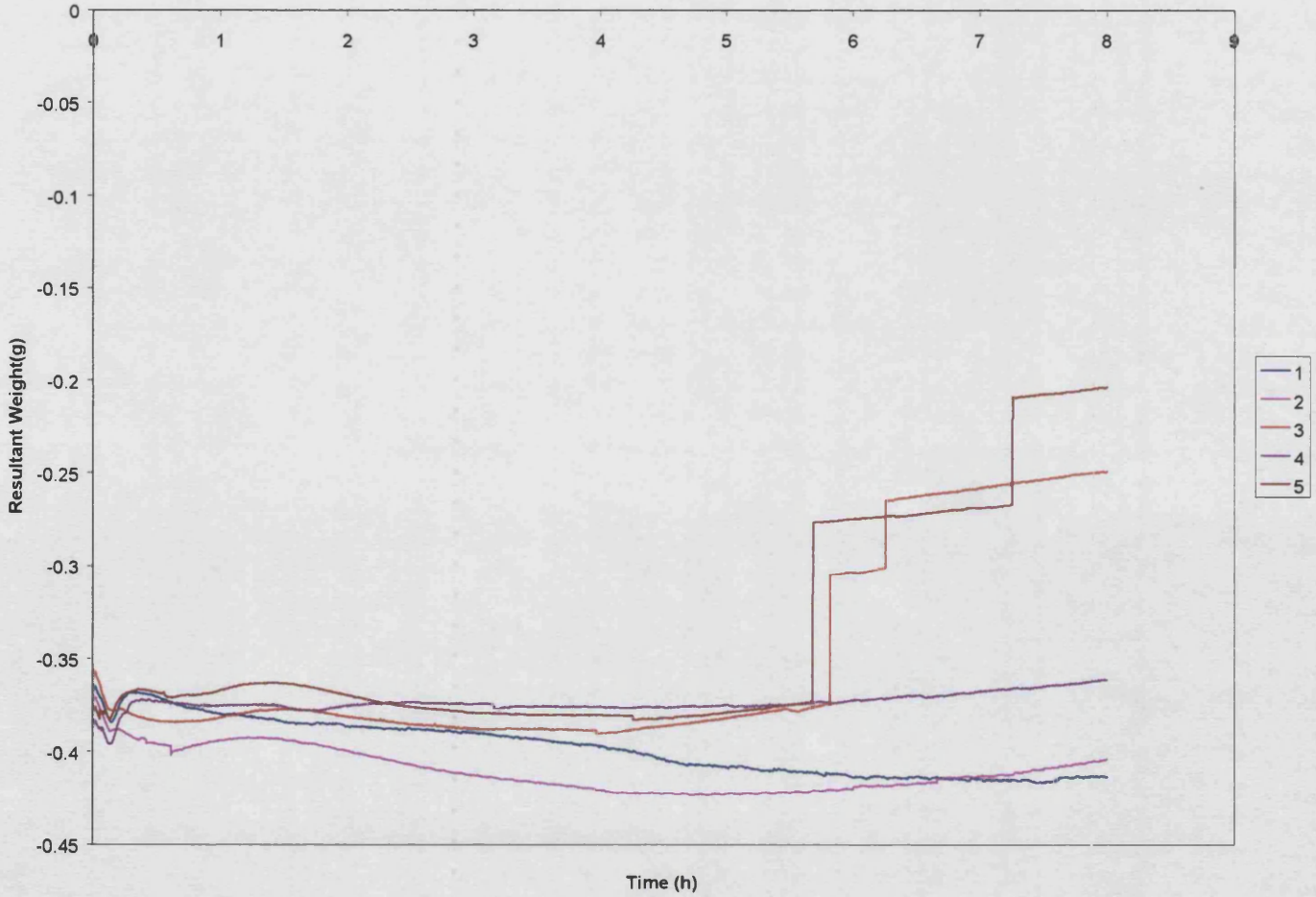

The graphs show that all of the generic capsules floated for the duration of the 8-hour test period. This was an unexpected result, as it was initially thought the capsules would not float for long periods. It is obvious that a floating capsule will be retained in the stomach for longer periods in some patients, but this would not cause much of a problem as long as the enteric coating remained intact.

Two of the graphs exhibit a sudden decrease in buoyancy after approximately five and a half hours. This sudden decrease is thought to be the release of a gas bubble from the capsule, which indicates that the enteric coating of the capsule has failed. This supposition was backed up by examination of the capsules after the test had concluded. The two capsules that were shown to exhibit a sudden decrease in buoyancy were the only capsules not intact after completion of the test. This indicates that there is a high degree of variation in the coating level of the capsules, resulting in some of the capsules remaining intact throughout the test and some of the capsules rupturing. If the capsules were to rupture in the stomach during the *in vivo* testing, the active omeprazole would be degraded by the acidic conditions, resulting in decreased Cmax blood levels. As this failure of the coating occurs after five and a half hours, it would not have caused a problem during the *in vivo* testing if the capsules had not floated. It is the floating of the capsules that will prolong the residence time in the stomach, thereby enabling the enteric coating to rupture, leading to degradation of the active drug. This variation in coating would not have been detected in the *in vitro* dissolution work because the acid pre-test only lasted for two hours.

7.3 Conclusions

The buoyancy apparatus has been used to help us to understand the problems that can be associated with *in vitro – in vivo* correlation. It has been shown that the apparatus, when used in conjunction with visual inspection, can explain *in vivo* results that were previously not understood. If the buoyancy apparatus had been used before the *in vivo* work had been performed, it would have been possible to predict the failure of the trial. Work could then have focused on finding a way around the floating/coating problem, rather than waiting for the results of an expensive clinical trial.

CHAPTER 8

DISCUSSION AND CONCLUSIONS

8.1 General discussion

The aims of this project were to develop and test various novel *in vitro* apparatus capable of identifying, and optimising, the vital characteristics of floating dosage forms.

The rational design of *in vitro* experiments is essential for the thorough understanding of any dosage form. It is perhaps even more important when considering the various intrinsic factors that influence the ability of a formulation to float. Floating dosage forms, in particular, have been shown to have a low degree of *in vitro – in vivo* correlation, hence there is a real need for apparatus capable of accurately predicting the behaviour of such dosage forms *in vivo*.

The most important factor to consider when designing floating dosage forms is the ability of a formulation to float upon the gastric fluids. It is not enough, however, to take a pre-testing density reading as an indicator of a dosage forms ability to float, as this does not take into account the many dynamic interactions that occur between a formulation and a test medium during testing. It is also unsatisfactory to simply state whether a dosage form floats or not, as it is much more preferential to quantitate the force with which a formulation is floating. This gives the formulator an idea of the robustness of the dosage form, and an indication as to what to expect when confronted with different stomach conditions *in vivo*.

A buoyancy apparatus was therefore developed that was capable of quantitating the dynamic floating profile of a dosage form over a functional time period. The apparatus consisted of a temperature regulated water bath linked via a force transmitter device to a computer for data logging. It has been shown that the apparatus can distinguish between the floating profiles of slightly modified formulations, helping the understanding of the dynamic interactions that are occurring within a dosage form during testing. The technique has been used to assess both gas powered and aerogel formulations successfully. Finally, the apparatus has been used to assess an *in vivo* failure and to explain the reasons for the lack of clinical success.

An integral part of many floating dosage forms is the ability to either trap or generate gas to aid buoyancy. Understanding and controlling the rate of gas release from a dosage form would enable the formulator to tailor a dosage form to meet their needs. A pressure vessel has therefore been designed and developed, that is capable of accurately

measuring the rate and extent of gas evolution from a floating system. The glass vessel is temperature regulated and linked, via a calibrated pressure transducer, to a personal computer for data logging.

It has been shown that the pressure vessel is capable of distinguishing between the gas release profiles of similar dosage forms. The rate of gas release has been used, along with the results from the buoyancy apparatus, to explain the buoyancy profiles seen for particular dosage forms. The apparatus has successfully measured gas-powered and aerogel floating formulations.

The third parameter associated with the floating ability of a dosage form is swelling. Density is inversely proportional to the volume of a dosage form, therefore if a tablet swells when immersed in medium, so the density of that dosage form will decrease correspondingly, hence aiding buoyancy.

A method that enabled real time quantification of the swelling of a floating dosage form was therefore developed. The apparatus consisted of a temperature regulated water bath, situated below a digital camera. Images from the camera were taken at pre-determined intervals and then subjected to an image analysis process to determine swelling/erosion. The method was shown to successfully produce a dynamic swelling profile and to identify the differences between similar formulations. The results were used, in conjunction with pressure vessel data, to explain why a particular buoyancy profile was seen for a particular formulation. The apparatus was shown to successfully measure gas-powered and aerogel floating formulations.

The amount of sodium bicarbonate has been shown to be of importance for floating dosage forms. However, an increase in the amount of bicarbonate does not always result in increased buoyancy throughout the duration of a test. The three dynamic methodologies could however be used to optimise the amount of bicarbonate needed in a formulation in order to achieve a desired floating profile.

The three dynamic apparatus have been shown to be most useful in unison, in order to explain the characteristics of a floating dosage form. It would be possible to use the information to tailor a formulation to produce a desired floating profile under chosen conditions. The combined results from the apparatus would also enable the formulator to understand the likely results of any *in vivo* tests, without the need to waste time and money conducting such tests. It is the scientific understanding of the mechanisms that lead to the floating of a dosage form which will enable the production of better formulations, therefore

the developed apparatus could play an integral part in the future development of floating dosage forms.

8.2 Further work

Having developed apparatus capable of identifying and accurately quantifying the parameters that influence the floating profile of a dosage form, further work should concentrate on the development of a novel gas-powered formulation. The dynamic testing methodologies should be utilised to develop and optimise the formulation, as well as to understand the interactions that occur during testing.

The optimised dosage form should then ideally be used in an *in vivo* study utilising gamma scintigraphy to study the position of the dosage form in the stomach. The *in vitro* testing should also be conducted after addition of the gamma emitter in order to assess the potential impact upon buoyancy parameters.

One *in vivo* failure has already been explained using the apparatus. Work by other authors in the literature should be investigated to assess the reasons for their lack of *in vitro – in vivo* correlation. Work should concentrate initially on gas-powered dosage forms.

Apparatus have been developed that measure buoyancy, swelling and gas production. One further parameter that should be investigated is the gel strength produced during swelling. Gel strength will have a direct effect on the ability of a formulation to trap any gas produced as well as on the dissolution parameters of the formulation. The development of a dynamic gel strength test would enable the formulator to have control over a further parameter that will have an effect on floating properties. Some work has been conducted in this area by Yang et al (1998) using a texture analyser (Stable Micro Systems, Surrey, UK). This method could possibly be adapted to measure the strength of the polymer gel layer that some floating dosage forms produce.

The effect of different mediums in the dynamic testing apparatus should also be investigated. Conditions in the stomach are not always identical, so the effect of changing medium conditions, such as viscosity and acidity, should be determined.

CHAPTER 9

REFERENCES

Agyilirah, G.A., Green, M., DuCret, R. and Banker, G.S. (1991) Evaluation of the gastric retention properties of a cross-linked polymer coated tablet versus those of a non disintegrating tablet. Int. J. Pharm. 75 : 241 – 247

Anderson, N.R., Banker, G.S. and Peck, G.E. (1982) Quantitative evaluation of pharmaceutical effervescent systems I. Design of testing apparatus. J. Pharm. Sci. 71 : 3-6

Bechgaard, H. and Ladefoged, K. (1978) Distribution of pellets in the gastrointestinal tract. The influence on transit time exerted by the density or diameter of the pellets. J. Pharm. Pharmacol. 30 : 690 – 692

Bechgaard, H., Christensen, F.N., Davis, S.S., Hardy, J.G., Taylor, M.J., Whalley, D.R. and Wilson, C.G., (1985) Gastrointestinal transit of pellet systems in ileostomy subjects and the effect of density. J. Pharm. Pharmacol. 37 : 718 – 721

Brener, W., Hendrix, T.R. and McHugh, P.R. (1983) Regulation of the gastric emptying of glucose. Gastroenterology 85 : 76 – 82

British Pharmacopoeia Commission (1993) Production of decarbonated water. *In*: The British Pharmacopoeia, 1998. Volume II. A67. London: The Stationary Office

Brittain, H.G., Bogdanowich, S.J., Bugay, D.E., DeVincentis, J., Lewen, G. and Newman, A.W. (1991) Physical characterisation of pharmaceutical solids. Pharm. Res. 8 (8) : 963 – 973

Brunauer, S. and Emmett, P.H. (1937) The use of low temperature Van der Waals adsorption isotherms in determining the surface area of various adsorbents. J. Am. Chem. Soc. 59 : 1553 – 1564

Cargill, R., Caldwell, L.J., Engle, K., Fix, J.A., Porter, P.A. and Gardner, C.R. (1988) Controlled gastric emptying. 1. Effects of physical properties on gastric resident times of nondisintegrating geometric shapes in beagle dogs. Pharm. Res. 5 (8) : 533 – 536

Chan, K.K.H., Buch, A., Glazer, R.D., John, V.A. and Barr, W.H. (1994) Site differential gastrointestinal absorption of benazepril hydrochloride in healthy volunteers. Pharm. Res. 11 (3) : 432 – 437

Ch'ng, H.S., Park, H., Kelly, P. and Robinson., J.R. (1985) Bioadhesive polymers as platforms for oral controlled delivery. II.: Synthesis and evaluation of some swelling, water-insoluble bioadhesive polymers. J. Pharm Sci. 74 (4) : 399 – 405

Christensen, F.N., Davis, S.S., Hardy, J.G., Taylor, M.J., Whalley, D.R. and Wilson, C.G. (1985) The use of gamma scintigraphy to follow the gastrointestinal transit of pharmaceutical formulations. J. Pharm. Pharmacol. 37 : 91 – 95

Chueh, H.R., Zia, H. and Rhodes, C.T. (1995) Optimization of Sotalol floating and bioadhesive extended release tablet formulations. Drug Dev. Ind. Pharm. 21 (15) : 1725 – 1747

Code, C.F. and Marlett, J.A. (1975) The interdigestive myo-electric complex of the stomach and small bowel of dogs. J. Physiol. 246 : 289 – 309

Cook, J.D., Carriaga, M., Kahn, S.G., Schalch, W. and Skikne, B.S. (1990) Gastric delivery system for iron supplementation. The Lancet 335 : 1136 – 1139

Cromer, A.H. (1981) Physics for the life sciences, Chapter 7: Fluids. 2nd Ed. Int. Student. Edition. McGraw-Hill Intern Book Co. Tokyo, Japan. 134-153

Davis, S.S., Hardy, J.G., Taylor, M.J., Whalley, D.R. and Wilson, C.G. (1984) The effect of food on the gastrointestinal transit of pellets and an osmotic device (Osmet). Int. J. Pharm. 21 : 331 – 340

Davis, S.S., Hardy, J.G. and Fara, J.W., (1986a) Transit of pharmaceutical dosage forms through the small intestine. Gut 27 : 886 – 892

Davis, S.S., Hardy, J.G., Wilson, C.G., Feely, L.C. and Palin, K.J. (1986b) Gastrointestinal transit of a controlled release Naproxen tablet formulation. Int. J. Pharm. 32 : 85 – 90

Davis, S.S. (1986c) The design and evaluation of controlled release dosage forms for oral delivery. S.T.P. Pharma. 2 :1015 – 1022

Davis, S.S., Stockwell, A.F., Taylor, M.J., Hardy, J.G., Whalley, D.R., Wilson, C.G., Bechgaard, H. and Christensen, F.N. (1986d) The effect of density on the gastric emptying of single– and multiple– unit dosage forms. Pharm. Res. 3 : 208 – 213

Dees, P.J. and Polderman, J. (1981) Mercury porosimetry in pharmaceutical technology. Powder Technol. 29 : 187 – 197

Desai, S. and Bolton, S. (1993) A floating controlled-release drug delivery system : In vitro – in vivo evaluation. Pharm. Res. 10 (9) : 1321 – 1325

Deshpande, A.A, Shah, N.H., Rhodes, C.T. and Malick, W. (1997) Development of a novel controlled-release system for gastric retention. Pharm. Res. 14 (6) : 815 – 819

Duchene, D., Touchard, F. and Peppas, N.A. (1988) Pharmaceutical and medical aspects of bioadhesive systems for drug administration. Drug Dev. Ind. Pharm. 14 : 283 – 318

Fordtran, J.S., Morawski, S.G., Santa Ana, C.A. and Rector Jnr, F.C. (1984) Gas production after reaction of sodium bicarbonate and hydrochloric acid. Gastroenterology 87 : 1014 – 1021

Ganderton, D. and Selkirk, A.B. (1969) The effect of granule properties on the pore structure of tablets of sucrose and lactose. J. Pharm. Pharmacol. 22 : 345-353

Gerogiannis, V.S., Rekkas, D.M., Dallas, P.P. and Choulis, N.H. (1993) Floating and swelling characteristics of various excipients used in controlled release technology. Drug Dev. Ind. Pharm. 19 (9) : 1061 – 1081

Gliko-Kaber, I., Yagen, B., Baloum, M. and Rubinstein, A. (2000a) Phosphated cross-linked guar for colon-specific drug delivery I. Preparation and physicochemical characterisation. J. Control. Release 63 : 121 – 127

Gliko-Kaber, I., Yagen, B., Baloum, M. and Rubinstein, A. (2000b) Phosphated cross-linked guar for colon-specific drug delivery II. In vitro and in vivo evaluation in the rat. J. Control. Release 63 : 129 – 134

Grass, G.M., and Morehead, W.T. (1989) Evidence for site-specific absorption of a novel ACE inhibitor. Pharm. Res. 6 (9) : 759 – 765

Groning, R. and Heun, G. (1984) Oral dosage forms with controlled gastrointestinal transit. Drug Dev. Ind. Pharm. 10 (4) : 527 – 539

Gupta, P.K., Leung, S.S. and Robinson, J.R. (1990) Bioadhesives / Mucoadhesives in drug delivery to the gastrointestinal tract. In Lenaerts, V and Gurny, R. (Eds), Bioadhesive Drug Delivery Systems, CRC Press, Boca Raton, pp 65 – 92

Harder, S., Fuhr, U., Beerman, D. and Staib, A.H., (1990) Ciprofloxacin absorption in different regions of the human gastrointestinal tract. Investigations with the hf-capsule. Br. J. Clin. Pharmac. 30 : 35 – 39

Harris, D., Fell, J.T., Taylor, D.C., Lynch, J. and Sharma, H.L. (1989) Oral availability of a poorly absorbed drug, hydrochloreothiazide, from a bioadhesive formulation in the rat. Int. J. Pharm. 56 : 97 – 102

Hilton, A.K. and Deasy, P.B. (1992) In vitro and in vivo evaluation of an oral sustained release floating dosage from of amoxycillin trihydrate. Int. J. Pharm. 86 : 79 – 88

Hunt, J.N. and Knox, M.T. (1968) A relation between the chain length of fatty acids and the slowing of gastric emptying. J. Physiol. 194 : 327 – 336

Hunt, J.N. and Knox, M.T. (1972) The slowing of gastric emptying by four strong acids and three weak acids. J. Physiol. 222 : 181 – 208

Hunt, J.N. (1980) A possible relationship between the regulation of gastric emptying and food intake. Am. J. Physiol. 239 : G1 - G4

Iannuccelli, V., Coppi, G., Bernabei, M.T. and Cameroni, R (1998a) Air compartment multiple-unit system for prolonged gastric residence. Part I. Formulation study. Int. J. Pharm. 174 : 47 – 54

Iannuccelli, V., Coppi, G., Sansone, R. and Ferolla, G. (1998b) Air compartment multiple-unit system for prolonged gastric residence. Part II In vivo evaluation. Int. J. Pharm. 174 : 55 – 62

Ichikawa, M., Kato, T., Kawahara, M., Watanabe, S. and Kayano, M. (1991) A new multiple-unit oral floating dosage system. I. In vivo evaluation of floating and sustained-release characteristics with p-Aminobenzoic Acid and Isosorbide Dinitrate as model drugs. J. Pharm. Sci. 80 (12) : 1153 – 1156

Ingani, H.M., Timmermans, J. and Moes, A.J., (1987) Conception and in vivo investigation of peroral sustained release floating dosage forms with enhanced gastrointestinal transit. Int. J. Pharm. 35 : 157 – 164

Johnson, F.A., Craig, D.Q.M., Mercer, A. and Chauhan, S. (1998) The use of image analysis as a means of monitoring bubble formation in alginate rafts. Int. J. Pharm. 170 : 179 – 185

Karim, A., Burns, T., Janky, D. and Hurwitz, A. (1985) Food-induced changes in Theophylline absorption from controlled release formulations. Part II. Importance of meal composition and dosing time relative to meal intake in assessing changes in absorption. Clin. Pharmacol. Ther. 38 : 642 - 647

Kaus, L.C., Fell, J.T., Sharma, H. and Taylor, D.C. (1984a) On the intestinal transit of a single non-disintegrating object. Int. J. Pharm. 20 : 315 – 323

Kaus, L.C., Fell, J.T, Sharma, H. and Taylor, D.C. (1984b) Gastric-emptying and intestinal transit of non-disintegrating capsules – the influence of Metoclopramide. Int. J. Pharm. 22 : 99 – 103

Kaus, L.C. (1987) The effect of density on the gastric emptying and intestinal transit of solid dosage forms: comments on the article by Davis et al. Pharm. Res. 4 : 78

Kelly, K.A., (1981) Motility of the stomach and gastroduodenal junction in Physiology of the Gastrointestinal Tract, Raven, New York 393 – 410

Khosla, R. and Davis, S.S., (1990) The effect of tablet size on the gastric emptying of non-disintegrating tablets. Int. J. Pharm. 62 : R9 - R11

Lentner, C. Ed. (1981) Geigy Scientific Tables, Vol. 1, 8th rev., Ciba-Geigy: Basle, Switzerland, p124

Li, S.P., Pendharker, C.M., Mehta, G.N., Karth, M.G. and Feld, K.M. (1993) Sucralfate as a bioadhesive gastric intestinal retention system: preliminary evaluation. Drug Dev. Ind. Pharm. 19 (19) : 2519 – 2537

Longer, M.A., Ch'ng, H.S. and Robinson, J.R. (1985) Bioadhesive polymers as platforms for oral controlled delivery. III: Oral delivery of Chlorothiazide using a bioadhesive polymer. J. Pharm. Sci. 74 (4) : 406 – 411

Matharu, R.S. and Sanghavi, N.M. (1992) Novel drug delivery system for Captopril. Drug Dev. Ind. Pharm. 18 (14) : 1567 – 1574

Mazer, N., Abisch, E., Gfeller, J-C., Laplanche, R., Bauerfeind, P., Cucala. M., Lukachich. M. and Blum, A. (1998) Intragastric behaviour and absorption kinetics of a normal and 'floating' modified-release capsule of Isradipine under fasted and fed conditions. J. Pharm. Sci. 77 (8) : 647 – 657

Menon. A,. Ritschel, W.A., and Sakr, A. (1994) Development and evaluation of a monolithic floating dosage form for Furosemide. J. Pharm. Sci. 83 (2) : 239 – 245

Newman, A. W. (1995) Micromeritics, Physical characterisation of pharmaceutical solids, 253-280 Marcel Dekker, New York

Oth, M., Franz, M., Timmermans, J. and Moes, A. (1992) The bilayer floating capsule : A stomach-directed drug delivery system for Misoprostol. Pharm. Res. 9 (3) : 298 – 302

O'Reilly, S. Wilson, C.G., and Hardy, J.G. (1987) The influence of food on the gastric emptying of multiparticulate dosage forms. Int. J. Pharm. 34 : 213 – 216

Park, K. and Robinson, J.R. (1984) Bioadhesive polymers as platforms for oral-controlled drug delivery : method to study bioadhesion. Int. J. Pharm. 19 : 107 – 127

Rosa Jimenez-Castellanos, M., Zia, H. and Rhodes, C.T. (1994) Design and testing in vitro of a bioadhesive and floating drug delivery system for oral application. Int. J. Pharm. 105 : 65 - 70

Rouge, N, Buri, P. and Doelker, E. (1996) Drug absorption sites in the gastrointestinal tract and dosage forms for site-specific delivery. Int. J. Pharm. 136 : 117 – 139

Sangekar, S., Vadino, W.A., Chaudry, I., Parr, A., Beihn, R. and Digenis, G., (1987) Evaluation of the effect of food and specific gravity of tablets on gastric retention time. Int. J. Pharm. 35 : 187 – 191

Sheth, P.R. and Tossounian, J.L., U.S. Patent Application 559 107, (1975)

Sugito, K., Ogata, H, Goto, H., Noguchi, M., Kogure, T., Takano, M., Maruyama, Y. and Sasaki, Y. (1990) Gastrointestinal transit of non-disintegrating solid formulations in humans. Int. J. Pharm. 50 : 89 – 97

Talukdar, M.M. and Kinget, R. (1995) Swelling and drug release behaviour of xanthan gum matrix tablets. Int. J. Pharm. 120 : 63 – 72

Talwar, N., Sen, H. and Staniforth, J.N. (2001) US patent 6 261 601

Talwar, N., Staniforth, J.N. and Tobyn, M.J. (2001) World patent 01 10419

Thacharodi, D.K. and Kampal, A. (1999) European patent 0 960 620

Thairs, S., Ruck, S., Jackson, S.J., Steele, R.J.C., Feely, L.C., Washington, C. and Washington, N. (1998) Effect of dose size, food and surface coating on the gastric residence and distribution of an ion exchange resin. Int. J. Pharm. 176 : 47 – 53

Thanoo, B.C., Sunny, M.C. and Jayakrishnan, A. (1993) Oral sustained release drug delivery systems using polycarbonate microspheres capable of floating on the gastric fluid. J. Pharm. Pharmacol. 45 : 21 – 24

Timmermans, J., Van Gansbeke, B. and Moes, A.J. (1989) Assessing by gamma scintigraphy the in vivo buoyancy of dosage forms having known size and floating form profiles as a function of time. Proc. of the 5th Int. Conf. On Pharmaceutical Technology 1 : 42 - 51

Timmermans, J. and Moes, A.J. (1990a) Measuring the resultant-weight of an immersed test material . I. Validation of an apparatus and a method dedicated to pharmaceutical applications. Acta Pharm. Technol. 36 : 171 – 175

Timmermans, J. and Moes, A.J. (1990b) Measuring the resultant-weight of an immersed test material II. Examples of kinetic determinations applied to monolithic dosage forms. Acta Pharm. Technol. 36 : 176 – 180

Timmermans, J. and Moes, A.J., (1990c) How well do floating dosage forms float? Int. J Pharm. 62 : 207 – 216

Timmermans, J. and Moes, A.J., (1993) The cut off size for gastric emptying of dosage forms. J. Pharm. Sci. 82 : 854

Timmermans, J. and Moes, A.J., (1994) Factors controlling the buoyancy and gastric retention capabilities of floating matrix capsules : new data for reconsidering the controversy. J. Pharm. Sci. 83 : 18 – 24

Tobyn, M.J., Johnson, J.R. and Dettmar, P.W. (1996) Factors affecting in vitro gastric mucoadhesion. II. Physical properties of polymers. Eur. J. Pharm. Biopharm. 42 : 56 – 61

Van Brakel, J., Modry, S. and Svata, M. (1981) Mercury Porosimetry : State of the art. Powder Technol., 29 : 1 – 12

Wagner, J.G., Veldkamp, W. and Long, S. (1958) J. Amer. Pharm. Assoc. 47 : 681 – 685

Watanabe, S., Kayano, M., Ishino, Y. and Miyao, K. (1976) US Patent 3 976 764

Weiner, K., Graham, L.S., Reedy, T., Elashoff, J. and Meyer, J.H. (1981) Simultaneous gastric emptying of two solid foods. Gastroenterology 81 : 257 – 266

Whitehead, L., Fell, J.T., Collet, J.H., Sharma, H.L. and Smith, A-M. (1999) Floating dosage forms : an in vivo study demonstrating prolonged gastric retention. J. Control. Release 55 : 3 – 12

Wilson, C.G. and Hardy, J.G. (1985) Gastrointestinal transit of an osmotic tablet drug delivery system. J. Pharm. Pharmacol. 37 : 573 – 575

Yang, L., Eshraghi, J. and Fassihi, R., (1999) A new intragastric delivery system for the treatment of helicobacter pylori associated gastric ulcer : in vitro evaluation. J. Control. Release. 57 : 215 – 222

Yang, L. and Fassihi, R. (1996). Zero-order release kinetics from a self correcting floatable asymmetric configuration drug delivery system. J. Pharm. Sci. 85 (2) : 170 – 173

Yang, L., Johnson, B. and Fassihi, R. (1998) Determination of continuous changes in the gel layer thickness of poly(ethylene oxide) and HPMC tablets undergoing hydration : a texture analysis study. Pharm. Res. 15 : 1902 – 1906

Yuasa, H., Takashima, Y. and Kanaya, Y. (1996) Studies on the development of intragastric floating and sustained release preparation I. Application of calcium silicate as a floating carrier. Chem. Pharm. Bull. 44 (7) : 1361 – 1366

Yuen, K.H., Deshmukh, A.A., Newton, J.M., Short, M. and Melchor, R. (1993) Gastrointestinal transit and absorption of Theophylline from a multiparticulate controlled-release formulation. Int. J. Pharm. 97 : 61 - 77